



AFTAC

Air Force Technical Applications Center

**Directorate of Nuclear Treaty Monitoring
Research Division**

Seismic Site Survey for New Regional Seismic Array Station in Morocco

**Dean A. Clauter, Phillip J. Lindstedt, Phillip F. Venanzi, and
James P. Neely**

22 August 2005

**Approved for Public Release;
Distribution is Unlimited**



(This page intentionally left blank.)



AFTAC

Air Force Technical Applications Center

**Directorate of Nuclear Treaty Monitoring
Research Division**

Seismic Site Survey for New Regional Seismic Array Station in Morocco

**Dean A. Clauter, Phillip J. Lindstedt, Phillip F. Venanzi, and
James P. Neely**

22 August 2005

**Approved for Public Release;
Distribution is Unlimited**



Report AFTAC-TR-05-005 has been reviewed and is approved for publication.



DAVID R. RUSSELL, SES
Director, Nuclear Treaty Monitoring



GUY D. TURNER, Colonel, USAF
Commander

The overall classification of this report is UNCLASSIFIED.

Addressees: Please notify AFTAC/TT, 1030 S. Highway A1A, Patrick Air Force Base FL32925-3002, if there is a change in your mailing address (including an individual no longer employed by your organization) or if your organization no longer wishes to be included in the distribution of future reports of this nature.

REPORT DOCUMENTATION PAGEForm Approved
OMB No. 0704-0188

The public reporting burden for this collection of information is estimated to average 1 hour per response, including the time for reviewing instructions, searching existing data sources, gathering and maintaining the data needed, and completing and reviewing the collection of information. Send comments regarding this burden estimate or any other aspect of this collection of information, including suggestions for reducing the burden, to the Department of Defense, Executive Services and Communications Directorate (0704-0188). Respondents should be aware that notwithstanding any other provision of law, no person shall be subject to any penalty for failing to comply with a collection of information if it does not display a currently valid OMB control number.

PLEASE DO NOT RETURN YOUR FORM TO THE ABOVE ORGANIZATION.

1. REPORT DATE (DD-MM-YYYY) 22-08-2005		2. REPORT TYPE Technical		3. DATES COVERED (From - To)	
4. TITLE AND SUBTITLE Seismic Site Survey for a New Seismic Array Station in Morocco				5a. CONTRACT NUMBER	
				5b. GRANT NUMBER	
				5c. PROGRAM ELEMENT NUMBER	
				5d. PROJECT NUMBER	
6. AUTHOR(S) Dean A. Clauter, Phillip J. Lindstedt, Phillip F. Venanzi, and James P. Neely				5e. TASK NUMBER	
				5f. WORK UNIT NUMBER	
7. PERFORMING ORGANIZATION NAME(S) AND ADDRESS(ES) Air Force Technical Applications Center (AFTAC/TTR) 1030 South Highway A1A Patrick AFB FL 32925-3002				8. PERFORMING ORGANIZATION REPORT NUMBER AFTAC-TR-05-005	
9. SPONSORING/MONITORING AGENCY NAME(S) AND ADDRESS(ES) Air Force Technical Applications Center (AFTAC/TTR) 1030 South Highway A1A Patrick AFB FL 32925-3002				10. SPONSOR/MONITOR'S ACRONYM(S)	
				11. SPONSOR/MONITOR'S REPORT NUMBER(S)	
12. DISTRIBUTION/AVAILABILITY STATEMENT A; Approved for Public Release; Distribution is Unlimited					
13. SUPPLEMENTARY NOTES					
14. ABSTRACT A seismic site survey in Morocco was conducted jointly with the Centre National Pour La Recherche Scientifique et Technique during January and February 2005. For three separate locations near Oujda (Site 1), Midelt (Site 2), and Tinerhir (Site 3), a portable seismic array was deployed. Seismometers were also installed in a tunnel at an existing seismic station near Midelt (MDT) for comparison. Data from the array at each site were used to determine the characteristics of the seismic background noise and the capability of each site to record regional events in Morocco. The logistics and feasibility of installing a 4-kilometer aperture array were investigated for each potential site. The noise and event analysis indicate that the southern site south of Tinerhir is far superior to the other two proposed locations. Logistically, the southern site is acceptable for installation and support of an array. Included in the report are detailed logistical, geophysical, and geological investigations at the proposed sites, and the analysis of the seismic noise and event data collected.					
15. SUBJECT TERMS Seismic Site Selection; Seismic; Noise Survey; Regional Event Analysis; Morocco Seismic Investigation; USAEDS					
16. SECURITY CLASSIFICATION OF:			17. LIMITATION OF ABSTRACT U	18. NUMBER OF PAGES 136	19a. NAME OF RESPONSIBLE PERSON Dean A. Clauter
a. REPORT U	b. ABSTRACT U	c. THIS PAGE U			19b. TELEPHONE NUMBER (include area code) 321-494-5266

(This page intentionally left blank.)

Contents

	<u>Page</u>
List of Figures	vii
List of Tables	ix
Acknowledgments	x
Introduction	1
Site Survey Format	1
Site Selection Criteria	1
Site Selection Process	1
Pre-Survey Studies	2
General Location Map of Survey Areas	3
General Geologic Map of Survey Areas	4
Site 1 (Oujda) Description	6
Geologic Summary	7
Noise Survey	9
Cultural Noise Sources	9
Accessibility	10
Communications Considerations	10
Power	10
Land Owner	10
Site 2 (Midelt) Description	11
Geologic Summary	11
Noise Survey	13
Cultural Noise Sources	13
Accessibility	14
Communications Considerations	14
Power	14
Land Owner	14
Site 3 (Tinerhir) Description	15
Geologic Summary	15
Noise Survey	21
Cultural Noise Sources	21
Accessibility	21
Communications Considerations	21
Power	21
Land Owner	22

	<u>Page</u>
Noise Spectra Analysis	23
Introduction	23
Objective of Noise Spectra Computation	23
Noise Data Presentation	24
Noise Data Results	24
Discussion	38
Event Location Analysis	39
Introduction	39
Calibration of Travel Times for P and S Waves	39
Event Analysis	45
Discussion	50
Comparison of the Attributes of Each of the Candidate Sites	51
Attribute Comparison	52
Conclusion	52
References	52
Distribution	53
Appendix A - Sensor Coordinates	A-1
Appendix B - Calibration and Spectral Computation Methods and Results	B-1
Appendix C - Power Spectral Noise Plots	C-1
Appendix D - Event Tables	D-1

List of Figures

	<u>Page</u>
Figure 1	Location Map of Survey Areas 3
Figure 2a	Geologic Map of Survey Areas 4
Figure 2b	Legend for Figure 2a 5
Figure 3a	Geologic Map of Site 1 6
Figure 3b	Legend for Figure 3a 7
Figure 4	Landsat Image of Site 1 8
Figure 5	Topographic Map of Site 1 9
Figure 6	View of Site 1 10
Figure 7	Geologic Map of Site 2 11
Figure 8	Landsat Image of Site 2 12
Figure 9	Topographic Map of Site 2 13
Figure 10	View of Site 2 14
Figure 11a	Geologic Map of Site 3 15
Figure 11b	Legend for Figure 11a 16
Figure 12	Topographic Map of Site 3 17
Figure 13	High Resolution Topographic Map of Site 3 18
Figure 14	Landsat Image of Site 3 19
Figure 15	Site 3 Spot Image 20
Figure 16	View of Site 3 21
Figure 17	Location of Mine in Relation to Site 3 22
Figure 18	Daytime Power Spectral Density for Site 1 25
Figure 19	Daytime Power Spectral Density for Site 2 26
Figure 20	Daytime Power Spectral Density for Site 3 27
Figure 21	Daytime Power Spectral Density for Midelt Vault 28
Figure 22	Daytime Power Spectral Density Comparison All Sites 29
Figure 23	Nighttime Power Spectral Density Comparison All Sites 30
Figure 24	Power Spectral Density Comparison for Site 3 Mine Shots 31
Figure 25	Summary Noise Values at 1 Hz 35
Figure 26	Summary Noise Values at 6 Hz 36
Figure 27	Weekend and Weekday Nighttime Noise Values at 1 Hz 37
Figure 28	Morocco P-wave Model 43
Figure 29	Morocco S-wave Model 44
Figure 30	Site 1 Recorded Event Locations 45
Figure 31	Site 2 Recorded Event Locations 46
Figure 32	Site 3 Recorded Event Locations 47

Figure 33	MDT Recorded Event Locations	48
Figure 34	All Recorded Event Locations	49

List of Tables

	<u>Page</u>
Table 1 Daytime Noise Values (All Sites)	32
Table 2 Nighttime Noise Values (All Sites)	33
Table 3 Summary Table of Daily Averages	34
Table 4 Recording Times and Duration at Sites	39
Table 5 List of Reference Events in Morocco During Survey	40
Table 6 P- and S-Wave Reference Event Travel Time Data	41
Table 7 Site Comparisons	51

Acknowledgments

This report presents information gathered and provided by a number of people from both the Centre National Pour La Recherche Scientifique Et Technique Laboratoire De Geophysique (CNRST) of Morocco and the Air Force Technical Applications Center (AFTAC) of the United States of America. We would like to acknowledge the many contributions from the staff of the CNRST under the direction of Dr. Aomar Iben Brahim, without which the survey would not have been possible. Principal researchers assisting in the field survey included Dr. El Mouraouah Azelarab, Birouk Abdelouahad, and Kasmi Mohamed. The technicians were Amedou Mohamed and Zouhri Hamid. We had three drivers, as well: Dahou Hassan, Kamal Hassan, and Tazrouti Driss. The authors would like to thank Mr. Tony Calenda and Mr. Doug Dale of AFTAC for their technical support preparing the equipment for the survey. Dr. Nazieh Yacoub and Mr. Jon Creasey of AFTAC provided software and helped with the travel time analysis. In addition, the authors would like to thank Mr. Peter Chisolm of the U.S. Embassy in Rabat, Morocco, for all his support in making the survey a success.

Introduction

The Air Force Technical Applications Center (AFTAC), in cooperation with the Centre National Pour La Recherche Scientifique et Technique Laboratoire De Geophysique (CNRST), recently investigated potential seismic array sites in Morocco. Three potential sites were identified and investigated to determine which was the most viable. This report describes the site investigation process and summarizes the results of the site surveys.

Site Survey Format.

The site survey format in this report includes:

- Area map showing survey station sites
- General description of site and surrounding area
 - Site description
 - Site geology
 - Noise spectra
 - Noise and event data
 - Topographic map showing coordinates and elevation
- Accessibility
- Power availability
- Communications availability
- Site comparison tables

Site Selection Criteria.

Several criteria are used in the site selection process. Information related to these criteria are addressed in this report. The criteria are:

- Lowest seismic noise level
- Highest signal-to-noise ratio
- Competent rock for seismometer emplacement
- Suitable topography for line-of-sight radio telemetry
- Physical accessibility via existing roads
- Power/communications availability
- Logistical supportability

Site Selection Process.

The basic steps for site selection are:

- Conduct literature study to select candidate locations for site surveys
- Conduct field survey at each candidate location and collect seismic noise data
- Compile and evaluate all data

The site investigation for the Moroccan seismic array followed this process.

Pre-Survey Studies

The initial step in selecting candidate sites was to gather available information on the area, including topography, geology, climate, and other characteristics which are considered in the site selection process. Geologic and topographic maps were obtained for several areas and were used to identify potential array locations. In this initial search, the main consideration focused on identifying sites with a high probability of finding granite at the surface for adequate sensor coupling and regional signal detection. In addition, the topography of the site had to facilitate line-of-sight radio communications within a 4-kilometer array aperture. Fourteen sites were initially selected for the investigation throughout northern and central Morocco. Eleven sites were eliminated because they were too close to a sea coast, too small to support an array, or had too much relief. The following paragraphs provide descriptions of the tectonic setting, geology, and cultural activities found in the areas of the three remaining sites.

Appendix A provides pre-survey material consisting of maps and imagery.

General Location Map of the Survey Areas.

The general survey areas are shown on the Morocco country map indicated by green circles in Figure 1 below. Site 1 is located about 60 kilometers (km) southwest of the town of Oujda and about 80 km south of the Mediterranean Sea coast. Site 2 is located about 50 km west of the town of Midelt between the High Atlas Mountains to the north and the Middle Atlas Mountains to the south. Site 3 is located south of the High Atlas Mountains about 30 km south of the town of Tinerhir. Paved all-weather highways connect most major towns throughout the country. The roads into the survey areas are either gravel or unimproved dirt.

Location Map of Survey Areas



Figure 1. Political map of Morocco with the general areas of investigation circled.

General Geologic Map of Survey Areas.

On the geologic map shown (Figure 2) are outlined the boundary areas of the three sites identified for additional investigation. Each of these sites will now be described in more detail.

Geologic Map of Survey Areas



Figure 2a. Geology map of Morocco indicating locations of the three sites. Granitic rocks are denoted as solid red. Green circles show survey areas.

CARTE GÉNÉRALE QUATERNAIRE ET TERTIAIRE



Figure 2b. Legend for Figure 2b.

Site 1 (Oujda) Description.

Geology Summary. This area has a small granitic intrusive. A portion of a geologic map of this area follows Site 1 survey area is circled in black.

Geologic Map of Site 1

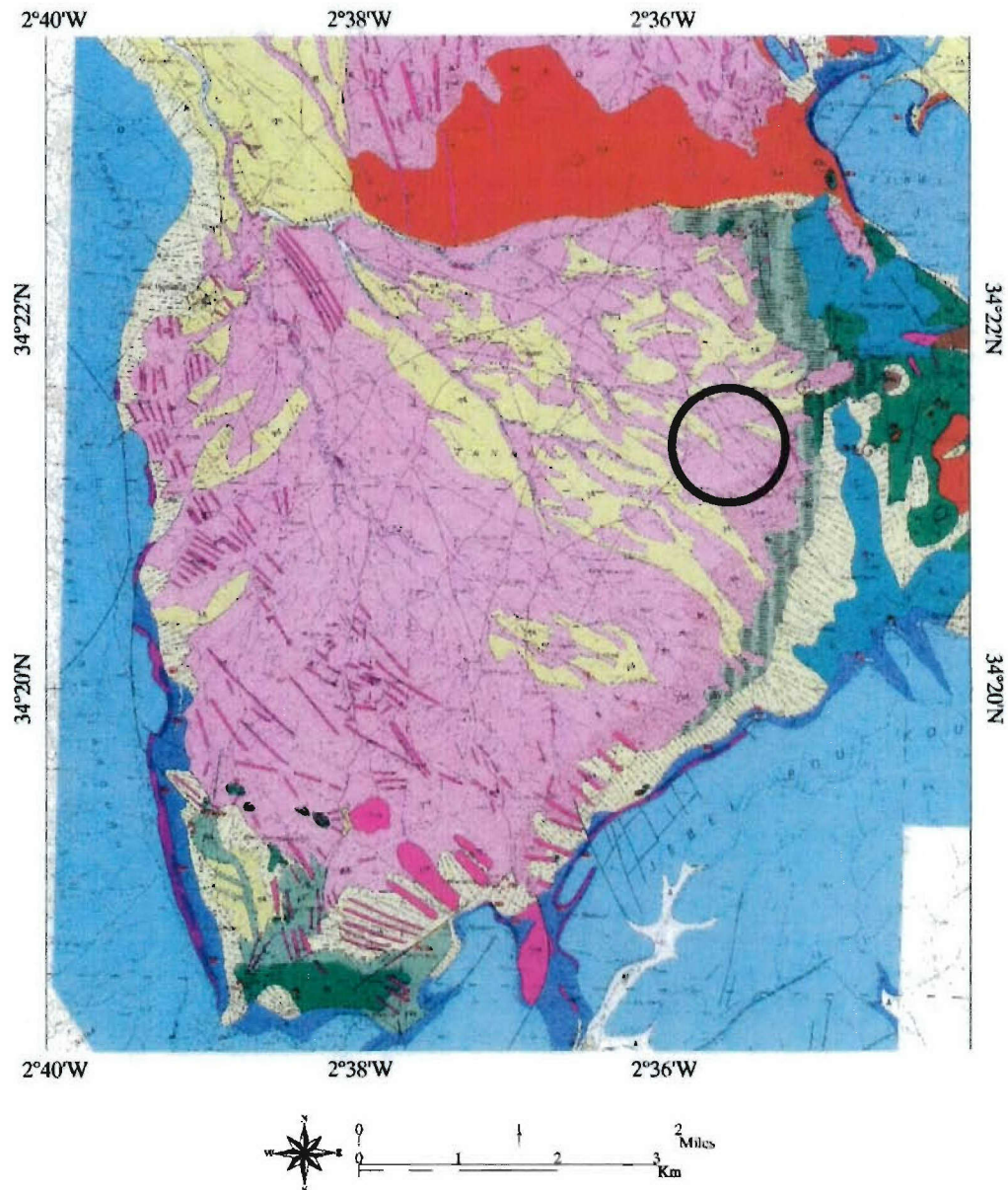


Figure 3a. Location of the granitic intrusive for Site 1.

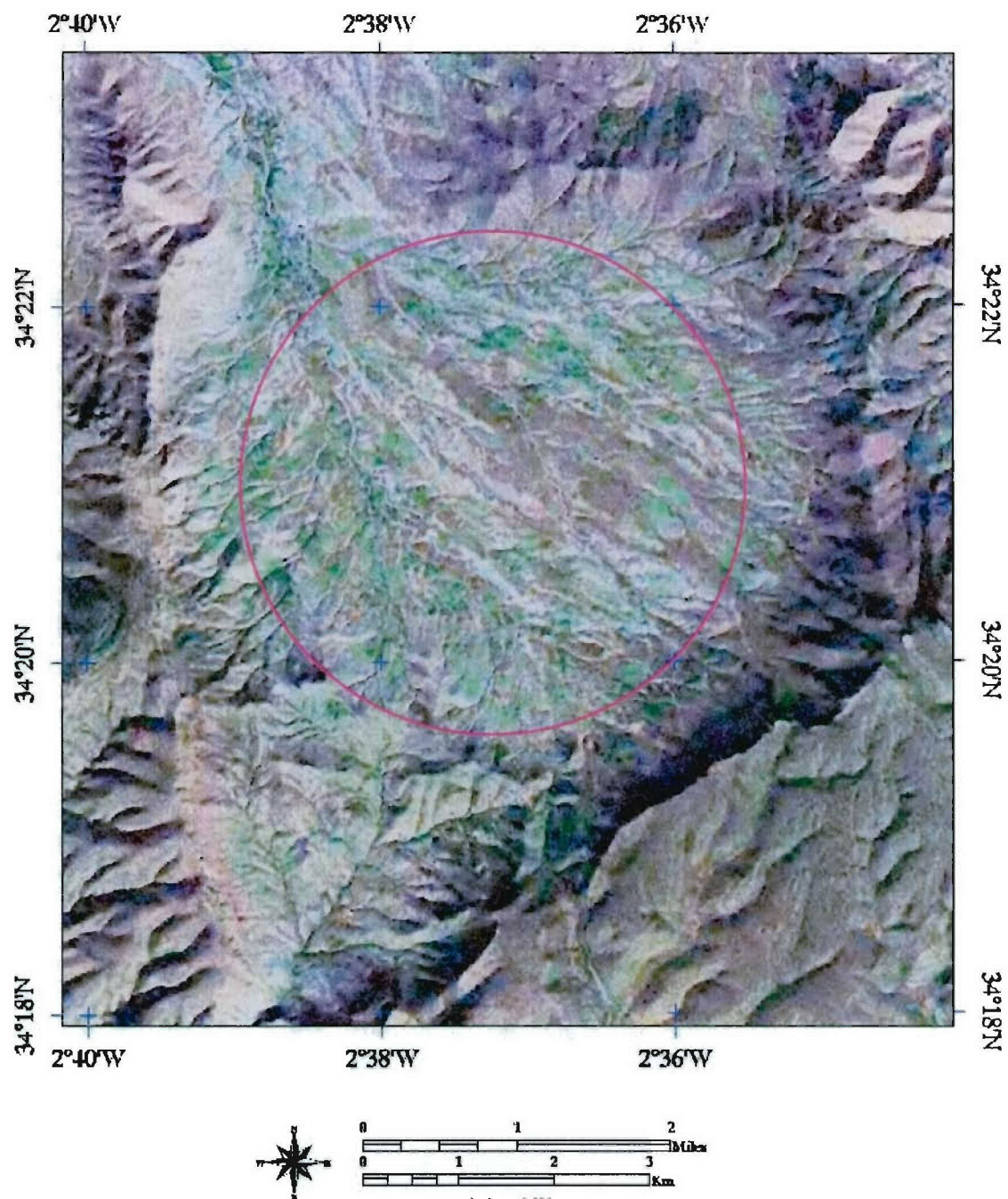


Figure 4. Landsat image of the area proposed for Site 1. Note the rough topography outside of the immediate area.

Noise Survey. Noise data were collected from a 5-sensor circular array with a diameter of approximately 1 km. See Appendix A, Sensor Coordinates, for the sensor locations. We used the highest hill in the middle of our 5-sensor array for our intrasite communications due to the many depressions and creek beds found in this rough terrain.

Topographic Map of Site 1

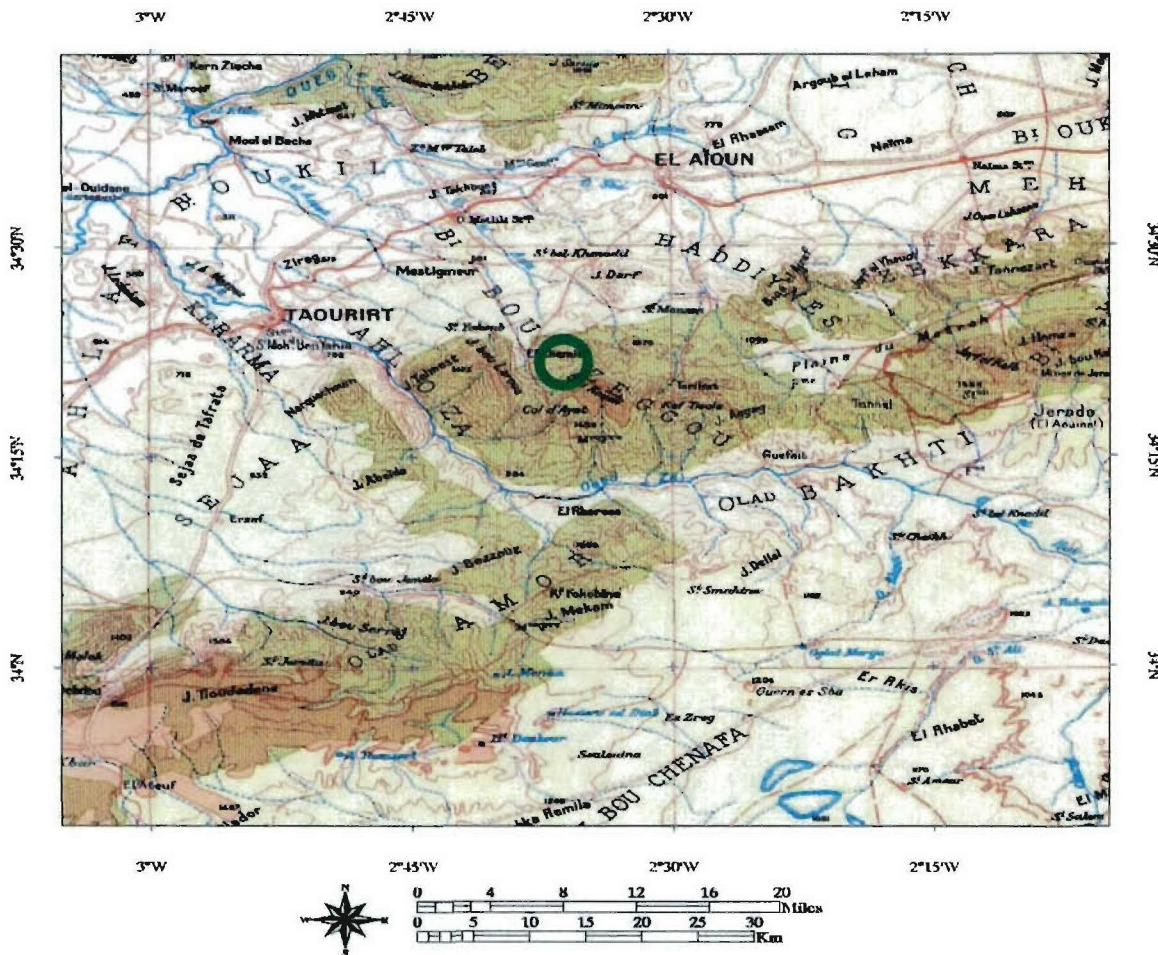


Figure 5. Map of Site 1 survey area. Site 1 is of low-to-moderate relief and is dissected by several small river valleys. An unimproved dirt road leads from the town of Tanacherfi east into Site 1.

Cultural Noise Sources. This is mainly an agricultural area used for farming and grazing. There are several wells in the area which use gasoline-powered pumps to irrigate the fields. There are dirt roads throughout the area and paved roads to the west and north of the site. Traffic appears to be light. No heavy industry or power generation exists in this area. About 15 km south of the site, the Moulouya River is dammed by a 100-meter dam. No hydroelectric power is generated by this dam. Dozens of daily explosions were noted in the analysis, coming from the east.

View of Site 1



Figure 6. Photo of Site 1 survey area.

Accessibility. Access to the survey area is via paved road to the town of Tanacherfi, and through the center of the proposed array area. Dirt roads lead off of this paved road into other locations in the proposed array area.

Communications Consideration. A microwave link was noted in the town, and a nearby high mountain top had an army communications center and a television transmission tower.

Power. Commercial power is available approximately 2 km from site.

Land Owner. The land is community/township owned.

Site 2 (Midelt) Description.

Geology Summary. The area of Site 2 has a small granitic intrusive, surrounded by sedimentary rocks. The granitic rocks are exposed at the surface with, at most, several meters thickness of the sedimentary rocks on top.

Geologic Map of Site 2

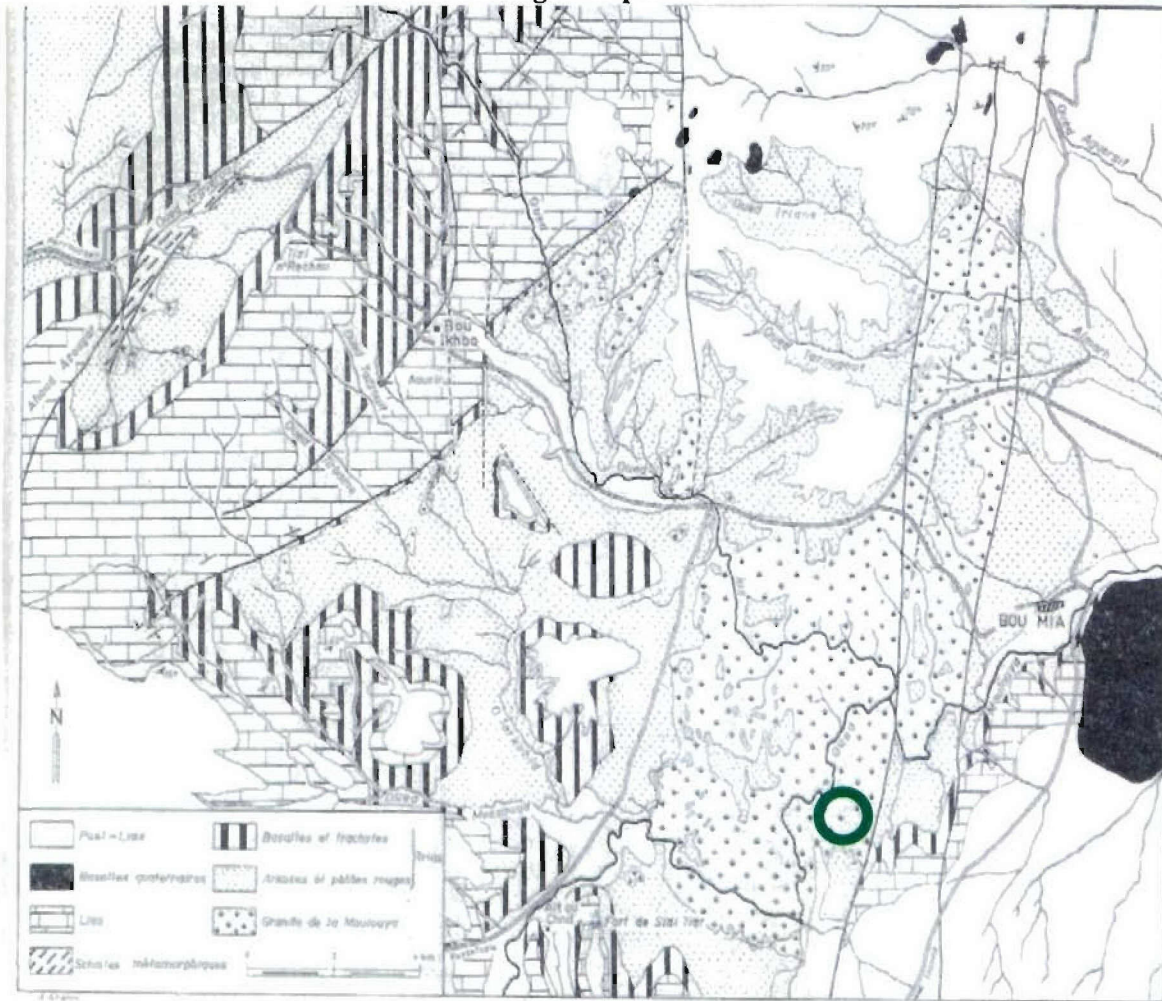


Figure 7. Location of the survey area for Site 2.

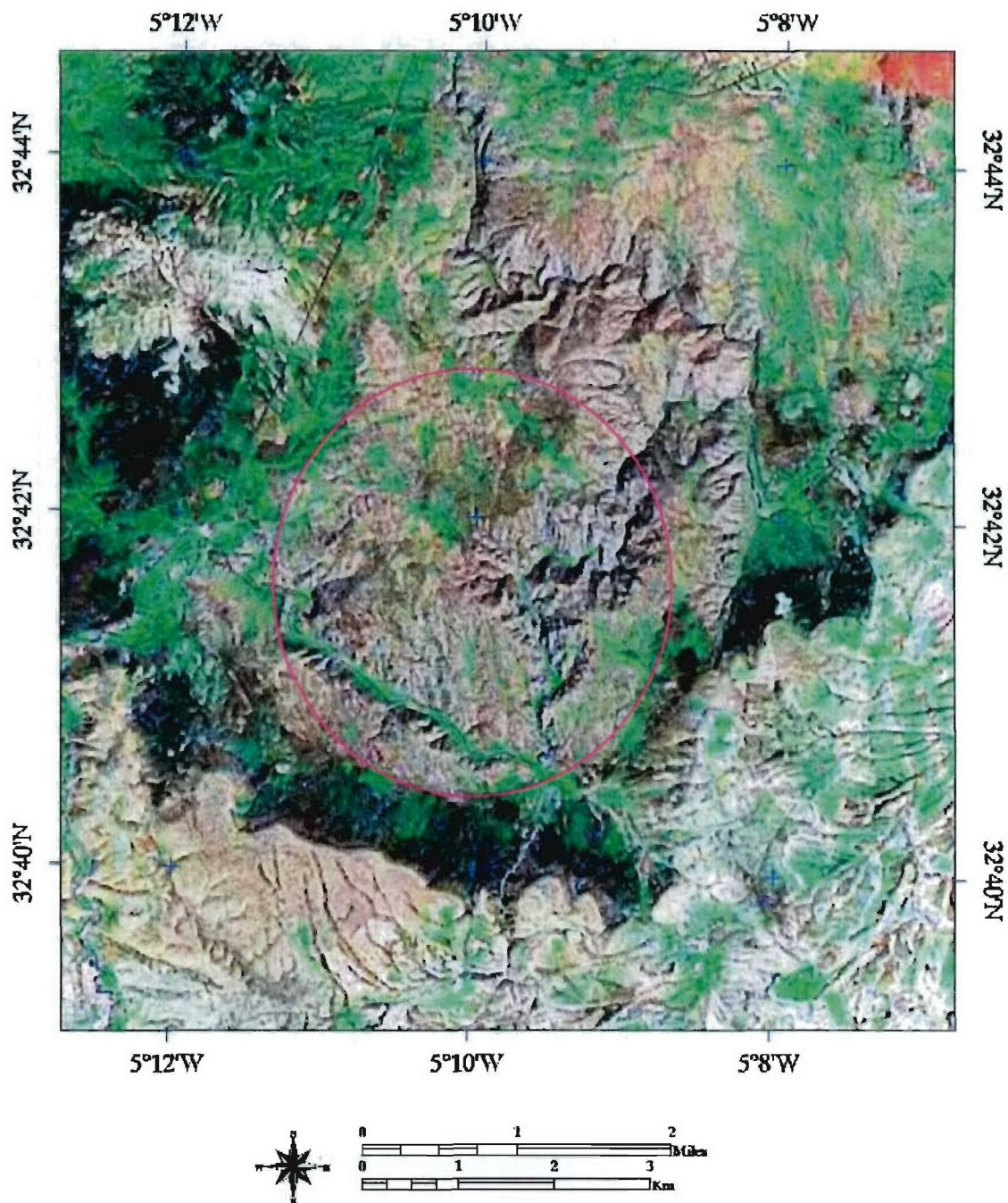


Figure 8. Landsat image of granite for Site 2 with a 4 km array superimposed. Note that the plateau is deeply dissected, and a highway runs along the north and west perimeters.

Noise Survey. Noise data were collected from a 3-sensor triangular array with a diameter of approximately 0.5 km. The array consisted of two Guralp ESPDs and one GS13. See Appendix A, Sensor Coordinates, for the sensor locations. Additional data were collected in the Midelt vault (MDT) located 46 km to the east, and used both for comparison to this site and in the event location procedures.

Topographic Map of Site 2

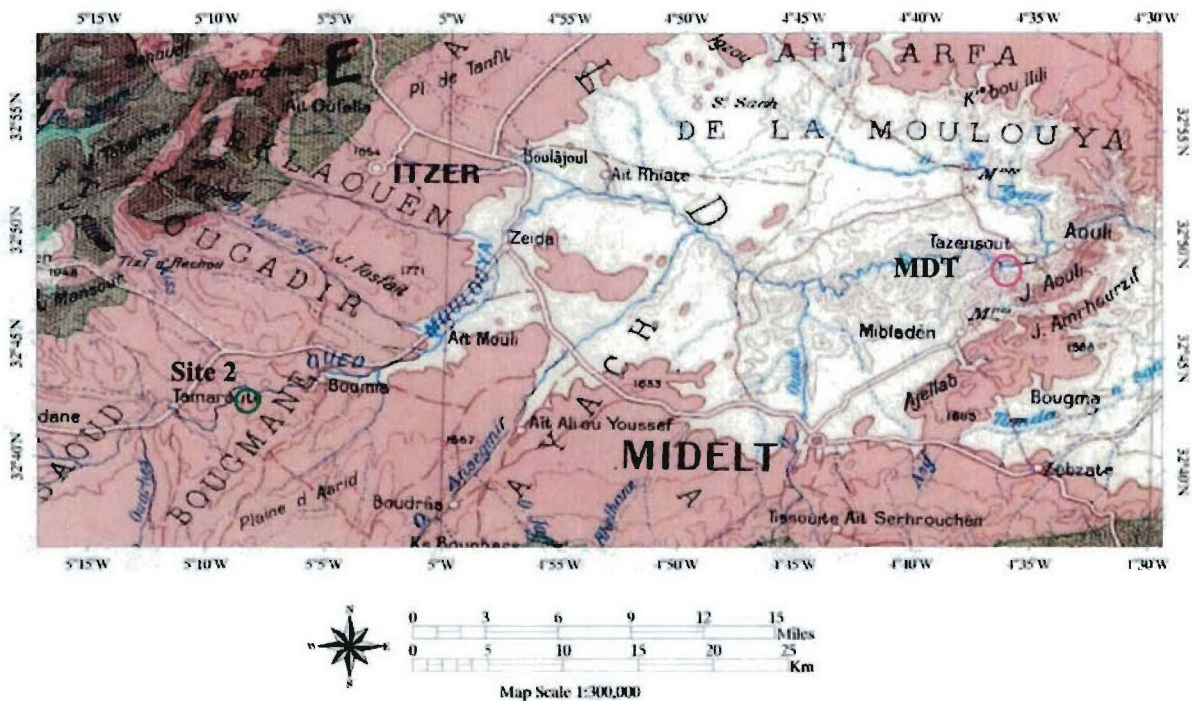


Figure 9. Site 2 data collection area. Approximate location of Site 2 survey area denoted by green circle. The site is located on a plateau of moderate relief which is dissected by a small river. The station MDT is located northeast of Mibladen along the Moulouya River and shown with a magenta circle.

Cultural Noise Sources. The area is surrounded by paved roads; however, the traffic is generally light and consists primarily of farm vehicles, light trucks, and automobiles. A high voltage transmission line with towers is on the northern half of the site. Drilling of a deep well was noted about 15 km from the site, and others may exist in the area for farming. The area near the site is mainly an agricultural area; however, there are many abandoned galena mines, some of which only appear to be recently abandoned. The prospects of reactivation appear low according to our host. Interestingly, the seismic noise data indicated a large difference in the background noise between the weekday and weekend for this site (see the accompanying noise section). In addition, the station MDT had a much lower background noise level overall. The source of this increased seismic noise is obviously due to cultural activities which were never identified as coming from the immediate vicinity of Boumia. Boumia is mainly a small village supporting agricultural activity in the surrounding countryside, with no heavy industry noted. A dam 150 meters tall is being constructed about 35 kilometers to the east along the Moulouya River. This dam is too far away to be of consequential significance with respect to the seismic noise level.

View of Site 2



Figure 10. View of Site 2, showing a typical sensor emplacement. Note the rolling topography on the plateau. However, looks are deceiving as the plateau is deeply dissected by stream beds running through this site as seen from the Landsat imagery in the map appendix.

Accessibility. Paved roads surround the perimeter of the proposed site on all sides, with the last 3 km of the survey area accessible by a dirt farm road.

Communications Consideration. A microwave communications tower was also noted on a nearby hill north of Boumia on the northern portion of the granite and another in the village of Boumia.

Power. Commercial power is available approximately 5 km from the survey site, with power lines noted parallel to the paved farm roads surrounding the site.

Land Owner. The land is state-owned.

Site 3 (Tinerhir) Description.

Geology Summary. This area has a very large Precambrian granitic intrusive, surrounded by volcanic extrusive rocks. In the actual proposed location of the array, there is a thick Quaternary layer of sediments whose depth was not determined, but could be as much as 100 meters thick in places based on the amount of sediment noted being delivered to the valley and the lack of outcrops. See the following photograph of the geologic map.

Geologic Map of Site 3

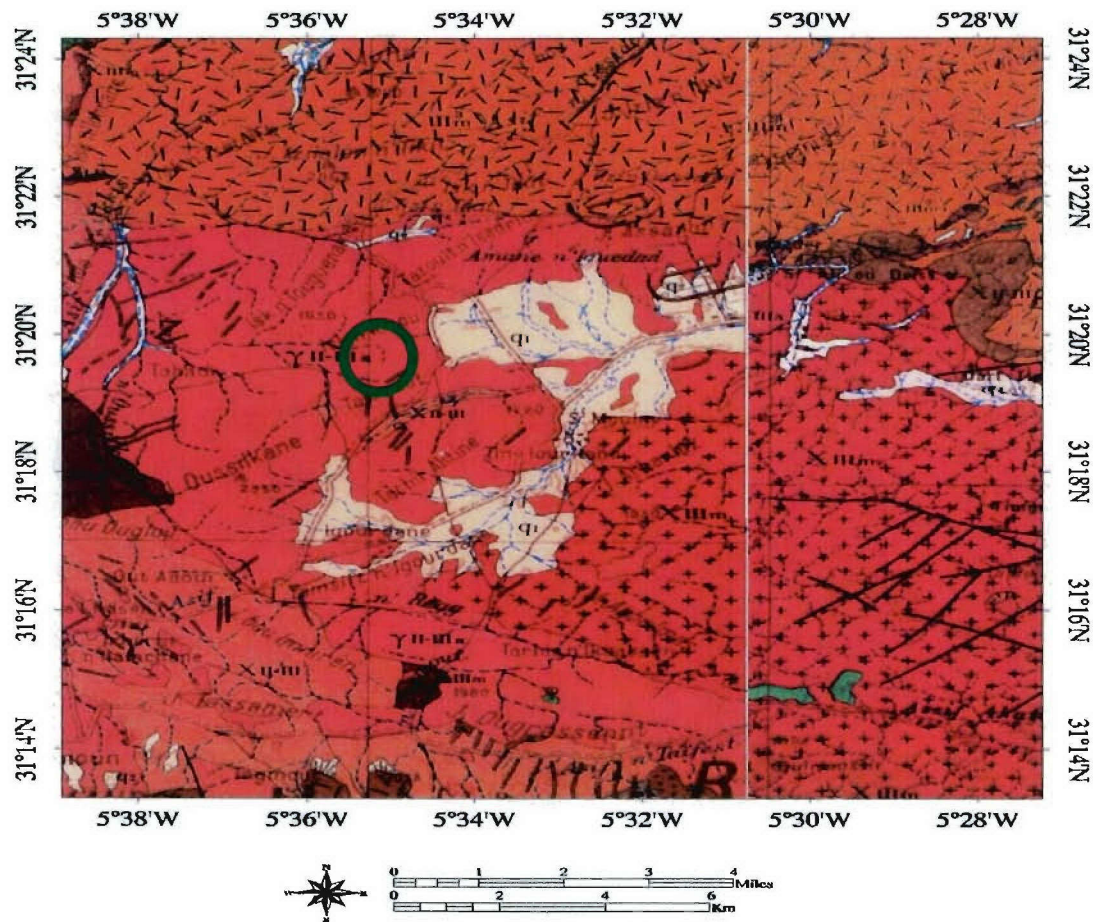


Figure 11a. Geological map of Site 3 granitic intrusive. Approximate location of Site 3 survey denoted by green circle. The granite appears to be a few meters below the surface in most places.

PRÉCAMBRIEN III MOYEN X_{III_m}

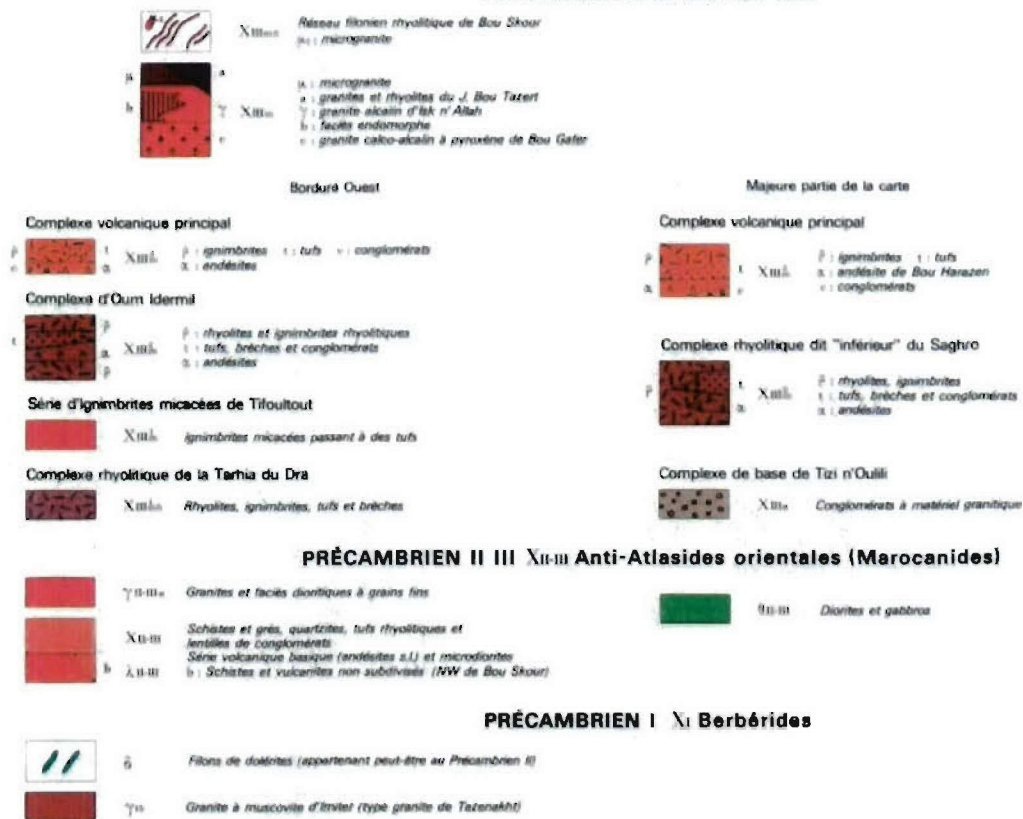
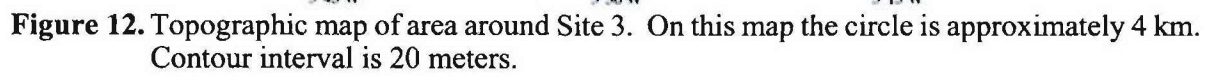


Figure 11b. Geology key to Figure 11a.

6°W 5°45'W 5°30'W 5°15'W



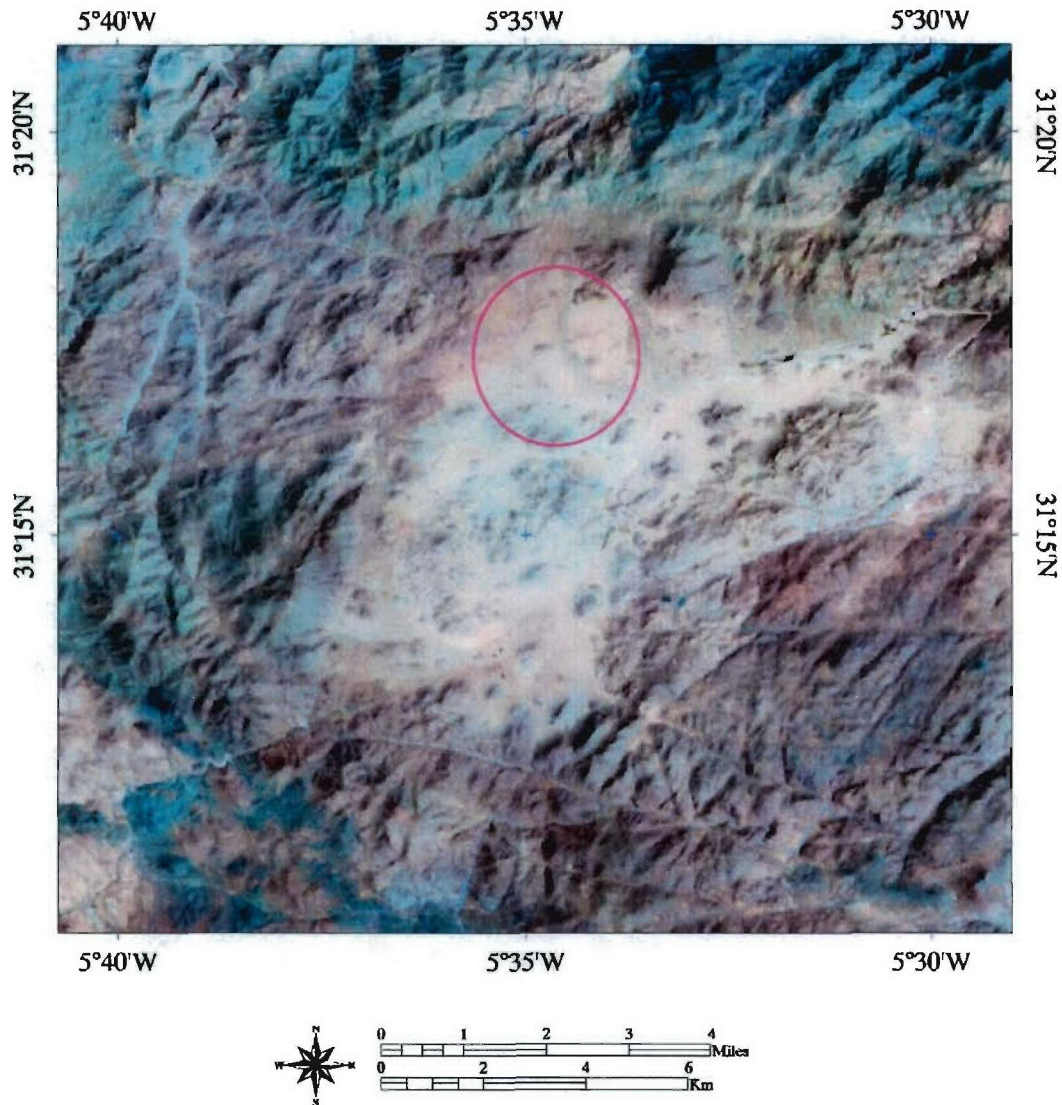


Figure 14. Landsat image of the Site 3 area as indicated in the geologic map. Note that the volcanics tend to have a bluish color tint while the granite is more reddish. One can clearly trace the granite/volcanic boundary in this photograph. The mountains in the lower right of the photograph, although in granite, are deeply dissected with 300-meter canyons, making location of the array in the mountains impossible. The only feasible area is that outlined by the circle.

Site 3 Spot Image

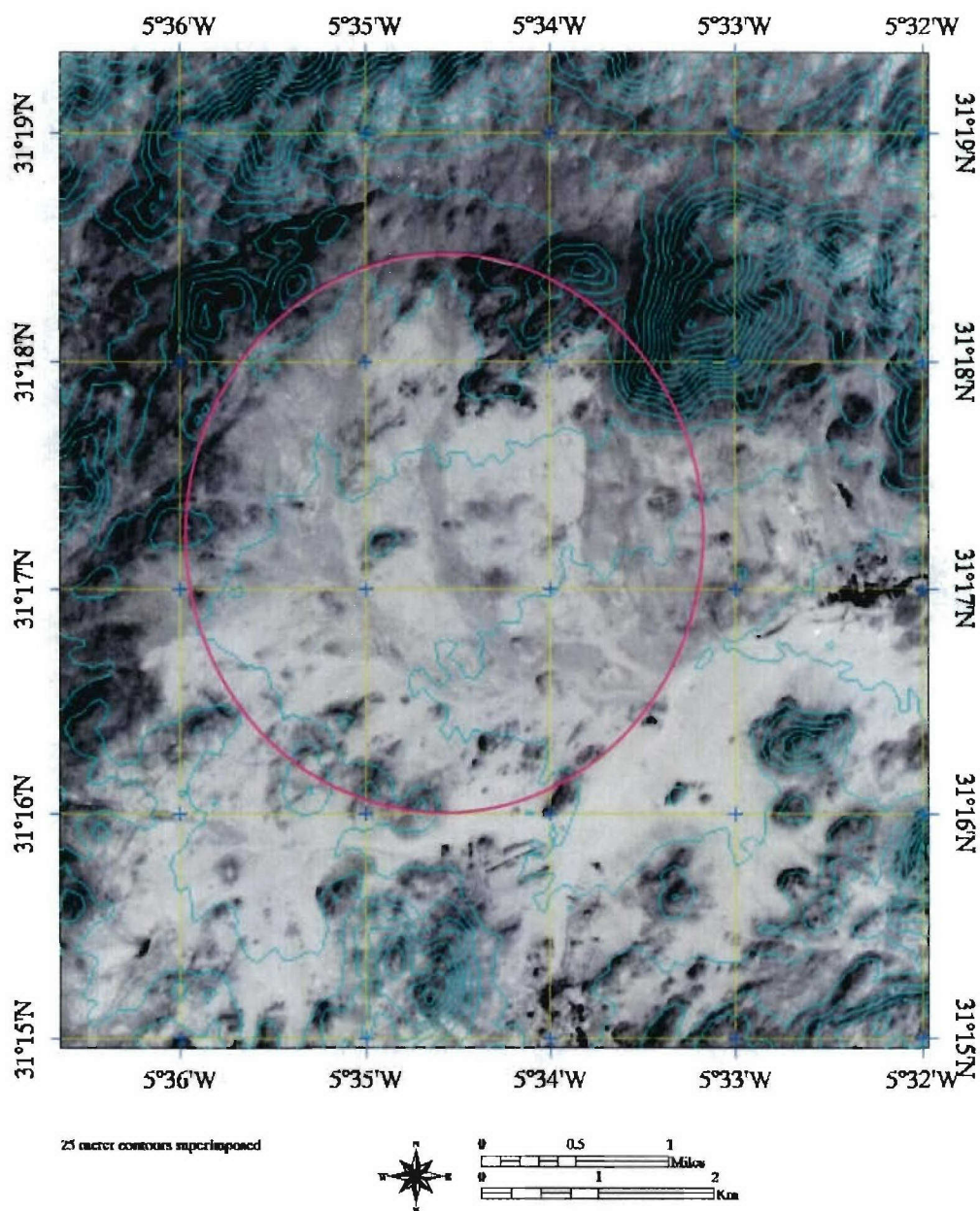


Figure 15. Spot image of Site 3 proposed array location with 25-meter contours superimposed. Proposed center is at approximately 31° 17' 19" N and 5° 34' 47" W. We would have a straight line-of-sight to all locations from the hill left of center with one contour line superimposed, without the use of repeaters. Note we are also outside the cultivated area.

Noise Survey. Noise data were collected from a 6-sensor circular array with a diameter of approximately 1 km. See Appendix A, Sensor Coordinates, for the sensor locations. In addition, a single short-period GS13 sensor was deployed in the center of the array. Data were collected for 6 days.

View of Site 3



Figure 16. View of Site 3, showing the levelness of the valley floor, and potentially thick sediments. This observation point is clearly shown on the Spot image (Figure 15) and is recommended for the approximate array center and communications collection point.

Cultural Noise Sources. This site is mainly an agricultural area used for grazing. Small explosions were detected from a mine/quarry located approximately 15 km to the northwest. The position of this quarry with respect to the array location is shown in Figure 17.

Accessibility. The area is accessible by dirt road.

Communications Consideration. No communications towers were noted in the area. Data may have to be transmitted by satellite from this location, due to its remoteness.

Power. No commercial power is available on-site. The closest location of a step-down transformer noted is in the village of Iknioul, which is 20 km away from the proposed site. It was observed, however, that the villagers in the adjacent town several kilometers away from the proposed array location had electric power. The villagers said the power was part of a separate cooperative from the main Moroccan power grid, and that the power was reliable.

Land Owner. The land is state-owned.

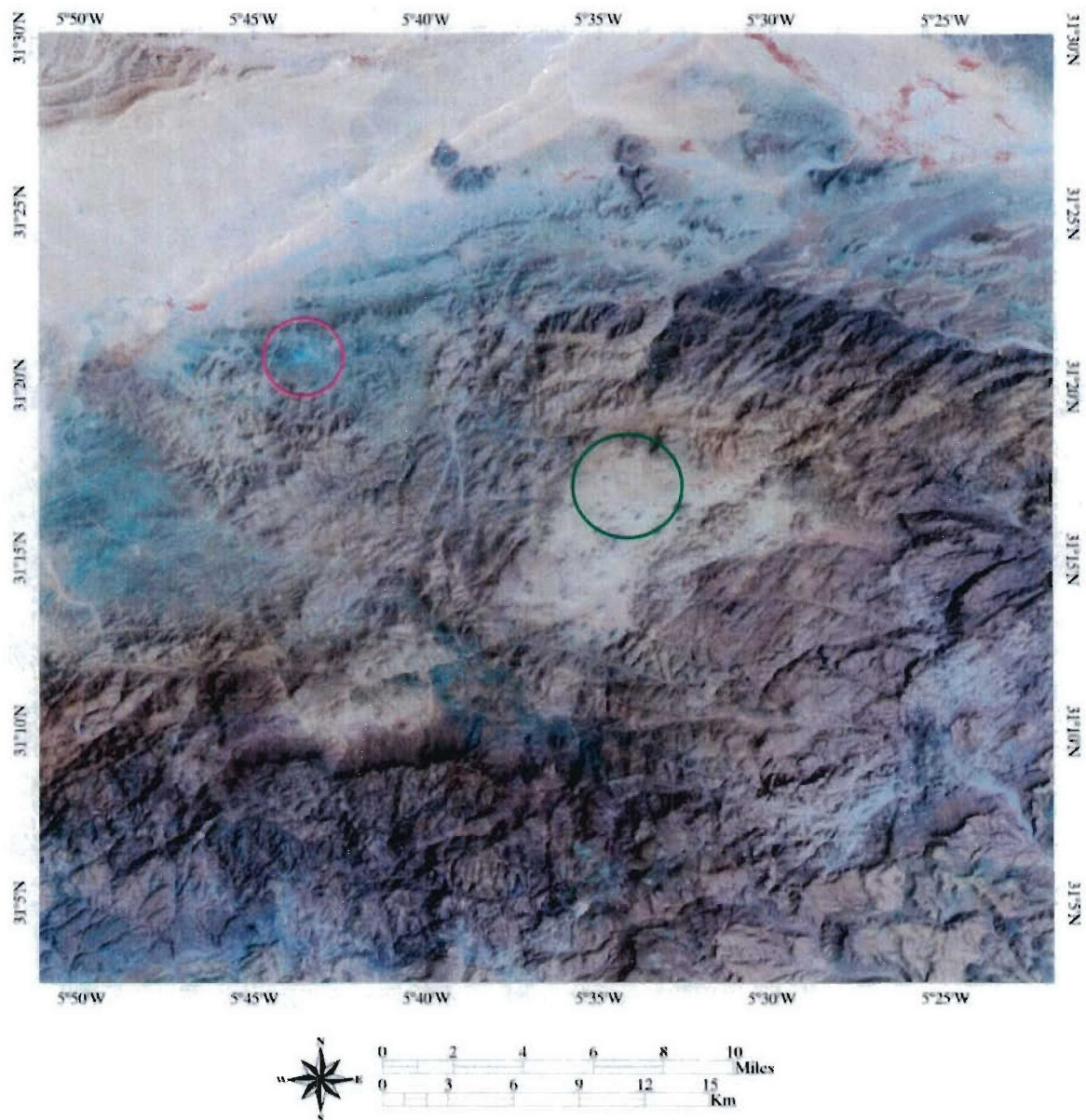


Figure 17. Location of mine is at $31^{\circ} 21' N$ and $5^{\circ} 44' W$, about 14 km from the proposed array location at $31^{\circ} 17' 19'' N$ and $5^{\circ} 34' 47'' W$. The mine has a blueish tint to it, and has a magenta circle surrounding it. The array location is indicated by a green circle. The rocks to the east and southeast are still in the granite body but are too highly dissected with canyons, several hundred meters deep, for easy array emplacement. The rocks at about the 4 o'clock position on the green circle have 300 meters relief, which is difficult to see at this scale.

Noise Spectra Analysis

Introduction.

Seismic data were collected at each survey location and the Midelt (station MDT) vault. For Site 1, the instruments consisted of five 3-component broadband Guralp sensors. At Site 2, the data were collected using two vertical broadband Guralp sensors and one short-period Geotech GS13. A full array of five Guralp sensors was intended for Site 2, but due to difficulties operating the equipment, only two of the Guralps provided data. At the Midelt vault, located in a horizontal mine shaft 100 meters inside a mountain with 100 meters of overburden, we set up three GS13s and a Reftek 130 digitizer/data recorder. At Site 3, we collected data from six broadband Guralp sensors, and a GS13 connected to a Reftek 130. The Guralps were connected to a radio network and data were forwarded to a central collection point. There were frequent dropouts on the Guralp system data. These dropouts complicated the data analysis, but were acceptable since only segments of the data were of interest. For Site 1, only Guralp sensors were used for the noise analysis. At Sites 2 and 3, noise spectra were determined with both the Guralp and Reftek digitizers and seismometer systems. The Guralp seismometer is an active sensor. The GS13 seismometer is a passive sensor, with a large voltage output. The system noise on the Guralps was larger than the background noise above about 7 Hertz (Hz), as can be seen in the spectral plots of Figure 5, Appendix B, comparing the Reftek and Guralp systems. Details of the calibration procedures used are provided in Appendix B, Calibration and Spectral Methods and Results, along with the instrument nominal response curves for phase and amplitude.

Objective of Noise Spectra Computation.

Our objective was to compare noise spectra for day and night, and workday and weekend segments. For Site 1, we compared spectra on Wednesday and Saturday, and for Site 2 on Thursday and Saturday. For Site 3, however, we never managed to obtain a full day of weekend data so, consequently, data on Wednesday and Friday were used. The samples chosen for analysis were 5-minute segments occurring between 0600 and 1800 local time for daytime segments, and segments occurring between 1800 and 0600 local time for nighttime segments. This allowed comparison of background seismic noise between systems for both day and night conditions. Noise conditions are generally quieter at night. We would find the quietest 5-minute period in each half hour block of data for the noise spectra computation. An appropriate data waveform segment for noise analysis is background noise containing no seismic events, no spikes or gaps due to an error in data transmission, and without clipping. After the appropriate data waveforms were selected, the mean and linear trend were removed from the data waveform. The power spectra were produced by auto-correlating the waveform segment using overlapping windows. The windows were formed using a Hanning window function, with an overlap of 50%. The auto-correlation was averaged over the number of windows used, the discrete Fourier transform was taken to produce the power spectral density, and the instrument frequency response was removed from the power spectra by the process of deconvolution. For each 300-second (5-minute) waveform segment, representing 12,000 points at a sampling rate of 40 samples per second, a total of 30 15-second (600-point) windows were used. The spectra were then stacked to determine mean values and standard deviations.

Noise Data Presentation.

Data are reported in a series of tables presented here at 1 and 6 Hertz, and representative power spectra are displayed for each site. The complete series of power spectra measured are shown in the Power Spectral Noise Plots, Appendix C. In addition, the actual spectra themselves show the characteristics of the noise over the entire frequency band of interest. Interesting features, such as spectral lines or peaks, show up and are generally due to man-made causes such as rock crushers, pumps, generators, and other cyclic sources of cultural noise. In addition, one can determine in which part of the frequency band the array will perform best. Three standard deviations are also shown on the plots from which the variability of the noise can be determined, along with the models for the Peterson New Low Noise and High Noise models (Jon Peterson, 1993). These Peterson models are an aggregate taken from a number of stations representing the lowest and highest noise measured at existing stations.

Noise Data Results.

The objective is to obtain a site with as low a noise value as possible. Generally speaking, sites more distant from the coast will have a lower noise value than those near a coastline. We have found from other site surveys that the coastal effect can be observed hundreds of kilometers inland. Another factor is the rock impedance (density times P-wave velocity). The contrast between high impedance intrusive rocks and lower impedance weathered country rocks naturally rejects horizontally arriving energy from nearby sources of noise while allowing for more vertically arriving energy from more distant sources. Thus, seismic observations made on high impedance granitic intrusives have consistently resulted in (1) lower overall noise and (2) higher signal-to-noise ratios, with higher density rocks performing better than low density rocks. There is also some indication that low density overburden on top of the high density rock will trap the wind noise (Young et al., 1996). For these reasons, we generally seek intrusive rock formations as far as possible from a coastline in areas of low cultural activity. If possible, boreholes are located in areas with some overburden. The spectral noise results, we will now show, support these generalities in Morocco.

A typical spectral curve for each site investigated is shown in Figures 18-21. These are plots of the displacement power as a function of frequency.

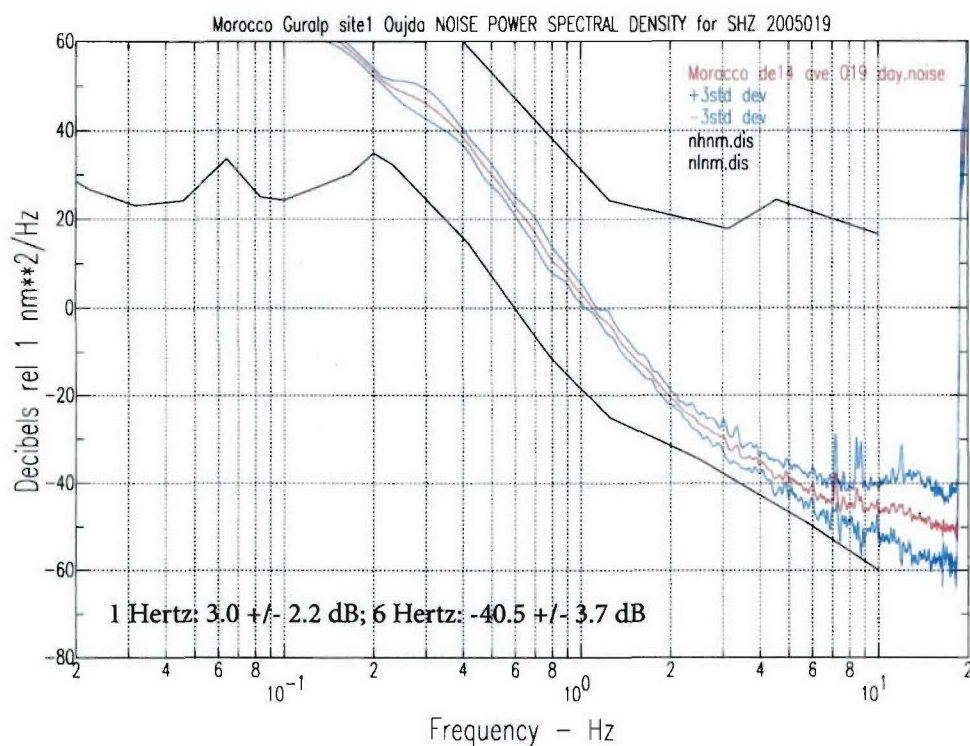


Figure 18. Daytime Power Spectral Density for Site 1. These data were computed on background noise segments with no regional events observed in the time domain traces. Note that at 1 Hz the power spectral density is above the reference level at 0 decibels (dB). In addition, there are several spectral lines noted here, one at approximately 7 Hz and one at 8.5 Hz. The large jump in the power at approximately 17 Hz is due to the effects of the anti-alias filter not being deconvolved, and is not real. In many cases, we are measuring instrument noise above 7 Hz for the Guralps.

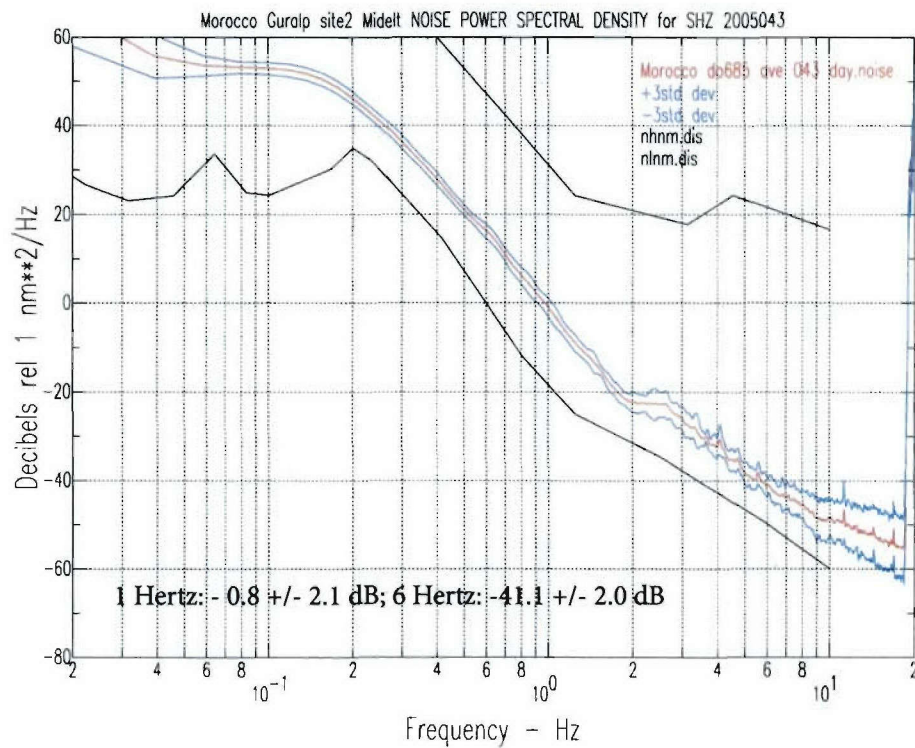


Figure 19. Daytime Power Spectral Density for Site 2. There is less variability for this spectrum, fewer large spectral peaks, and a slightly lower noise value at 1 Hz.

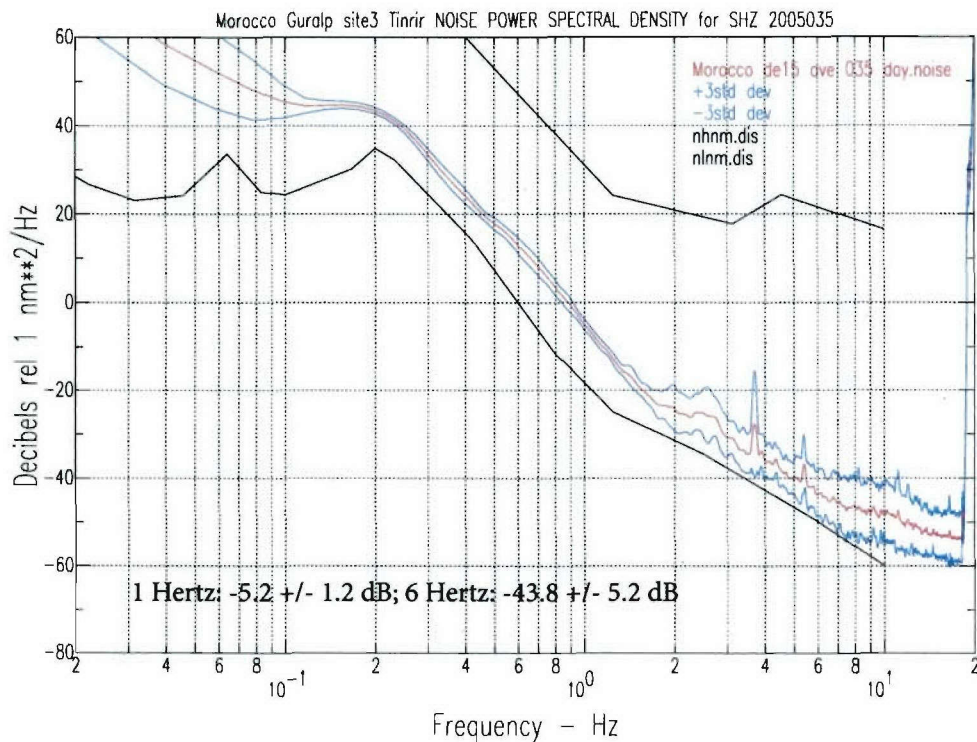


Figure 20. Daytime Power Spectral Density for Site 3. At 1 Hz, the power spectral density is considerably lower than the two previous sites. In addition, the power spectral density is lower for the higher frequencies with the exception of a notable peak at about 3.5 Hz. This peak disappears consistently at night as seen in Figure C-28 in Appendix C, confirming its cultural source.

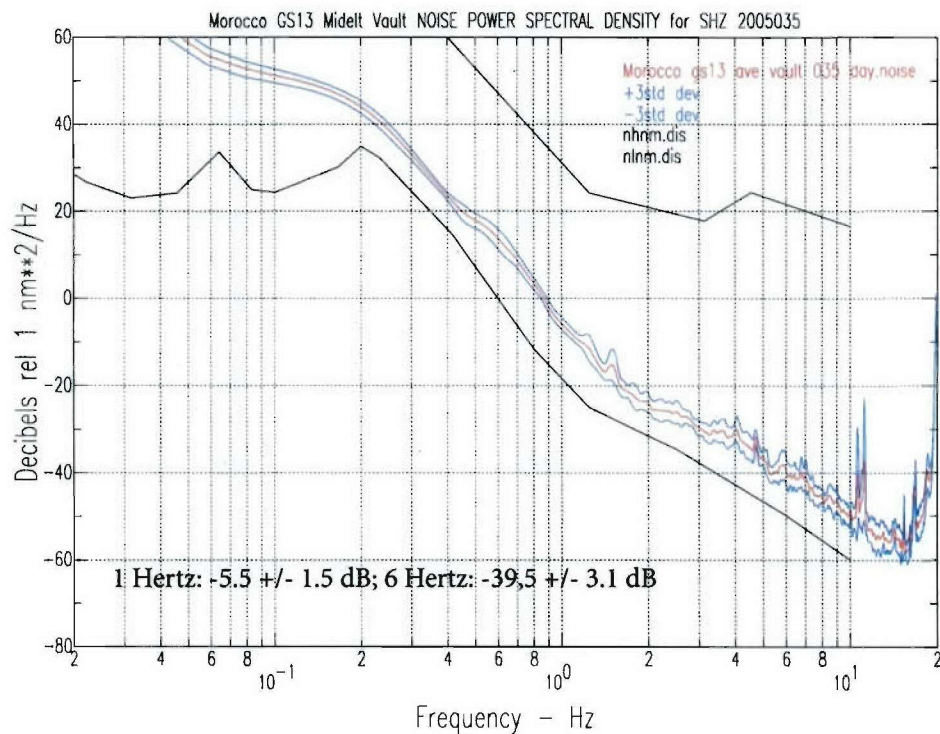


Figure 21. Daytime Power Spectral Density for the Midelt Vault. The power spectral density is comparable at 1 Hz to Site 3. In addition, we do not see the large spectral lines below 10 Hz, although there is a large one above 10 Hz. Also, the standard deviation is low, reflecting the fact that this site is below ground and wind noise attenuated.

We can also superimpose spectra from different sites for comparison. We show this in Figure 22 for daytime values, and in Figure 23 for nighttime values.

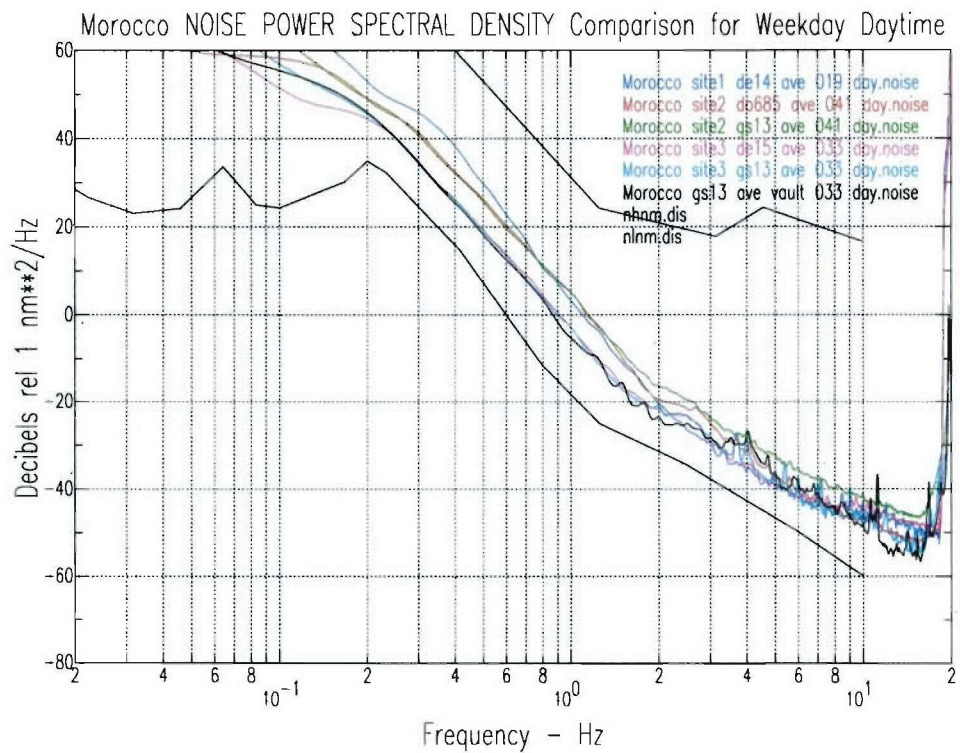


Figure 22. Weekday daytime values plotted for Sites 1, 2 and 3.

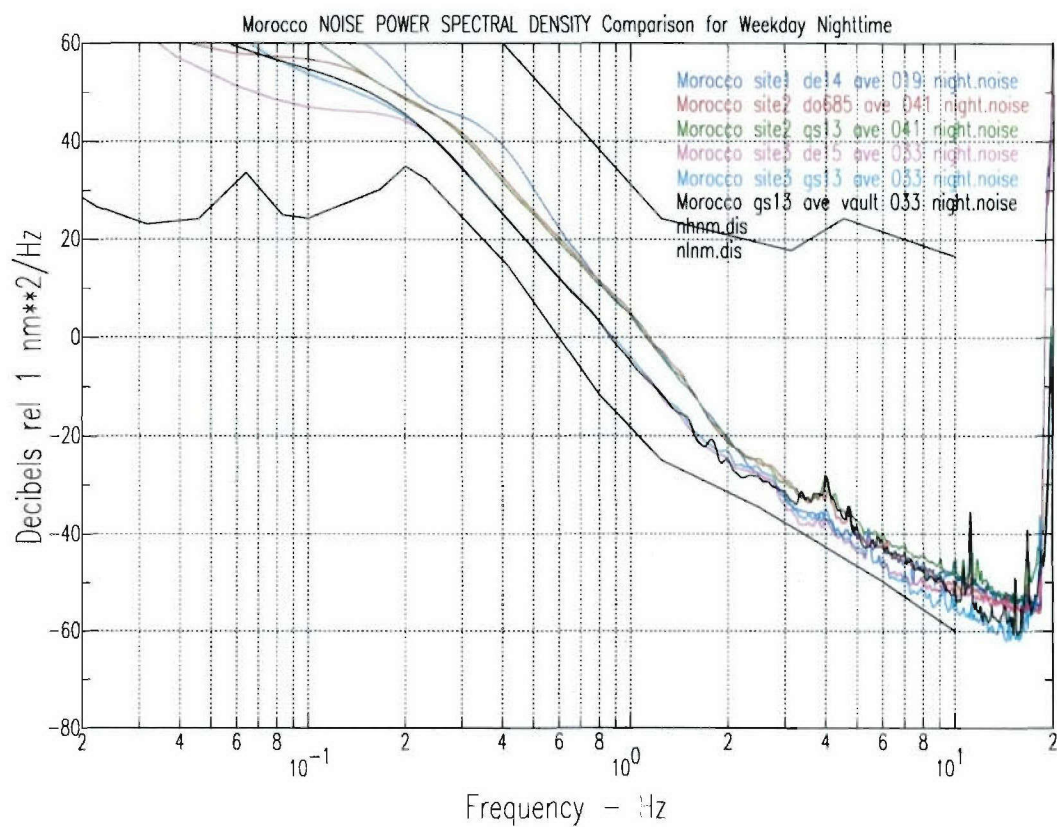


Figure 23. Comparison of power spectral values for weekdays at nighttime.

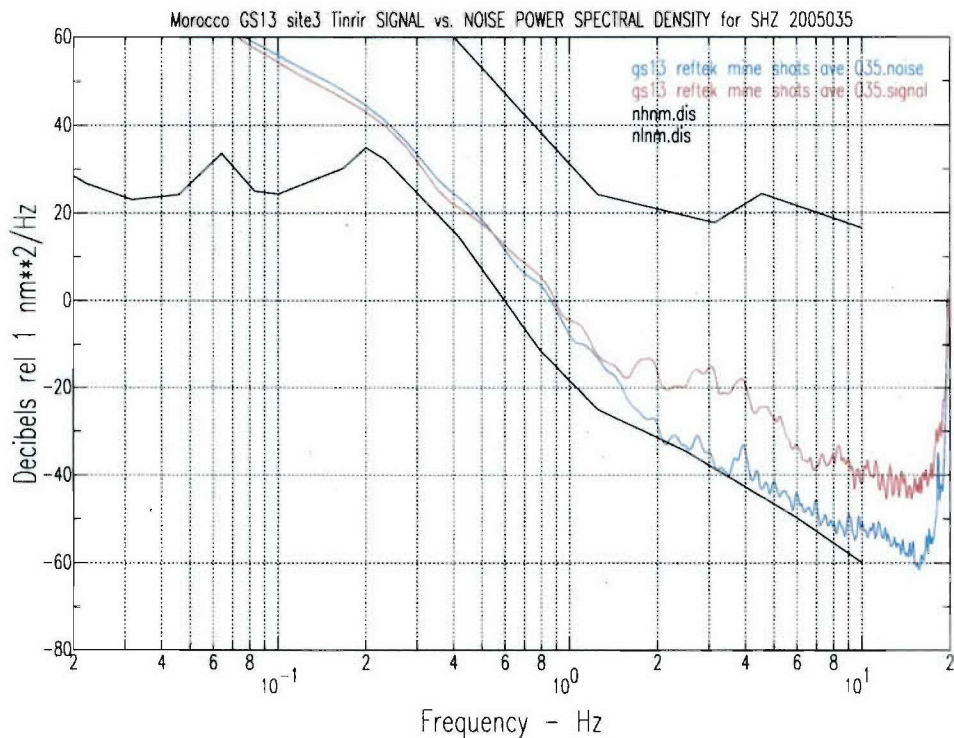


Figure 24. Power spectral density comparison for Site 3 mine blasts. Site 3 has a mine located 14 km to the northwest. At times, explosive shots were seen going through the temporary array from this direction. The spectra of one of these shots is presented in this figure in red, with the background noise in blue. The spectrum is spread out over most of the usable signal band, indicating the impulsive nature of the signals. The impulsive signals have a correlation coefficient of 0.6 across an array distance of 1 km perpendicular to the wavefront. The 4 km array will decorrelate these signals better than the temporary array which has only a 1 km aperture.

The values and averages at 1 and 6 Hz are summarized in Tables 1-3. Following these, some of these values are plotted in Figures 25-27, and a discussion of the observations follows in the next section.

Table 1: Daytime Noise Values (All Sites)

Name	Year / Day of Year	Displ. PSD (dB) rel to 1 nm²/Hz (1 Hz, Daytime)	Standard Deviation (dB) (1 Hz, Daytime)	Displ. PSD (dB) rel to 1 nm²/Hz (6 Hz, Daytime)	Standard Deviation (dB) (6 Hz, Daytime)
NLNM	N/A	-18.0	N/A	-49.8	N/A
NHNM	N/A	32.0	N/A	+21.6	N/A
Guralp site 1	2005019	+3.0	2.6	-40.5	3.7
Guralp site 1	2005023	-4.0	4.8	-39.8	5.8
Average site 1	N/A	-0.5	7.2	-40.1	0.8
MDT vault	2005033	-5.2	1.9	-39.1	3.1
MDT vault	2005035	-5.5	1.5	-39.5	3.1
Average MDT vault	N/A	-5.4	0.3	-39.3	0.5
Reftek site 2	2005041	+4.9	1.1	-35.6	2.7
Guralp site 2	2005041	+5.0	0.7	-39.8	2.6
Reftek site 2	2005043	-1.6	2.7	-37.9	3.6
Guralp site 2	2005043	-0.8	2.1	-41.1	2.0
Average site 2	N/A	+1.9	5.2	-38.6	3.5
Reftek site 3	2005033	-3.1	1.4	-46.1	4.2
Guralp site 3	2005033	-3.1	2.0	-42.5	2.5
Reftek site 3	2005035	-4.8	1.0	-41.3	4.8
Guralp site 3	2005035	-5.2	1.2	-43.8	5.2
Average site 3	N/A	-4.0	1.6	-41.3	3.9

Table 2: Nighttime Noise Values (All Sites)

Name	Year / Day of Year	Displ. PSD (dB) rel to 1 nm²/Hz (1 Hz, Nighttime)	Standard Deviation (dB) (1 Hz, Nighttime)	Displ. PSD (dB) rel to 1 nm²/Hz (6 Hz, Nighttime)	Standard Deviation (dB) (6 Hz, Nighttime)
NLNM	N/A	-18.0	N/A	-49.8	N/A
NHNM	N/A	32.0	N/A	+21.6	N/A
Guralp site 1	2005019	4.7	4.5	-43.1	3.9
Guralp site 1	2005023	-4.5	2.3	-46.3	3.3
Average site 1	N/A	+0.1	0.4	-44.7	3.3
MDT vault	2005033	-4.9	1.1	-42.0	1.6
MDT vault	2005035	-5.1	1.5	-41.1	3.0
Average MDT	N/A	-5.0	0.3	-41.6	0.9
Reftek site 2	2005041	4.5	1.2	-39.7	4.7
Guralp site 2	2005041	5.2	0.9	-43.1	2.4
Reftek site 2	2005043	0.7	2.7	-38.5	8.5
Guralp site 2	2005043	0.6	2.2	-43.7	2.0
Average site 2	N/A	+2.7	3.5	-41.2	3.7
Reftek site 3	2005033	-3.9	1.1	-45.3	5.5
Guralp site 3	2005033	-4.0	1.5	-47.1	2.6
Reftek site 3	2005035	-4.9	1.9	-43.7	3.3
Guralp site 3	2005035	-5.3	1.6	-47.2	2.4
Average site 3	N/A	-4.5	1.0	-45.8	2.4

Table 3: Summary Table of Daily Averages

Name	Displ. PSD (dB) rel to 1nm²/Hz (1 Hz, 24 hours)	Standard Deviation (dB) (1 Hz, 24 hours)	Displ. PSD (dB) rel to 1nm²/Hz (6 Hz, (24 hours)	Standard Deviation (dB) (6 Hz, 24 hours)
NLNM	-18.0	N/A	-49.8	N/A
NHNM	32.0	N/A	+21.6	N/A
Site 1	-0.2	6.9	-42.4	4.3
MDT vault	-5.2	0.4	-40.4	2.0
Site 2	+2.3	4.1	-39.9	3.9
Site 3	-4.3	1.3	-43.6	4.6

Summary Noise Values @ 1 Hertz

average-circle, day-square, night-diamond

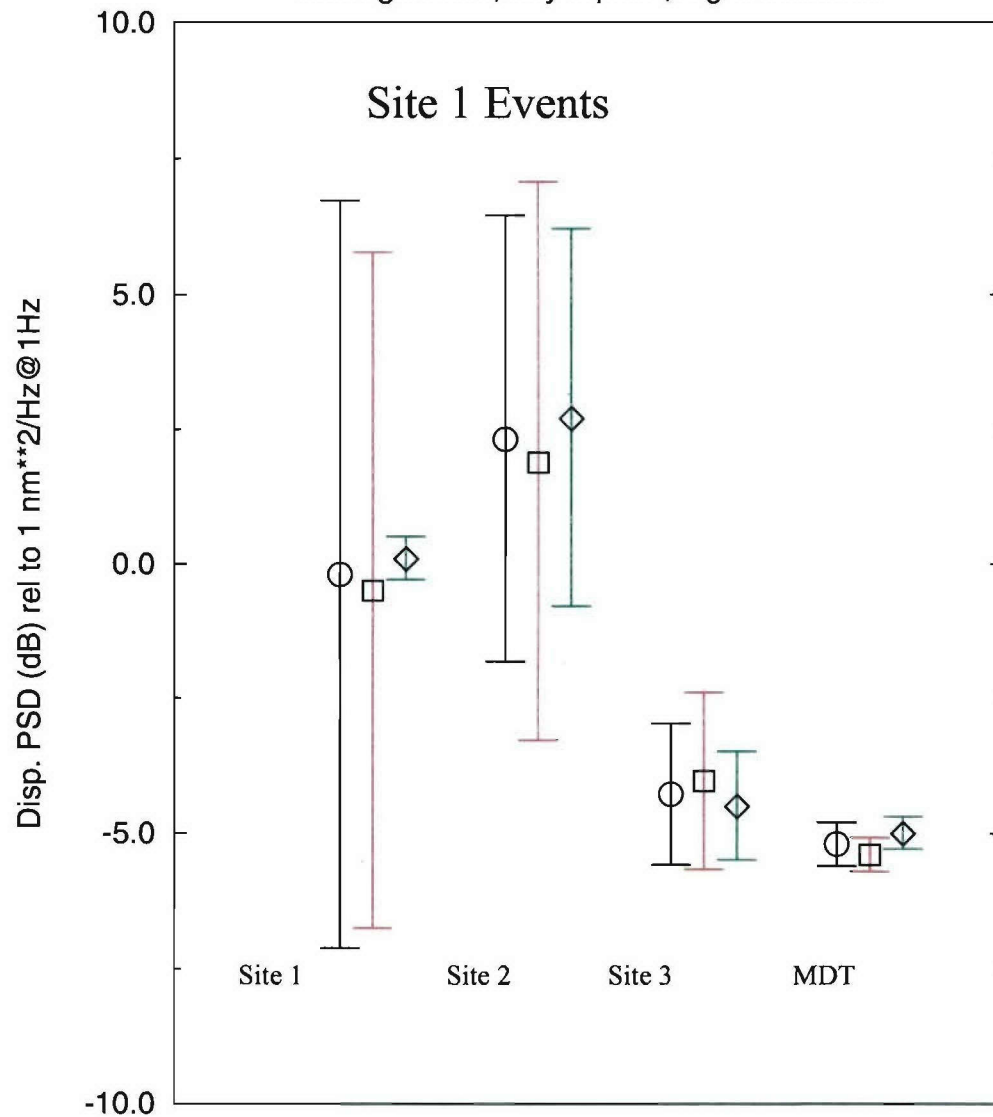


Figure 25. Summary values at 1 Hz for the three sites and MDT. It is clear that Site 3 and MDT have superior performance at 1 Hz.

Summary Noise Values @ 6 Hertz

average-circle, day-square, night-diamond

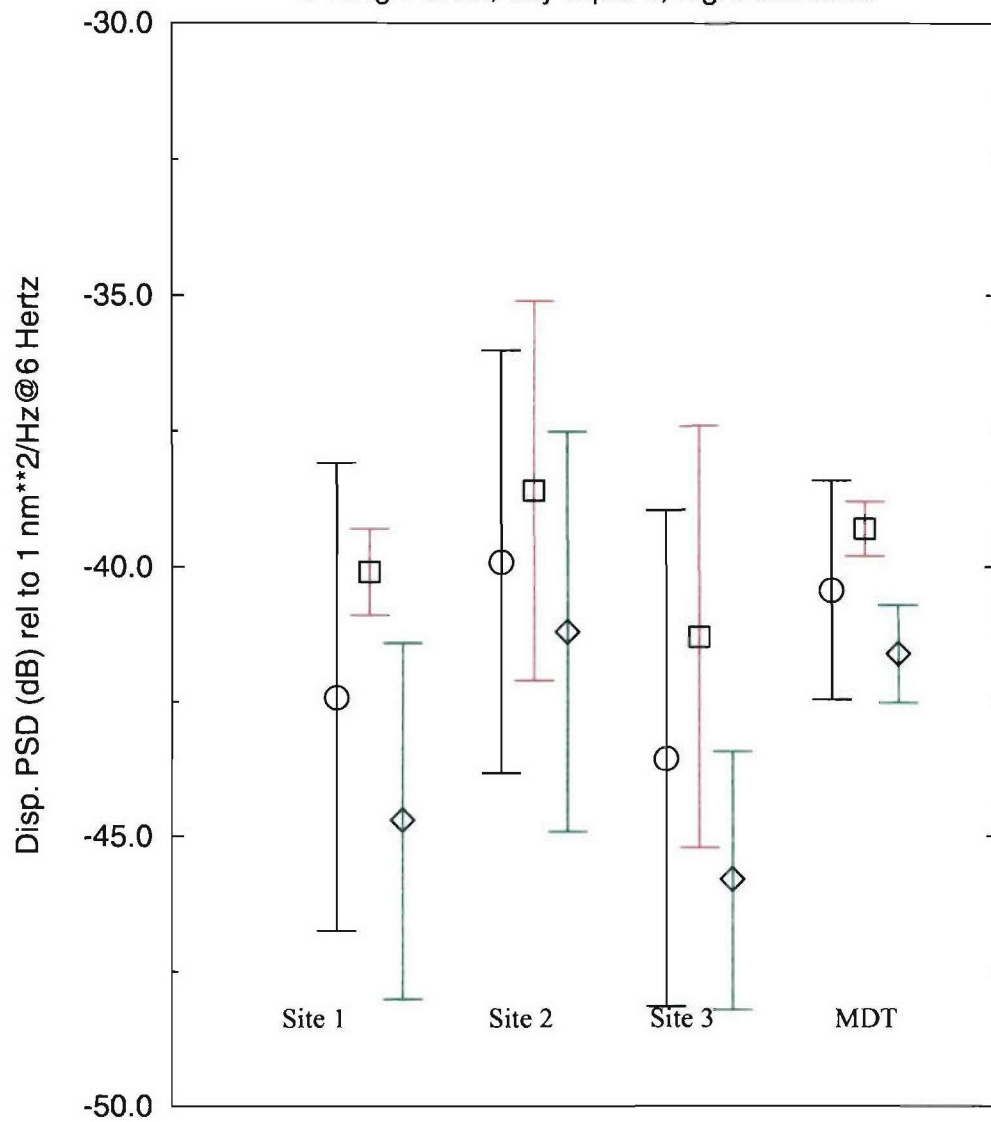


Figure 26. Comparison of daytime values at 6 Hz. Again, Site 3 has the lowest noise.

Weekday and Weekend noise @ 1 Hz

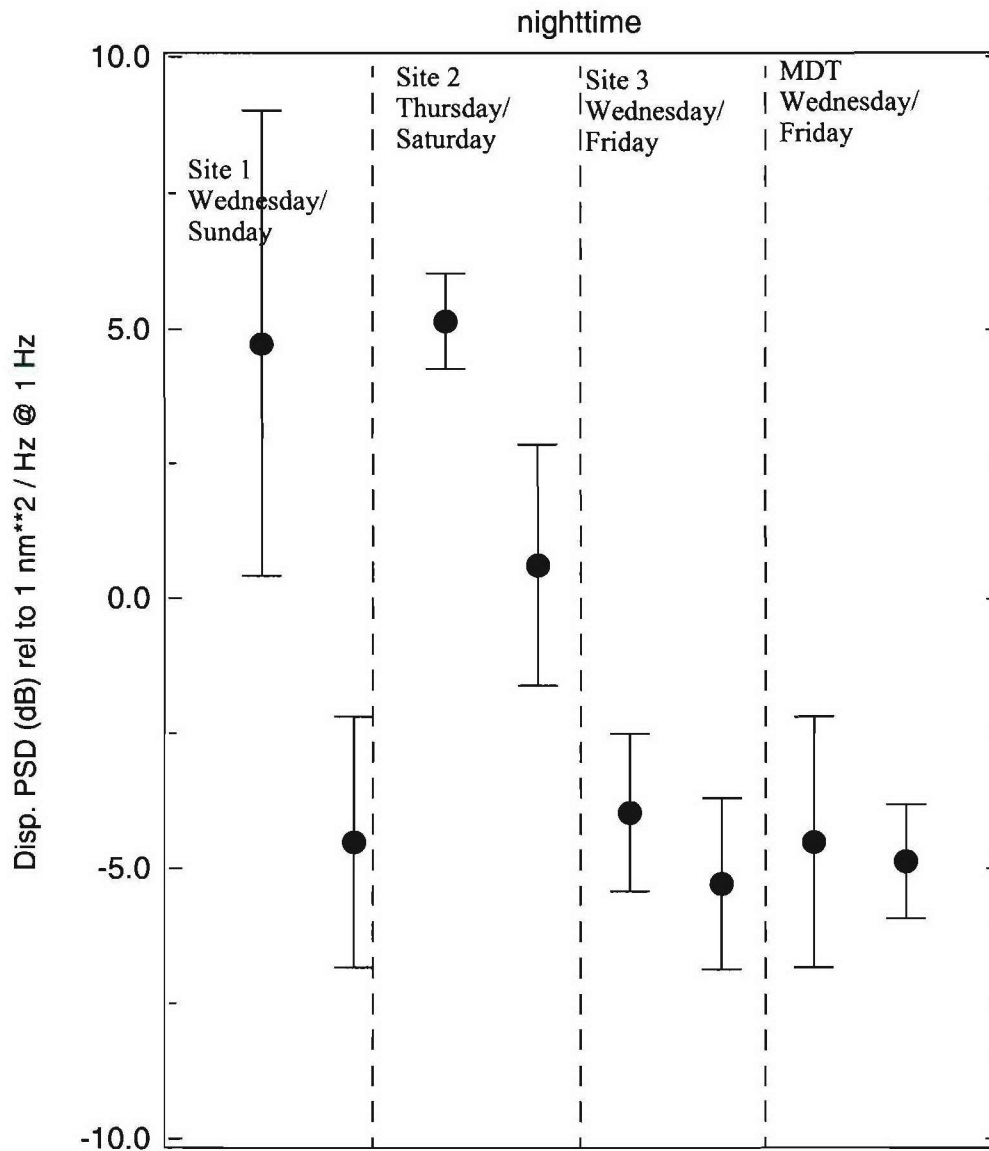


Figure 27. Comparison of 1 Hz noise values for Wednesday and Sunday for Sites 1 and 2, and for Wednesday and Friday for Sites 3 and MDT. It is obvious that at Sites 1 and 2, there is much more cultural noise present on workdays. The same data were not collected for Site 3; however, one can see that Wednesday is noisier than Friday. In addition, Sites 3 and MDT are much quieter overall.

Discussion.

Site 1 is much closer to the ocean than Sites 2 and 3, and would, therefore, be expected to have higher background noise values. What is surprising is that on weekends Site 1 is very quiet, indicating that the main cause of the increased noise is cultural, not due to its proximity to the coast. The high noise values measured at Site 2 were surprising, as the vault at MDT is only about 40 km to the east. The low value of the background noise for Site 3 was anticipated based on its distance from the coast. The fact that the cultural noise from the daytime is not much higher than for the nighttime indicates that overall cultural activity at Site 3 is not a major noise factor. The source of this noise is mainly the mine which is 14 km to the northwest. The mine noise would be effectively decorrelated by the 4 km diameter array. In addition, several dB noise reduction could be realized at 1 Hz and more at higher frequencies by putting the sensors in boreholes, making the site superior to MDT which is already in a vault.

Event Location Analysis

Introduction.

The main use of the proposed array by our host will be to monitor in-country seismicity. Therefore, one objective of our site survey was to determine the capability of each of the proposed sites to record regional events within Morocco. We wanted to demonstrate to our host that our main objective, which was to pick the quietest location in Morocco, was also consistent with their mission requirement to monitor in-country seismicity. To accomplish this objective, a large number of regional events were recorded from each of the three prospective array locations. We set up a temporary array at each of the three proposed site locations for the time periods described in Table 4. In addition, we deployed three GS13 seismometers and a Reftek130 digitizer in the vault at the Midelt site MDT along the three cardinal axes: north, east, and vertical, in order to provide a second station for input to the event formation process for Sites 2 and 3. We took the difference between the P and S arrival times and the temporary array azimuth to determine the locations. In addition, for a number of the events at Sites 2 and 3, we obtained arrival times and azimuth information from the sensors we placed in the Midelt vault. Location accuracies depended on the distance from the event, the number of contributing stations (which was either one or two), and the accuracy of the P and S arrival times and azimuth information. Our main objective was to determine the capability of each proposed array locations to detect regional events within Morocco and the approximate region within the country where they resided. Better locations could have been determined if we had also used the internal Moroccan network.

Table 4: Recording Times and Duration at Sites

Site	On-Time	Off-Time	Duration in Hours
1	1/19/2005 00:00	1/24/2005 08:00	128.0
2	2/09/2005 15:00	02/13/2005 07:30	88.5
3	1/30/2005 17:00	02/05/2005 08:00	135.0
MDT	1/26/2005 12:00	02/12/2005 10:00	410.0

Calibration of Travel Times for P and S Waves.

In order to use the S minus P times for distance determination we first had to calibrate the regional velocity curves for these phases. The Moroccans gave us the list of events in Table 5 which were located with their local network. We then found a number of these events that had been recorded at each of our temporary array locations and the Midelt vault. From this information, we generated the distance and arrival time information in Table 6. A linear regression was performed on the data in Table 6 and is shown in Figures 28 and 29 for P and S waves, respectively. The resulting regional travel time curves from the regressions were incorporated into the travel time models, which were subsequently used for location determination.

Table 5: List of Reference Events in Morocco During Survey

Event	Day	Month	Year	Hour	Min	Sec	Lat. N	Long. W	Mag	Locality	Site event observed
32	17	01	2005	18	38	12.39	34.988	3.897	3.1	TIFAROUINE (AL HOCEIMA)	1
33	17	01	2005	22	30	40.02	34.950	2.873	3.3	OULAD SETTOUT (NADOR)	1
34	19	01	2005	20	33	17.37	35.078	3.617	2.3	BNI MARGHNINE (NADOR)	none
35	19	01	2005	21	28	14.11	35.036	3.719	2.1	TROUGOUT (NADOR)	1
36	20	01	2005	00	07	17.08	35.056	3.692	2.3	TROUGOUT (NADOR)	1
37	21	01	2005	18	39	7.76	35.081	2.801	3.0	BOUARG (NADOR)	1
38	23	01	2005	19	07	25.16	33.671	5.962	2.7	KHEMISSET	1
39	26	01	2005	03	59	25.43	35.053	2.732	3.4	AREKMANE (NADOR)	none
40	26	01	2005	04	33	43.99	35.076	3.728	2.4	TROUGOUT (NADOR)	none
41	26	01	2005	06	30	4.85	34.623	9.712	3.1	ATLANTIQUE	none
42	28	01	2005	16	00	9.83	35.115	3.729	2.3	OULAD AMGHAR (NADOR)	MDT
43	29	01	2005	07	41	35.76	37.774	1.906	4.5	ESPAGNE	MDT
44	29	01	2005	19	28	34.22	36.608	7.517	3.5	ATLANTIQUE	MDT
45	30	01	2005	17	09	55.54	35.037	3.802	3.2	BNI BOUAYACHE (AL HOCEIMA)	MDT 3
46	30	01	2005	22	19	16.60	35.045	3.798	2.8	BNI BOUAYACHE (AL HOCEIMA)	MDT
47	30	01	2005	22	20	24.60	35.045	3.798	2.7	BNI BOUAYACHE (AL HOCEIMA)	3
49	02	02	2005	00	47	05.77	35.063	3.791	3.3	NEKKOUR	
50	03	02	2005	06	40	08.49	35.195	3.827	2.8	AIT YOUSSEF OUALI	MDT
51	03	02	2005	11	40	33.97	37.938	1.740	4.3	SUD D'ESPAGNE	MDT 3
52	03	02	2005	11	58	12.92	35.240	3.760	2.8	LARGE NADOR	MDT
53	03	02	2005	01	09	41.76	37.884	1.636	3.7	SUD D'ESPAGNE	MDT 3
54	04	02	2005	07	36	11.67	35.075	3.812	2.2	BNI BOUAYACHE (AL HOCEIMA)	MDT
55	04	02	2005	03	56	04.74	33.128	5.318	3.0	OUM RABIA (KHENIFRA)	MDT
56	05	02	2005	12	38	19.11	35.073	3.718	2.2	TROUGOUT (NADOR)	not observed

Table 5: List of Reference Events in Morocco During Survey (Continued)

Event	Day	Month	Year	Hour	Min	Sec	Lat. N	Long. W	Mag	Locality	Site event observed
57	05	02	2005	22	32	58.88	35.056	3.733	2.1	TROUGOUT (NADOR)	MDT
58	06	02	2005	02	46	05.77	35.208	3.983	3.3	IZEMOUREN (AL HOCEIMA)	MDT
59	07	02	2005	22	18	33.84	34.936	2.588	2.8	OULAD DAOUD ZKHANINE (NADOR)	MDT
60	08	02	2005	06	47	15.35	35.109	3.764	2.4	TROUGOUT (NADOR)	MDT
61	09	02	2005	05	24	41.05	35.075	3.707	2.9	TROUGOUT (NADOR)	MDT
62	11	02	2005	05	38	52.83	35.017	3.681	2.5	BNI MARGHNINE (NADOR)	MDT
63	12	02	2005	05	38	52.83	35.017	3.681	2.5	BNI MARGHNINE (NADOR)	site 2

Table 6: P- and S-Wave Reference Event Travel Time Data

Distance in kilometers	P-wave travel time in seconds	S- wave travel time in seconds
71.2	14.2	24.0
74.5	13.9	22.3
82.3	14.4	23.7
126.8	23.0	39.1
127.9	22.2	38.9
139.0	23.7	41.2
206.8	34.1	59.1
258.1	36.3	62.4
259.1	40.3	61.8
259.1	41.0	62.0
259.1	41.1	73.6
261.3	40.3	61.3
261.3	40.6	70.5
261.3	41.9	71.8
264.6	40.9	71.8
266.9	41.2	63.8
272.4	40.4	70.5
273.5	40.9	70.3
280.2	42.9	86.4
300.3	45.6	not observed
320.2	47.8	76.1

Table 6: P- and S-Wave Reference Event Travel Time Data (Continued)

Distance in kilometers	P-wave travel time in seconds	S- wave travel time in seconds
449.2	60.3	121.4
450.3	60.3	122.2
452.6	59.9	125.0
471.5	63.6	122.4
498.2	65.1	113.2
602.7	79.1	139.1
618.3	76.3	138.0
624.9	82.5	143.6
626.0	82.0	145.2
818.4	102.5	179.1
819.5	819.5	185.2

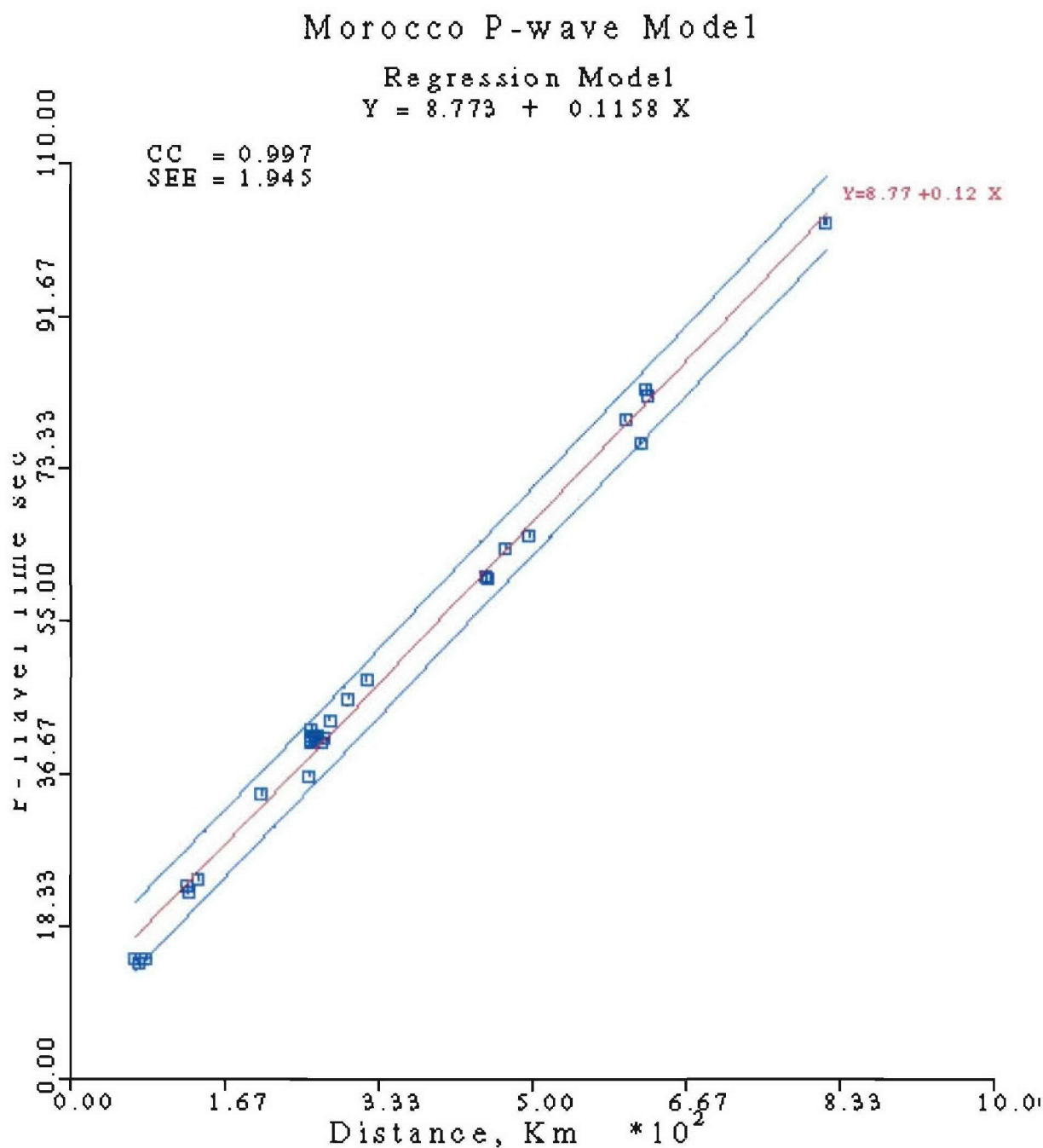


Figure 28. Linear regression and resulting P-wave travel time model. The P-wave velocity which is the reciprocal of the slope is 8.64 km per second. The error bars are also shown which are one standard deviation from the regression line. CC is the correlation coefficient, and SEE is the standard error estimate.

Morocco S-wave Model

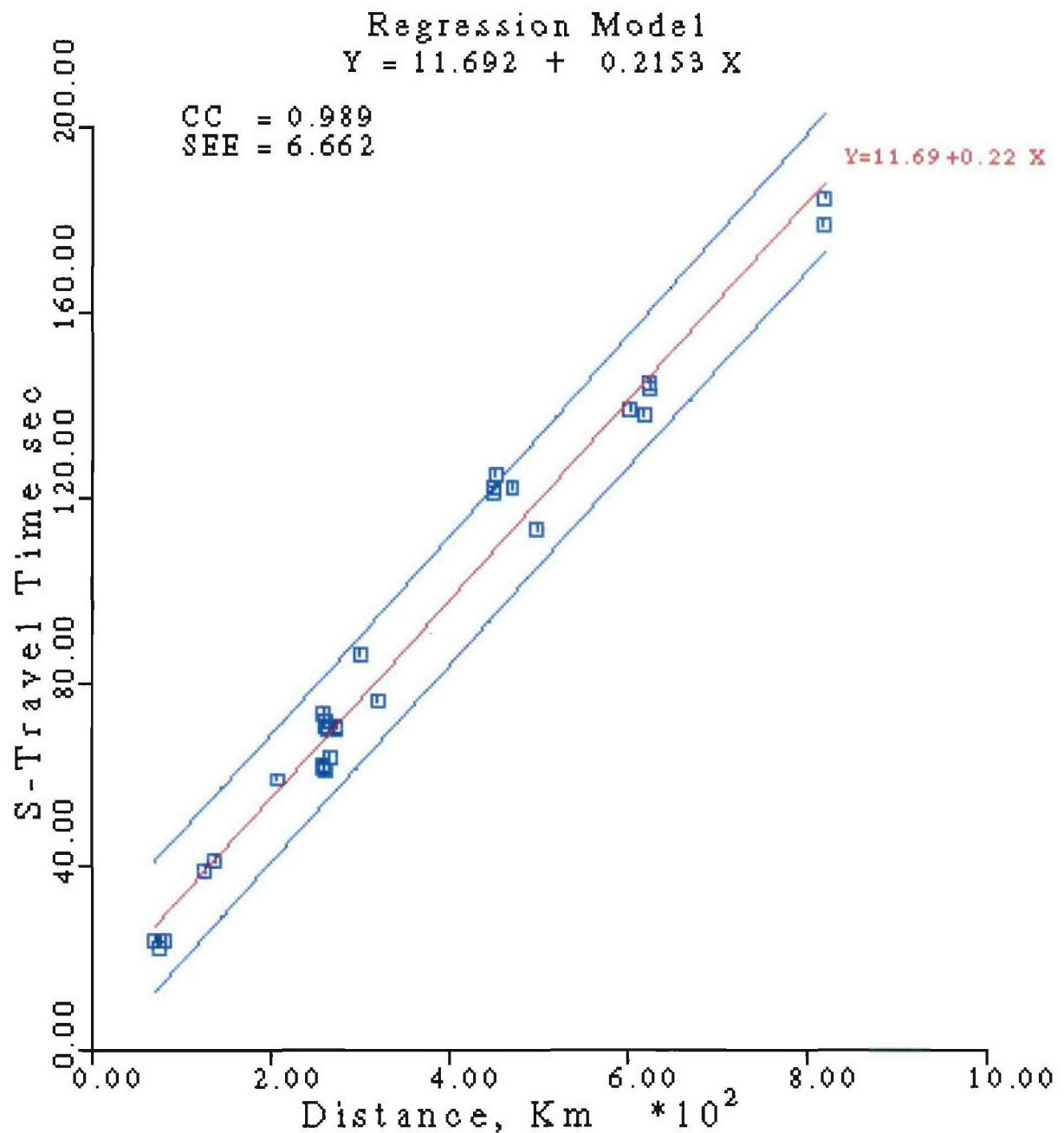


Figure 29. Linear regression and resulting S-wave travel time model. The S-wave velocity is the inverse of the slope or 4.6 km per second.

Event Analysis.

Tables in Appendix D, Event Tables, provide event latitude, longitude, and origin time for each of the three proposed site locations. Figures 30-33 provide event locations for those events detected at each of the three proposed sites and the Midelt station MDT. Figure 34 is a summary plot, with all events from Sites 1, 2, and 3 plotted.

Site 1 Recorded Event Locations

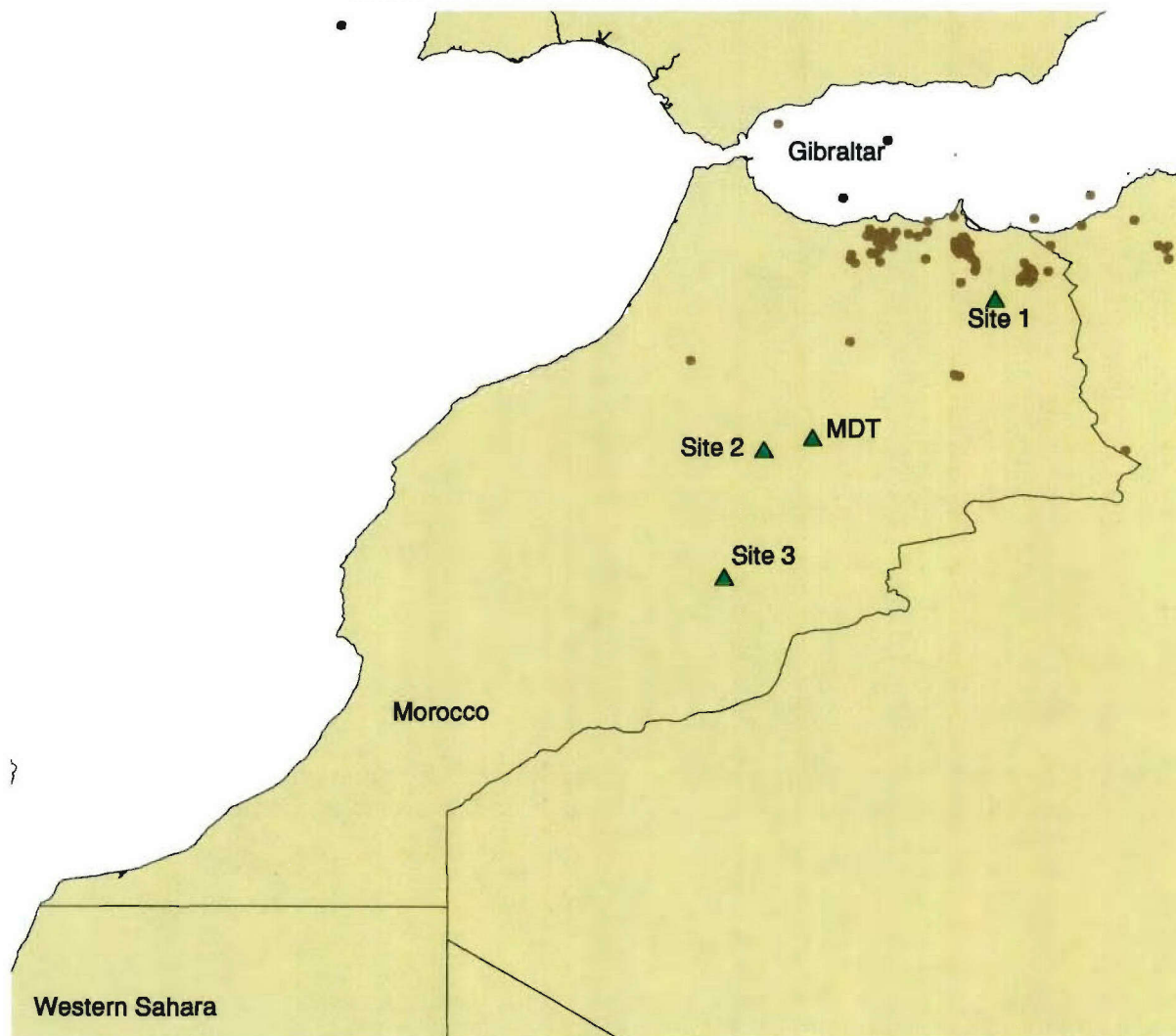


Figure 30. Events detected from proposed array Site 1. Note that event detectability is mainly in the northern area of Morocco.

Site 2 Recorded Event Locations

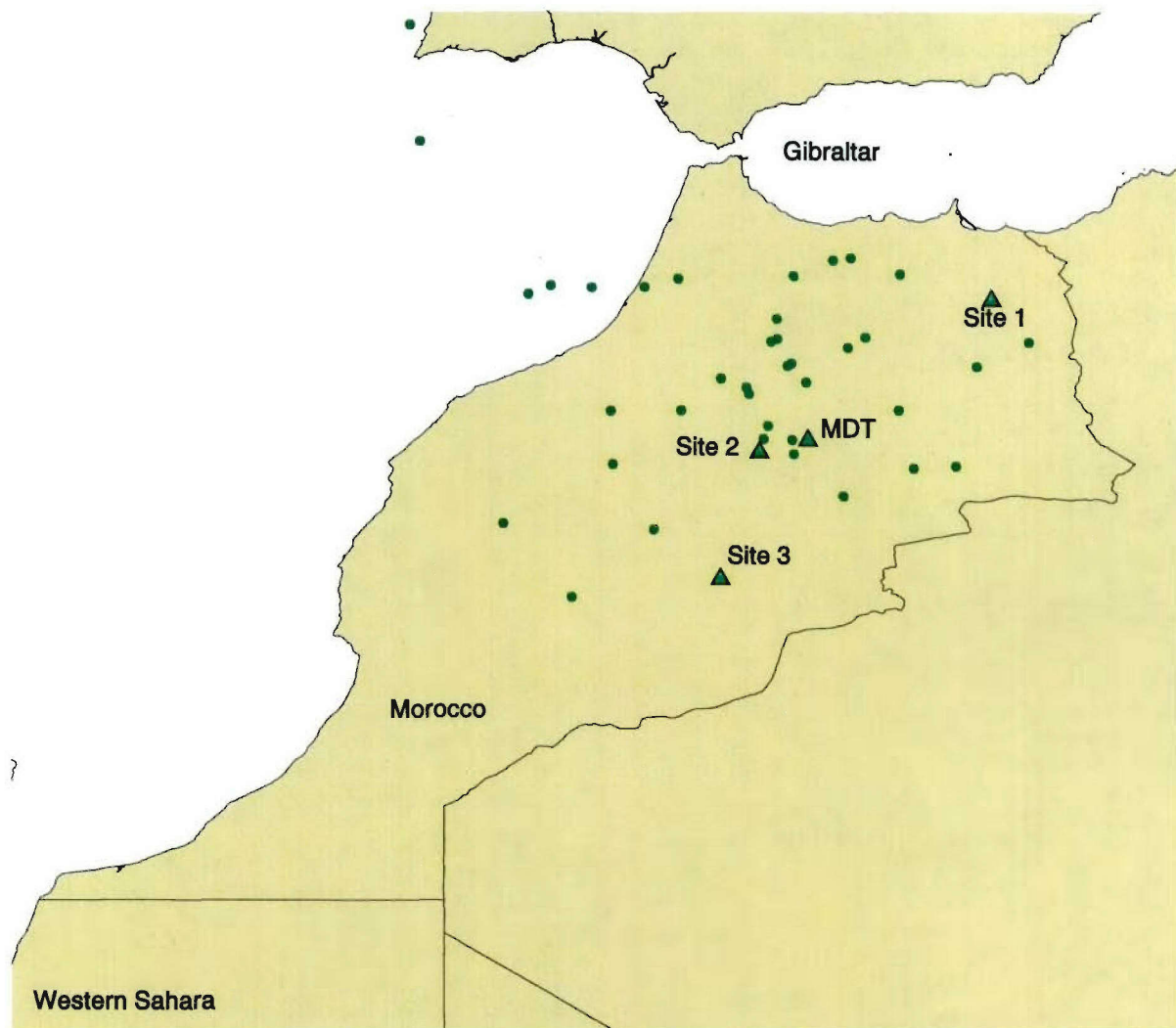


Figure 31. Events detected from proposed array Site 2. This site, being centrally located, detects mainly in an area surrounding the station, but a few events also in the north and the south.

Site 3 Recorded Event Locations

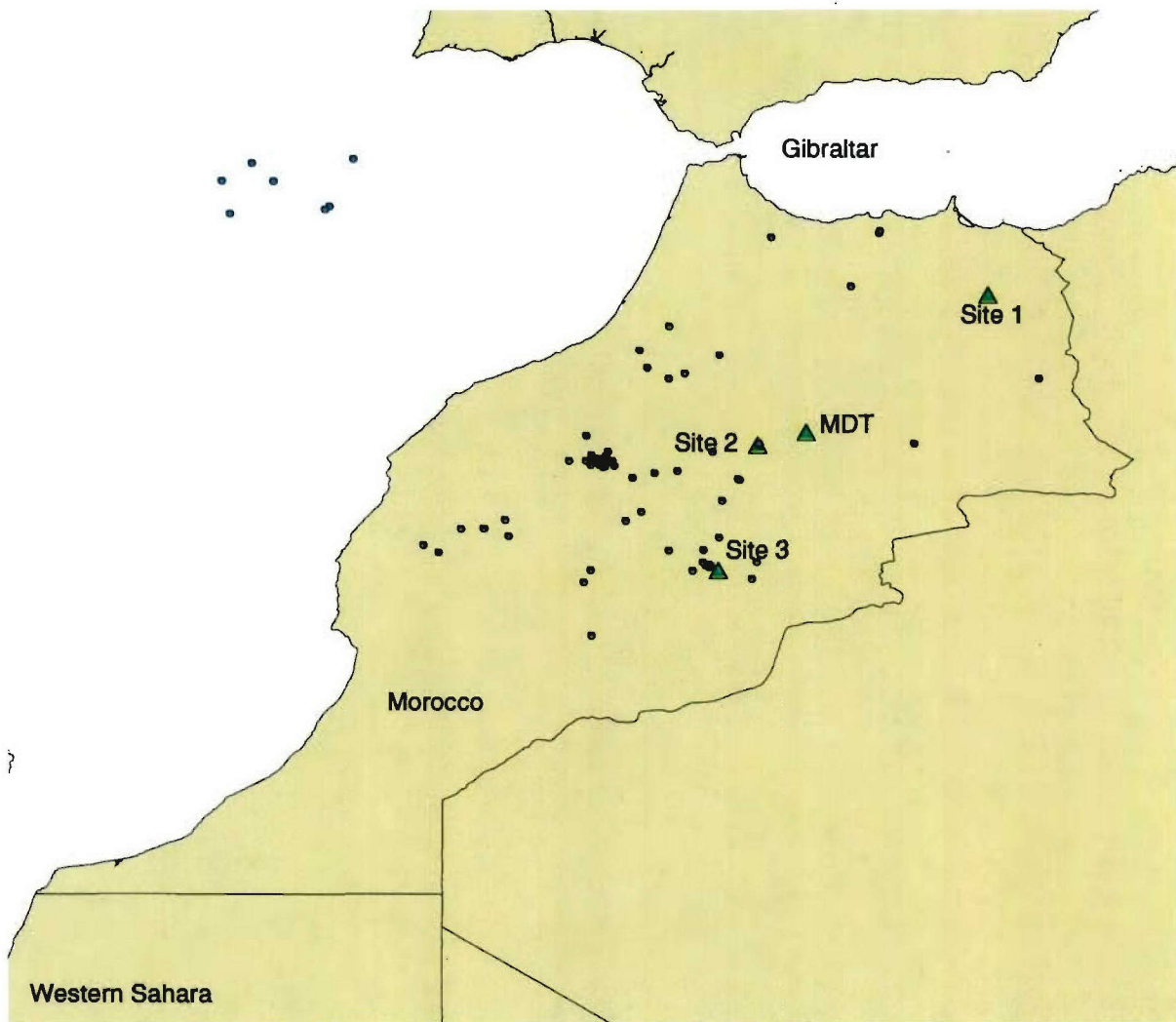


Figure 32. Events detected from proposed array Site 3. Site 3 detects many events both locally and elsewhere in Morocco, giving good detection capability throughout the country.

MDT Recorded Event Locations

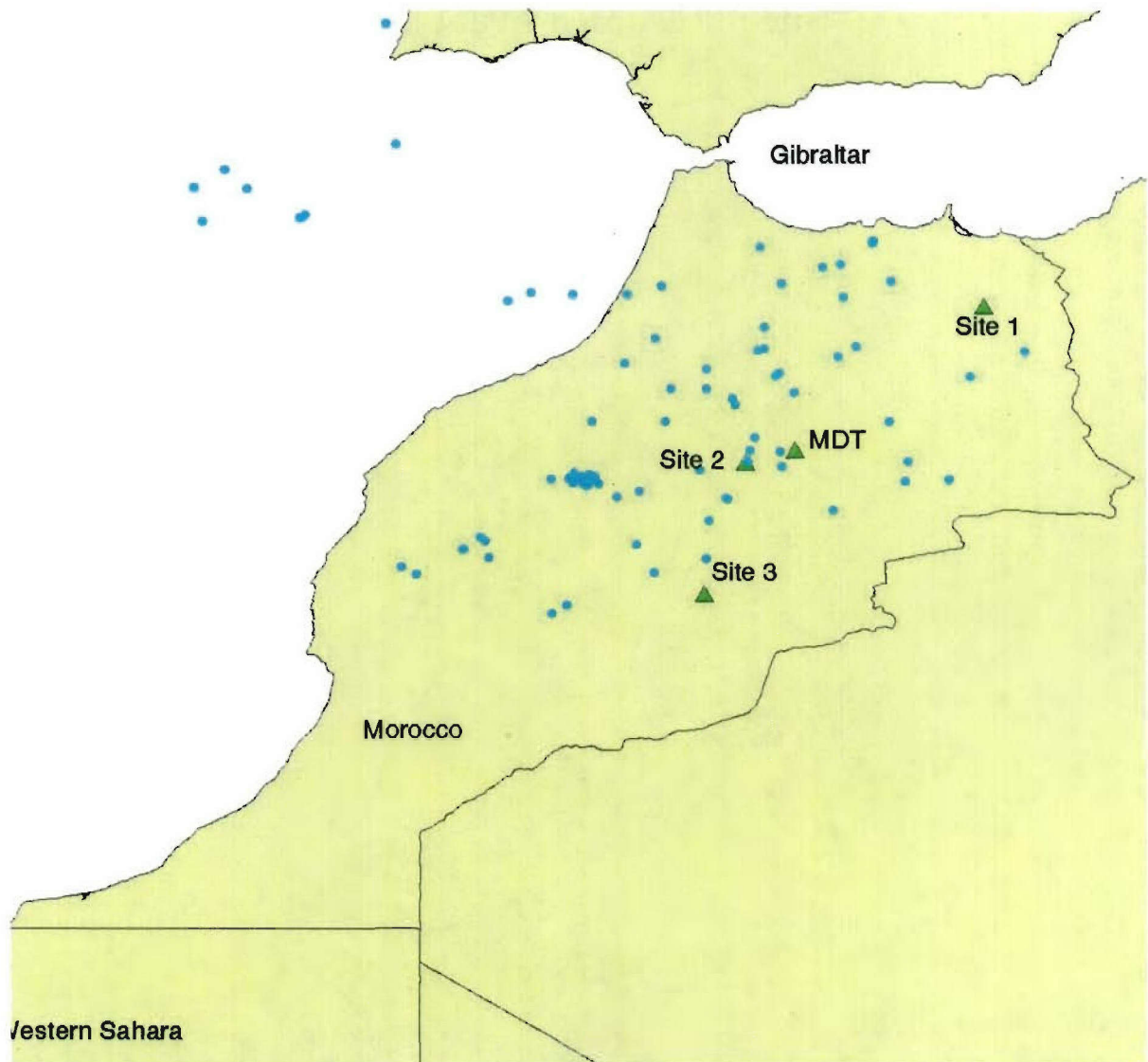


Figure 33. Events detected from the Midelt station MDT. This station is very good, having detected many of the events seen by Sites 2 and 3. Site 1 and MDT were not operational at the same time. One reason for the excellent performance observed from MDT is that the sensors, rather than being located on the surface, were located in a tunnel 100 meters in from the entrance.

All Recorded Event Locations

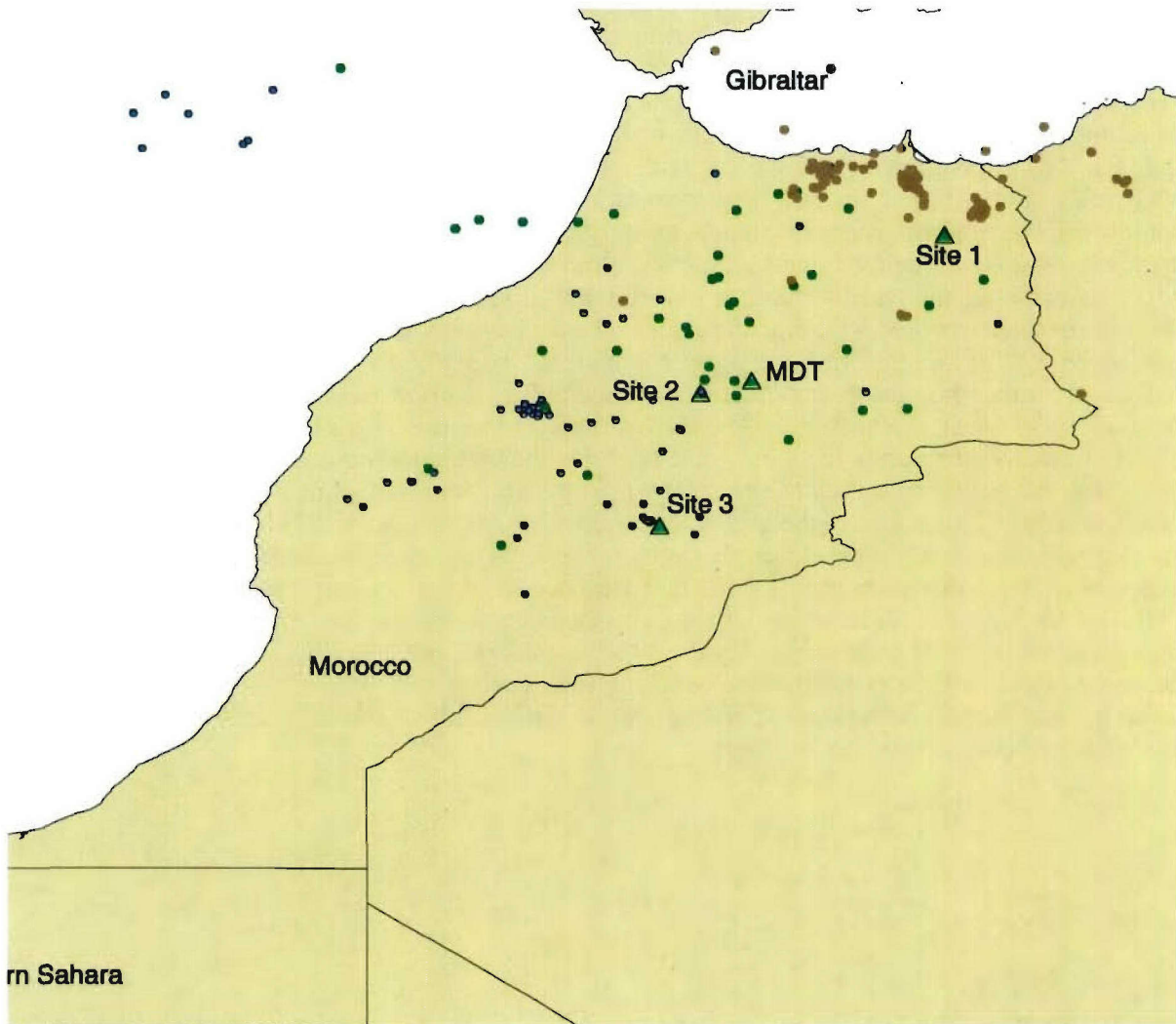


Figure 34. Events detected from locations of Site 1 (brown), Site 2 (green), and Site 3 (blue).

Discussion.

Signals detected from each of the proposed site locations were recorded on the vertical channels of individual sensors, with the arrays used to determine the directions and confirm the validity of the signals. The arrays were then used to determine the azimuth of the events and, in some cases, find secondary phase in the coda. The parameter indicative of event detection capability for each proposed location to the Moroccan seismic network is the areal coverage of events. The number of events detected at each site is a function of distance from active areas and the number of days the sensor was operational. From an operational perspective, spacial coverage will demonstrate how well a site will add to overall network performance since, with good spacial coverage, the station will contribute to more regional network station detections in all areas of Morocco. The areal extent of coverage for signals at Site 3 is almost equivalent with that found at the vault at MDT, even though the sensors at Site 3: (1) are at the surface and not protected nearly as well from the wind as those at the MDT vault, and (2) are also further away from most of the seismic activity than those at MDT. Beamforming at Site 3 will increase the signal-to-noise ratio by at least another 3 dB, and putting the sensors in boreholes will add at least 1 dB at 1 Hz, and more at higher frequencies to the array capability. The thick sediments found at Site 3 will have the additional effect of greatly attenuating the wind noise provided the boreholes are below the sediment layer and in the competent hard rock (Young, 1996). Site 1 performs the poorest of the three sites on areal coverage. This is due to the higher level of the background noise at this site which appears as both cultural and due to the closer proximity to the coast than the other sites, and the fact that its geographic location is not centrally located in Morocco. Site 1 would not assist in event formation in the southern half of Morocco, as indicated by the event formation data. However, Site 1 does pick up much of the aftershock activity from the recent large earthquake at Hocemia. From the event data alone, one cannot determine which of Sites 2 or 3 would make the greatest contribution to the internal Moroccan network. One has to look, additionally, at the noise data to determine the site with the best potential performance.

Comparison of the Attributes of Each of the Candidate Sites





































Green (Best)	Yellow (Neutral)	Red (Worst)
		

Table 7: Site Comparisons

Site Attribute	Site 1	Site 2	Site 3
Location			
Isolation from cultural noise			
Comparable to NLNM at 1 Hz			
Comparable to NLNM at 6 Hz			
Event analysis results			
Geology			
Competent rock			
Homogeneous geology			
Accessibility			
Existing roads to array location			
Accessibility within array area			
Communications			
Line-of-sight intrasite communications			
Power			
Power availability			
Land Owner			
Low risk to obtain access			

Attribute Comparison.

Attributes of the candidate sites are compared in Table 7. The attributes of an ideal site would be one which exhibits low seismic noise, and uniformity of rock type and composition. The site would be accessible via existing roads and allow for ease of data communications within the array with no relay towers or high antenna masks required to transmit the data. Power would be readily accessible and reliable. There would be no land ownership issues. For each of the characteristics, each site was given one of three ratings. A green rating indicates the candidate site is comparable to an ideal site for that characteristic. A yellow rating indicates a slight difference from the ideal site for that characteristic, and a red rating indicates the greatest difference from the ideal.

Geophysical and geological considerations of the site are the most important and, therefore, listed first under the headings of Location and Geology, followed by the logistical considerations of accessibility, communications, power, and land ownership. Table 7 indicates that Site 3 compared most favorably overall to these characteristics.

Conclusion.

The noise data summarized in Table 3 indicate that the existing station at MDT would outperform an array put at Site 2. Comparing the three perspective sites only, the noise values at Site 3 indicate that the noise value is the lowest of the three prospective sites. The event data indicate that Site 1 would not be a good candidate for an array station, due to the lack of event detection over the southern half of Morocco.

Based on the technical analysis of the seismic data and the ensuing discussion of the other attributes of the three potential sites in Morocco, we recommend Site 3 for the location of a new seismic array in Morocco. Site 3, located approximately 40 km southeast of Boumalne-du Dades in the Anti-Atlas Mountains, will provide the largest increase in detection and location capability for regional and teleseismic signals in northwestern Africa. Of all the sites investigated, Site 3 has the characteristics most closely matched to that of a quiet continental site, which is far away from both the ocean and cultural noise. Due to the remoteness of this site, it is also unlikely that it will be threatened in the future by additional cultural development.

References

- Peterson, Jon (1993). *Observations and Modeling of Seismic Background Noise*, Open-File Report 93-322, US Department of Interior Geological Survey, Albuquerque, New Mexico.
- Young, Christopher J., Eric P. Chael, Mitchell M. Withers, and Richard C. Aster (1996). A Comparison of the High-Frequency (>1 Hz) Surface and Subsurface Noise Environment at Three Sites in the United States, *Bulletin of the Seismological Society of America*, 86(5), 1516-1528.

Distribution

US Embassy (1 copy)
Rabat, Morocco

Centre National Pour La Recherche Scientifique
Et Technique Laboratoire De Geophysique (CNRST) (4 copies)
Morocco

AFTAC/TT (3 copies)
Patrick AFB FL

AFTAC/CA (STINFO) (2 copies)
Patrick AFB FL

(This page intentionally left blank.)

Appendix A

Sensor Coordinates

For each of the three perspective sites, an array of sensors was set up. Each sensor had a geographical position, which was important for determining the Frequency - Wavenumber (F-K) information of the events seen. The sensor data are presented in this appendix in a series of tables. The site location was taken as the location of the element with no offsets.

Table A-1: Site 1 Coordinates (Oujda Site)

Sensor Number	Instrument Number	Latitude	W. Longitude	North Offset (kilometers)	East Offset (kilometers)
1	not used				
2	DO685	34° 21' 23.0"	2° 35' 28.9"	0.0000	0.0000
3	DA84	34° 21' 10.1"	2° 35' 45.8"	-0.3984	-0.4309
4	DE14	34° 21' 02.4"	2° 35' 28.3"	-0.6363	0.0153
5	DE13	34° 20' 46.2"	2° 35' 55.7"	-1.1366	-0.6834
6	DE15	34° 20' 45.9"	2° 35' 37.0"	-1.1459	-0.2065

Table A-2: Site 2 Coordinates (Midelt Site)

Sensor Number	Instrument Number	Latitude	W. Longitude	North Offset (kilometers)	East Offset (kilometers)
1	DE14	32° 41' 04.0"	5° 09' 05.3"	0.0000	0.0000
2	DO685	32° 41' 16.0"	5° 09' 09.3"	0.3706	-0.1040
3	GS13	32° 40' 51.2"	5° 09' 15.6"	-0.3953	-0.2678

Table A-3: Site 3 Coordinates (Boumalne-du Dades Site)

Sensor Number	Instrument Number	Latitude	W. Longitude	North Offset (kilometers)	East Offset (kilometers)
1	DE15	31° 16' 51.2"	5° 35' 38.9"	0.0000	0.0000
2	DO685	31° 16' 40.4"	5° 35' 51.3"	-0.3336	-0.3273
3	DA84	31° 16' 56.9"	5° 35' 57.5"	0.1761	-0.4910
4	DE14	31° 17' 10.4"	5° 35' 46.2"	0.5930	-0.1927
5	DE13	31° 17' 00.5"	5° 35' 19.2"	0.2872	0.5200
6	DA53	31° 16' 43.1"	5° 35' 18.5"	-0.2502	0.5385

Coordinates for the Midelt Vault site were taken from the literature as 32.8170° N, 4.6140° W.

Appendix B

Calibration and Spectral Computation Methods and Results

The purpose of this appendix is to explain how the actual Guralp calib values were determined from the Morocco data, and how we calibrated the Reftek GS13 system. Calibrating the Guralp sensors was necessary in order to determine accurately the noise levels for all of the Morocco sites. The procedure to determine the calib values was provided by Guralp Systems, Inc. The procedure will be outlined in detail below for one Guralp data channel. The same procedure was followed for all Guralp channels. For the example below, the vertical channel of the collocated Guralp at site 3 was used.

To determine the theoretical calib values, we use the following equations:

$$(counts)/(m)/(s) = S/LSBout \quad (1)$$

Where S is the given sensitivity and LSBout is the least significant bit of the digitizer. Both are defined below on a per instrument basis.

$$(counts/m) = ((counts)/(m)/(s)) \times 2 \times \pi \times f \quad (2)$$

In equation (2), we convert from velocity to displacement.

$$((counts)/(nm)) = (counts/m)/(1.0e + 09) \quad (3)$$

Where in equation (3), we have converted from meters to nanometers.

$$((nm)/(count)) = 1/((counts)/(nm)) \quad (4)$$

Lastly, equation (4) takes the reciprocal to obtain the theoretical calib value.

To determine the actual calib values, we use the following equations from Guralp documents:

$$Vin = (Cin \times 2 \times LSBin) \quad (5)$$

Equation (5) calculates the input voltage, Vin, where Cin is the input counts, 0 to peak, from the input calibration, and LSBin is the least significant bit of the input channel (both are displayed in Tables B-2 and B-1, respectively).

$$Vout = (Cout \times LSBout) \quad (6)$$

In equation (6), we have calculated the output voltage from the measured calibration. Cout is the measured peak-to-trough output from the waveform in counts and LSBout is the least significant bit which is provided for each sensor in Table B-1.

$$Current = ((Vin)/R) \quad (7)$$

In equation (7), the current is defined as the input voltage calculated in equation (5) divided by the calibration resistor provided in Table B-1.

$$Acceleration = (Current)/K \quad (8)$$

In equation (8), the acceleration is defined as the current divided by K, the feedback coil constant provided in Table B-1 for each sensor.

$$Velocity = (Acceleration) / (2 \times \pi \times f) \quad (9)$$

Equation (9) converts from acceleration to velocity.

$$S = (V_{out}) / (Velocity) \quad (10)$$

Equation (10) computes the instrument sensitivity, S, derived from the data by taking the output voltage and dividing by the velocity from equation (9). We now convert the sensitivity to the calibration constant using the next four equations.

$$(counts)/(m)/(s) = S / LSB_{out} \quad (11)$$

Equation (11) is computed using the sensitivity from equation (10) divided by the least significant bit.

$$(counts/m) = ((counts)/(m)/(s)) \times 2 \times \pi \times f \quad (12)$$

Equation (12) converts from velocity to displacement.

$$((counts)/(nm)) = (counts/m) / (1.0e + 09) \quad (13)$$

Equation (13) converts from meters to nanometers.

$$((nm)/(count)) = 1 / ((counts)/(nm)) \quad (14)$$

Lastly, equation (14) takes the reciprocal to obtain the actual calib value.

An example using the above equations follows after Table B-1. The actual calibration value for the calibs are given in Table B-2, column 7, and are compared with the nominal values in column 9. The maximum difference from the nominal approaches 6.5%.

Table B-1: Instrument Constants Provided by Guralp Systems

Instrument	Channel	Sensitivity (V/m/s) S	LSB (uV/count) LSB _{out}	Input LSB (uV/count) LSB _{in}	Calibration Resistor (Ohms) R	Feedback Coil Constant (A/m/s ²) K
DE15/T3M21	BHZ	2,973	1.269	320.34	51,000	0.01756
DE15/T3M21	BHN	2,993	1.261	320.34	51,000	0.01848
DE15/T3M21	BHE	2,989	1.266	320.34	51,000	0.01831
DO685/T3K93	BHZ	2,957	1.272	320.50	51,000	0.01747
DO685/T3K93	BHN	2,965	1.277	320.50	51,000	0.01843

Table B-1: Instrument Constants Provided by Guralp Systems (Continued)

Instrument	Channel	Sensitivity (V/m/s) S	LSB (uV/count) LSBout	Input LSB (uV/count) LSBin	Calibration Resistor (Ohms) R	Feedback Coil Constant (A/m/s ²) K
DO685/T3K93	BHE	2,969	1.287	320.50	51,000	0.01849
DA84/T3F31	BHZ	2,927	1.274	323.88	51,000	0.01906
DA84/T3F31	BHN	2,973	1.275	323.88	51,000	0.01921
DA84/T3F31	BHE	2,950	1.276	323.88	51,000	0.01924
DE14/T3M14	BHZ	2,971	1.270	322.43	51,000	0.01733
DE14/T3M14	BHN	2,987	1.261	322.43	51,000	0.0186
DE14/T3M14	BHE	3,019	1.267	322.43	51,000	0.0182
DE13/T3M20	BHZ	2,970	1.286	324.52	51,000	0.01743
DE13/T3M20	BHN	2,998	1.273	324.52	51,000	0.01842
DE13/T3M20	BHE	2,996	1.269	324.52	51,000	0.01822
DA53/T3F13	BHZ	2,951	1.275	323.59	51,000	0.01849
DA53/T3F13	BHN	3,001	1.279	323.59	51,000	0.01962
DA53/T3F13	BHE	3,122	1.277	323.59	51,000	0.01912

1. Divide the sensitivity, 2,973 V/m/s, by the LSB, 1.269 uV/count, to get 2,342,789,598 counts/m/s.
2. Multiply by $2\pi f$, $f = 1$ Hz, to get $1.472018118 \times 10^{10}$ counts/m.
3. Divide by 1.0×10^9 to convert to nanometers from meters, to get 14.72018118 counts/nm.
4. Take the reciprocal to obtain the theoretical calib value of 0.067934 nm/count.

Next, to determine the actual calib value:

1. Inject a 1 Hz sine wave calibration from the digitizer to the sensor.
2. Measure the maximum and minimum count values on the input data which consist of four samples per second using an interpolation method described below and add the values to obtain the total input count value. For this example, we get 24,076.2 counts.
3. To obtain the input voltage, multiply by 320.34 uV/count to get 7.712569908 V.
4. Measure the maximum and minimum count values from the output data channel. Add the values to obtain the total output count value of 3,265,128 counts.
5. Multiply by 1.269 uV/count to get the output voltage of 4.143447432 V.

6. Next, divide the input voltage, 7.712569908 V, by the calibration resistor, 51,000 Ohms, to get 1.512268609e-04 Amps.
7. Then, divide by the Feedback coil constant, 0.01756 A/m/s/s, to get 8.612008026e-03 m/s/s.
8. Divide by $2\pi f$, $f = 1$ Hz, to get 1.370643647e-03 m/s.
9. Next, divide the output voltage, 4.143447432 V, by the velocity, 1.370643647e-03 m/s, to obtain the sensitivity of 3,022.993934 V/m/s.
10. Divide the sensitivity, 3,022.993934 V/m/s, by the LSB, 1.269 uV/count, to get 2,382,185,921 counts/m/s.
11. Multiply by $2\pi f$, $f = 1$ Hz, to get 1.496771558e+10 counts/m.
12. Divide by 1.0e+09 to get 14.96771558 counts/nm.
13. Finally, take the reciprocal to obtain the actual calib value of 0.066810 nm/count.

The actual calib value when compared to the theoretical calib value only yields a -1.655% difference.

The calib values used for the noise calculations are given in Table B-2, column 7. Calibrations were not successful at all sites. The calibrations used and the sites that they were taken at are given in columns 4 and 10.

Table B-2: Calibration Values for Guralps

Sensor	Channel	Input Voltage in Counts Cin	Site Observed	Measured Output Amplitude (counts) Cout	Calculated Value (nm/count)	% Difference from Nominal	Nominal Value (nm/count)	Calibration Used for Sites
DE14	3m14Z	11980.5	1	3,250,312	0.068122	0.131	0.068033	1, 3
DE14	3m14N	11946.2	1	3,070,118	0.067003	-0.277	0.067189	1, 3
DE14	3m14E	12043.6	1	3,146,498	0.067359	0.847	0.066793	1, 3
DE13	3m20Z	14440.5	1	3,831,213	0.069709	1.154	0.068914	1
DE13	3m20N	13744.8	1	3,695,609	0.065088	-3.686	0.067579	1
DE13	3m20E	15212.9	1	3,749,706	0.071781	6.481	0.067412	1
DE15	3m21Z	12038.1	1	3,265,128	0.066810	-1.655	0.067934	1, 3
DE15	3m21N	12213.2	1	3,136,564	0.067048	-0.009	0.067054	1, 3
DE15	3m21E	12784.3	1	3,157,497	0.070365	4.382	0.067411	1, 3
DO685	3k93Z	12417.1	1	3,185,880	0.071027	3.745	0.068463	1, 2
DO685	3k93N	11765.9	1	3,005,803	0.067619	-1.354	0.068547	1, 2
DO685	3k93E	12329.4	1	2,990,183	0.070996	2.908	0.068990	1, 2, 3

Table B-2: Calibration Values for Guralps (Continued)

Sensor	Channel	Input Voltage in Counts Cin	Site Observed	Measured Output Amplitude (counts) Cout	Calculated Value (nm/count)	% Difference from Nominal	Nominal Value (nm/count)	Calibration Used for Sites
DA84	3f31Z	no data	NA	no data	nominal value 0.069273	0	0.069273	1, 3
DA84	3f31N	no data	NA	no data	nominal value 0.068255	0	0.068255	1, 3
DA84	3f31E	no data	NA	no data	nominal value 0.068841	0	0.068841	1, 3
DA53	3f13Z	12210.2	3	3,057,769	0.069418	0.951	0.068764	2, 3
DA53	3f13N	12032.0	3	2,917,732	0.067560	-0.398	0.067830	2, 3
DA53	3f13E	12705.4	3	3,135,778	0.068116	4.634	0.065099	2, 3
DE13	3m20Z	14509.4	3	3,827,865	0.070103	1.725	0.068914	3
DE13	3m20N	14495.9	3	3,687,911	0.068789	1.790	0.067579	3
DE13	3m20E	14327.8	3	3,747,129	0.067651	0.355	0.067412	3
DO685	3k93Z	11889.2	3	3,190,707	0.067905	-0.815	0.068463	3
DO685	3k93N	12379.8	3	3,004,476	0.071178	3.838	0.068547	3
DO685	3k93E	11802.3	3	no data	0.070996	2.908	0.068990	NA
DE15	3m21Z	12038.1	3	no data	0.066810	-1.655	0.067934	NA
DE15	3m21N	12213.2	3	no data	0.067048	-0.009	0.067054	NA
DE15	3m21E	12784.3	3	no data	0.070365	4.382	0.067411	NA

In the following table, we repeated the measurements on four separate calibrations for sensor DE14/T3M14, channel (BHN). From this analysis we determined the measurement error for calibration.

Table B-3: Error Analysis Using Guralp Calibrations

Sensor	Channel	Input Voltage in Counts Cin	Measured Output Amplitude (counts) Cout	Calculated Value (nm/count)	Nominal Value (nm/count)	% Difference from Nominal	Mean Calculated Value (nm/count)	STD
DE14/T3M14	BHN	11752.8	3,063,978	0.066051	0.067189	-1.694	NA	NA
DE14/T3M14	BHN	11946.2	3,070,118	0.067003	0.067189	-0.277	NA	NA
DE14/T3M14	BHN	12336.5	3,060,207	0.069417	0.067189	3.316	NA	NA
DE14/T3M14	BHN	12463.2	3,070,086	0.069904	0.067189	4.041	NA	NA
DE14/T3M14	BHN	NA	NA	NA	NA	NA	0.068094	0.00186

Using the results from Table B-3, the non-systematic error is 2.732%, or 0.1171 dB. We had no

capability to measure the instrument constants provided by the manufacturer, which would be one source of systematic error.

Normalized system amplitude and system phase responses for Guralps and GS13s with Reftex digitizers follow. The normalized values were multiplied by the calib value at 1 Hz to determine the power spectra as a function of frequency.

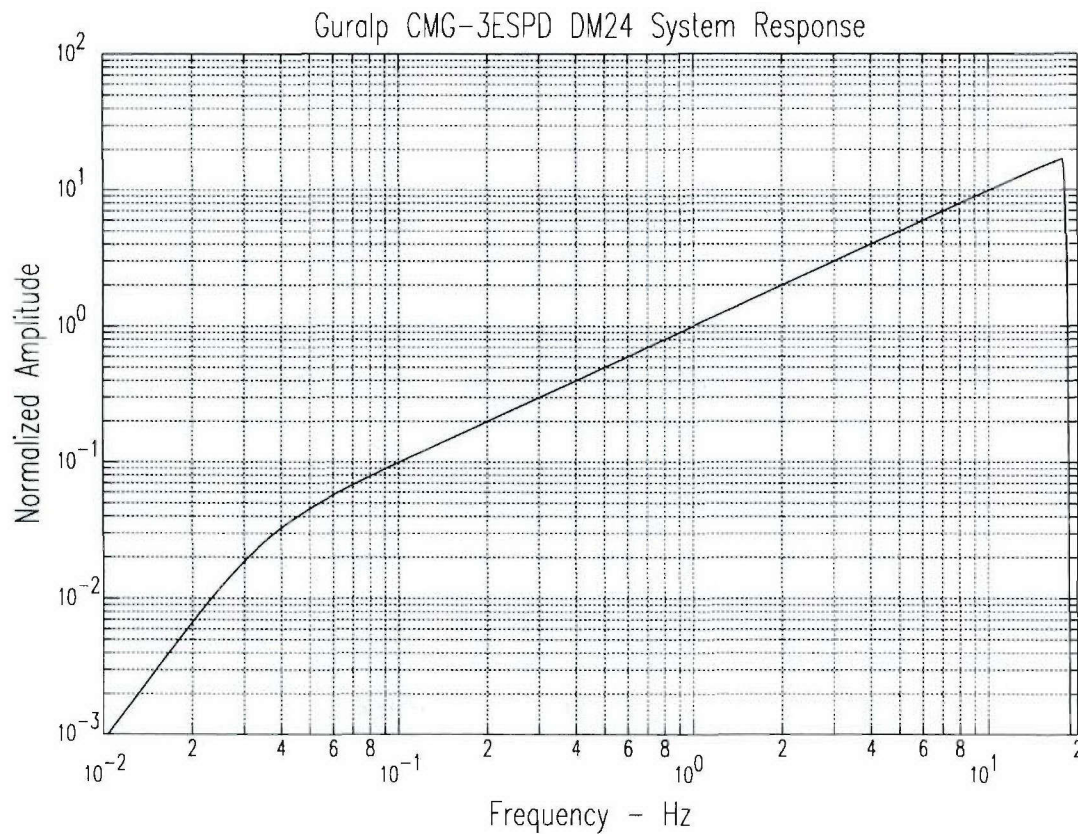


Figure B-1. Guralp CMG-3ESPD DM24 System amplitude response.

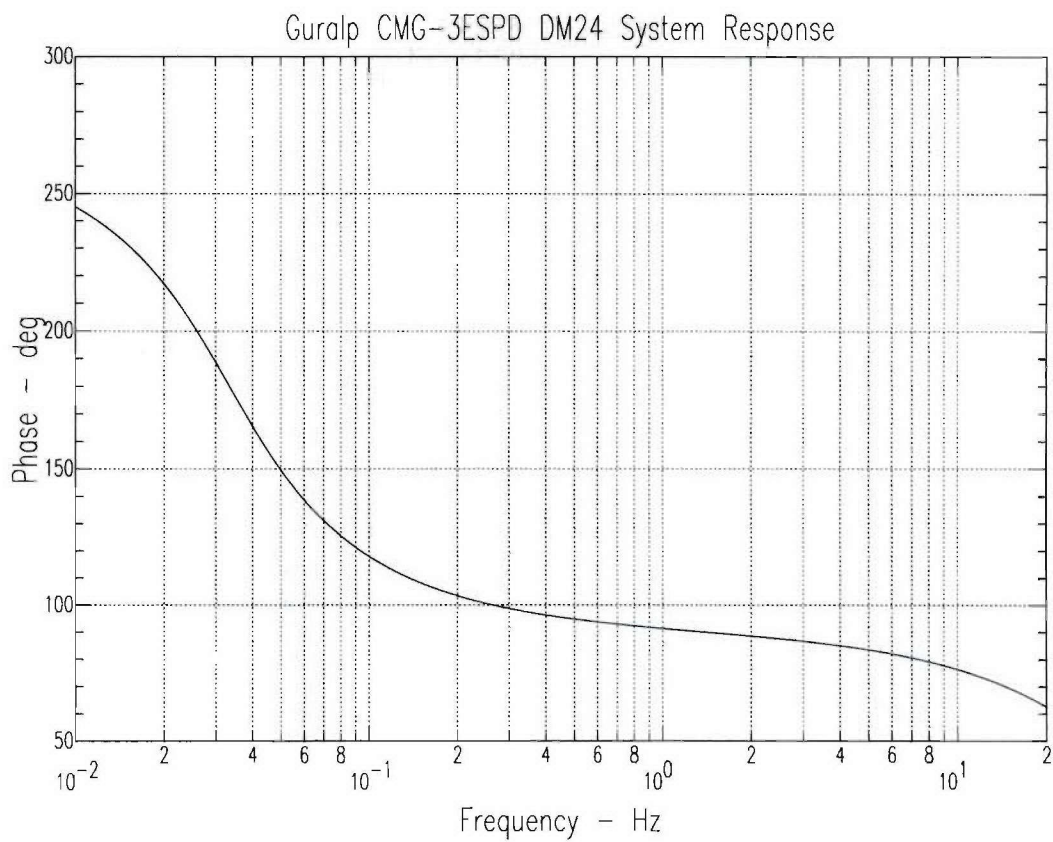


Figure B-2. Guralp CMG-3ESPD DM24 System phase response.

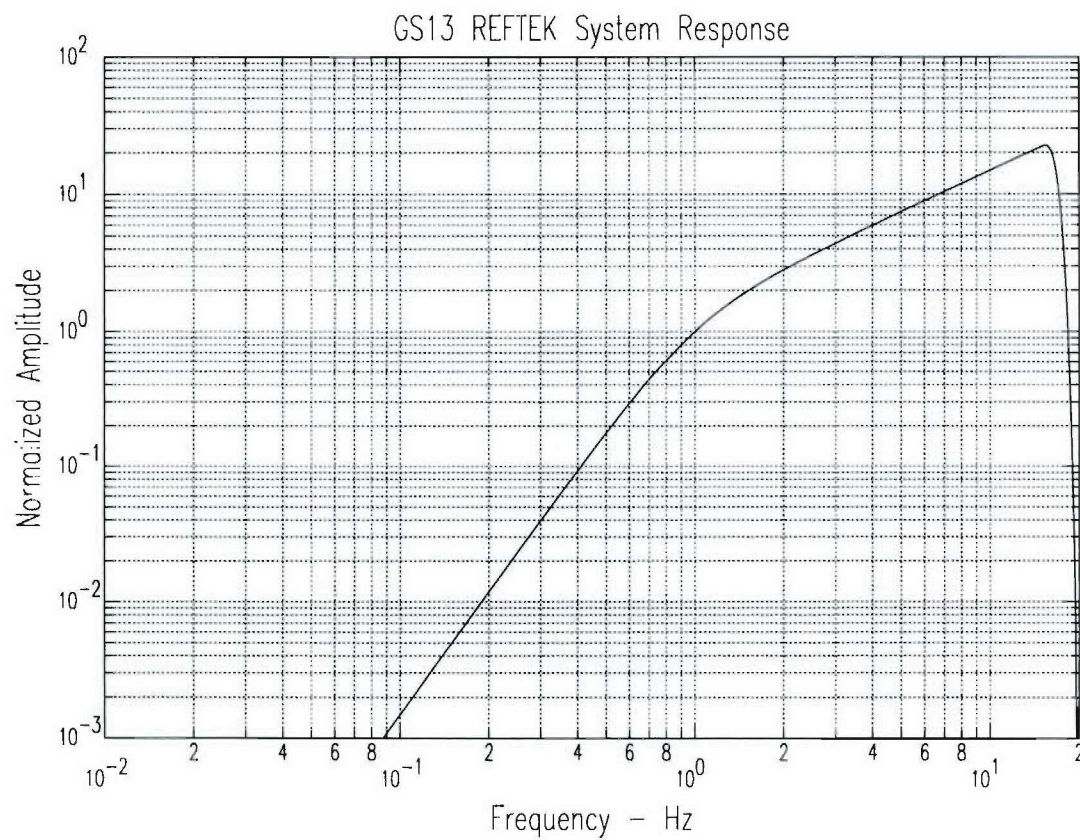


Figure B-3. Reftek/GS-13 System amplitude response.

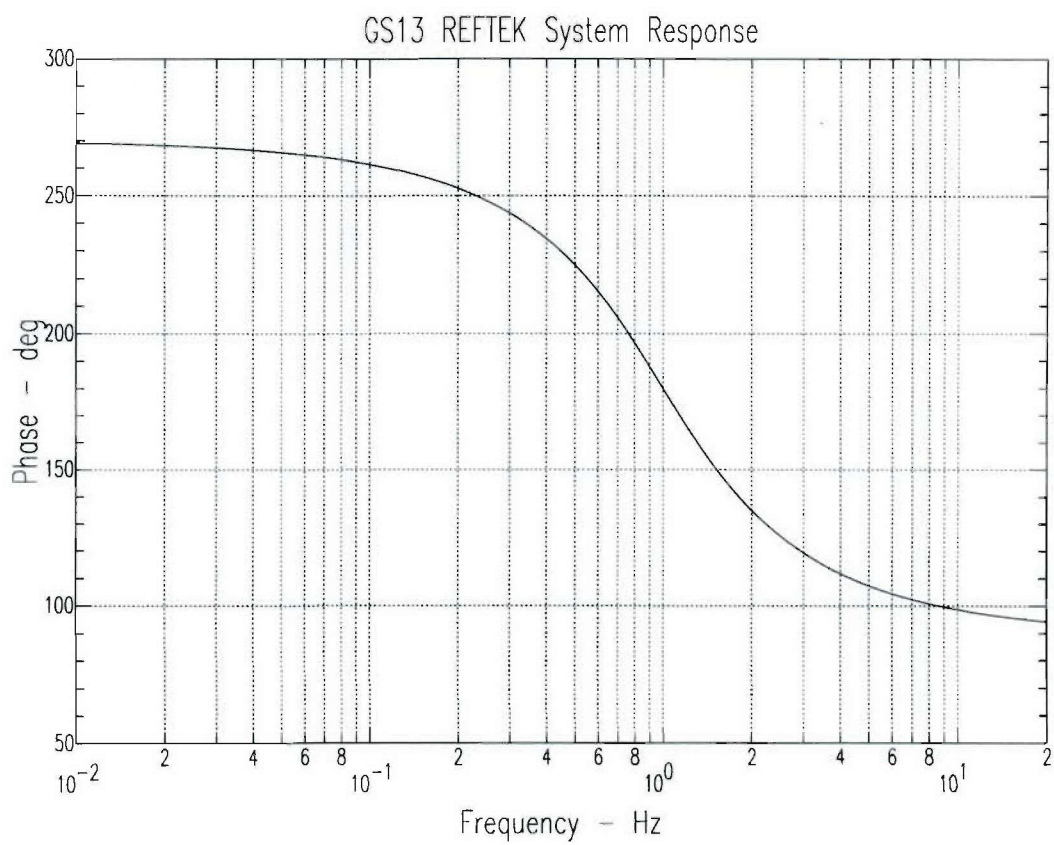


Figure B-4. Reftek/GS13 System phase response.

GS13 Reftek Calibrations.

Since the GS13 Reftek data were not calibrated in the field, the co-located Guralp at Site 3 (sensor DE15) was used to calibrate the GS13 Reftek data. A side-by-side noise analysis was performed on Site 3 data to determine the GS13 Reftek data calib value. As shown in Figure B-5 below, the GS13 Reftek data (red trace) matches the Guralp data (blue trace) at 1 Hz. For the Guralp data, a calib value of 0.066810 nm/count was used. For the GS-13 Reftek data, a calib value of 125,000 nm/count was used. Therefore, the 125,000 nm/count calib value was used to analyze all of the GS13 Reftek data for the Morocco survey.

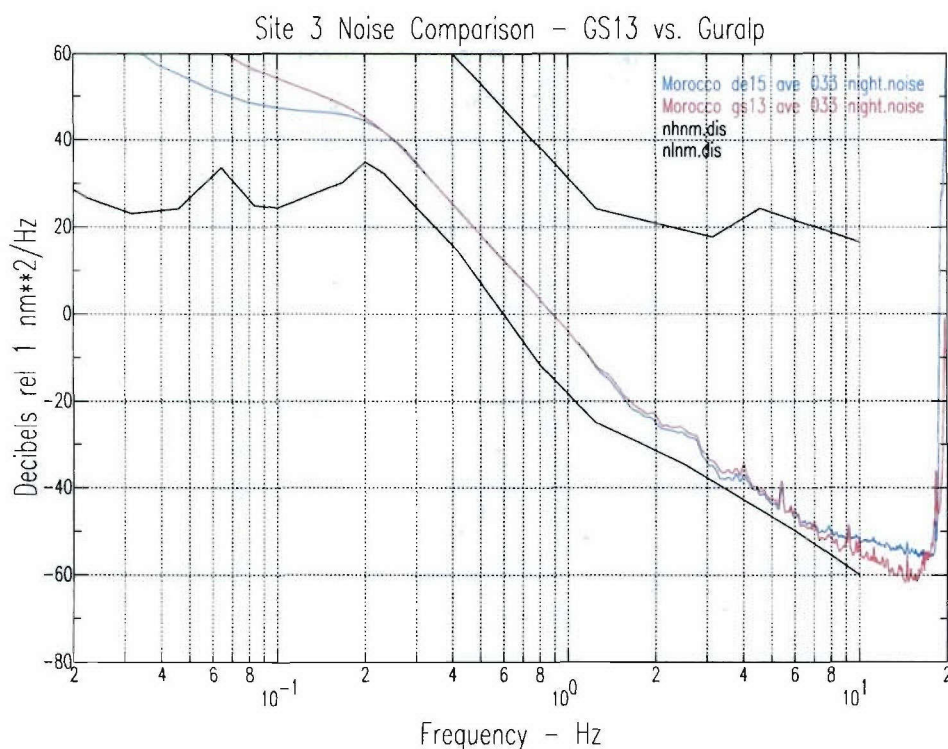


Figure B-5. Noise comparison between the GS13 Reftek and co-located Guralp systems. For a calib value of 125,000 (102 dB), the GS13 matches the DE15 instrument response at 1 Hz. Note also that for frequencies above about 7 Hz, the Guralp power spectra and the GS13 power spectra diverge. This is due to system noise from the Guralp system above 7 Hz. The higher level of power spectra above 17 Hz is due to the anti-alias filter.

Interpolation of Input Voltage from the Guralp Calibrator.

For the Guralps, we calibrated the instruments with a 1 Hz sinusoid for a duration of 1 minute. The input voltage for the calibrator was also recorded on a separate data channel, but only at a sample rate of four samples per second, and these points did not necessarily correspond to a minima or maxima on the sine wave function. Consequently, we had to interpolate between data points to find the maxima and minima for the input voltage. This was done by transforming the time domain

input signal calibrator data to the frequency domain, adding zeros in the frequency domain to the input spectra at the lowest frequencies, and then transforming the result back to the time domain. This procedure effectively increased the resolution of the time domain sinusoid. In addition, we found that the input voltage varied from cycle-to-cycle by several percent, which effectively limited the accuracy of the calibration. Using the nominal values for the instrument constants, we were then able to correct the theoretical instrument gain by a constant determined from the calibration data. This is now demonstrated in the next figure, where a sine wave with unity amplitude was phase shifted by $\pi/4$ degrees with only four points per cycle given. These data were then interpolated by the algorithm for curve fitting described above. Maximum value is, in fact, 0.999987 confirming the interpolation is done correctly for a true maxima of 1.00000.

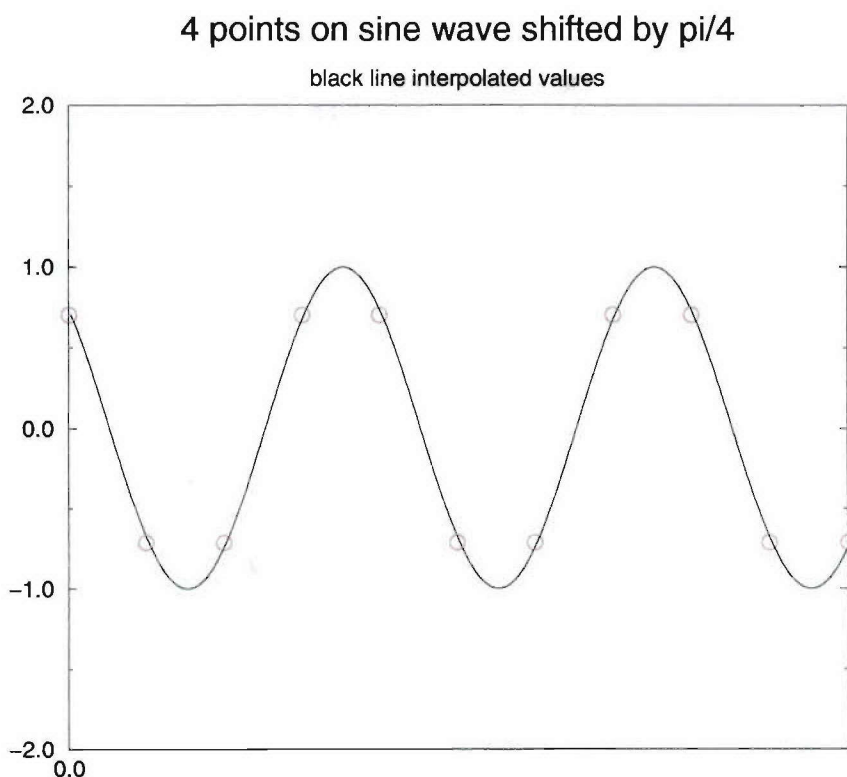


Figure B-6. A sine wave was interpolated from a waveform segment which has a 45° phase shift, with four points per cycle for 62 cycles. The interpolated values, plotted in black, were computed using the zero fill method described above. The true maximum is 1.00000, which is represented by here by 0.999987 for this test case. The same method was used for the calibration results, to obtain the true output voltage from the calibrator.

Appendix C

Power Spectral Noise Plots

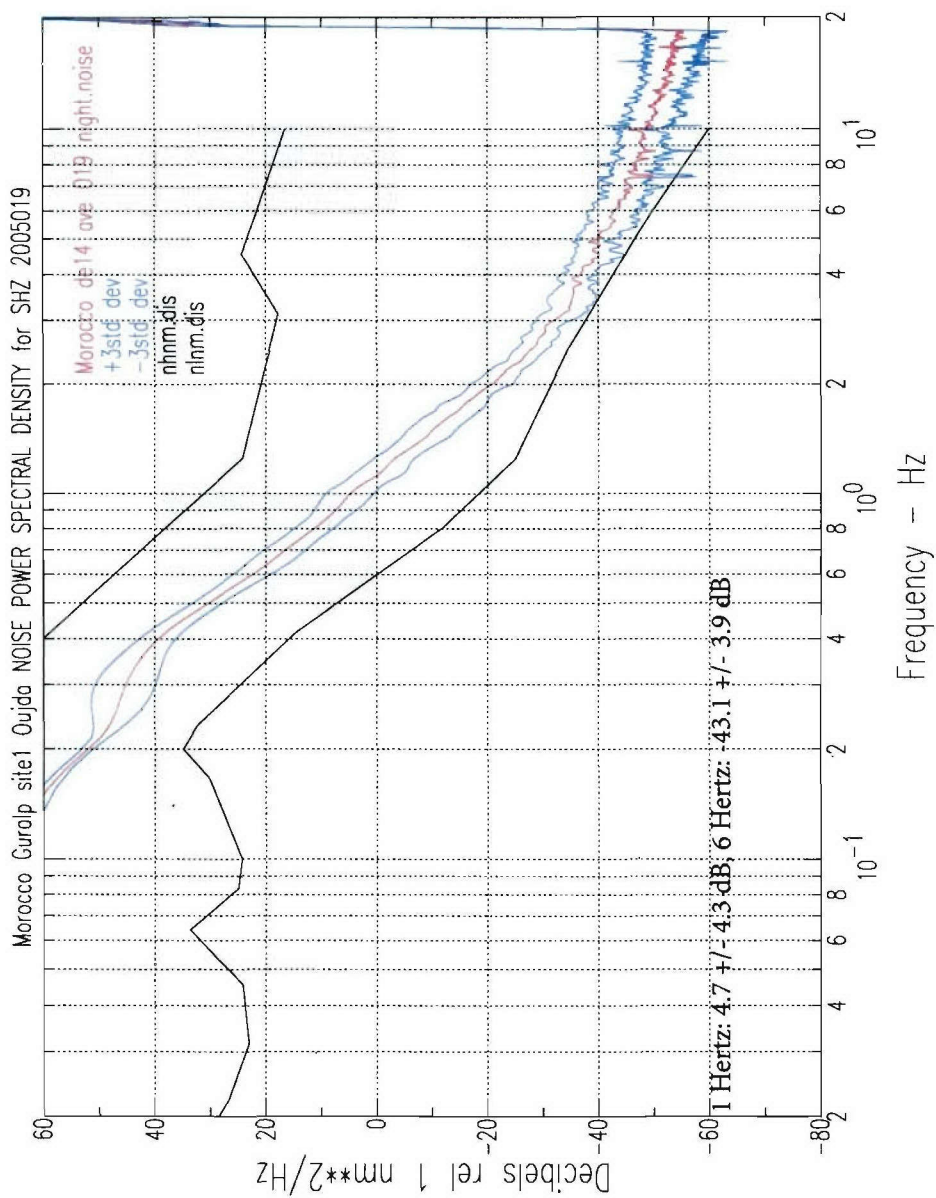


Figure C-1. Morocco Guralp Site 1, sensor DE14, DOY 019, night noise.

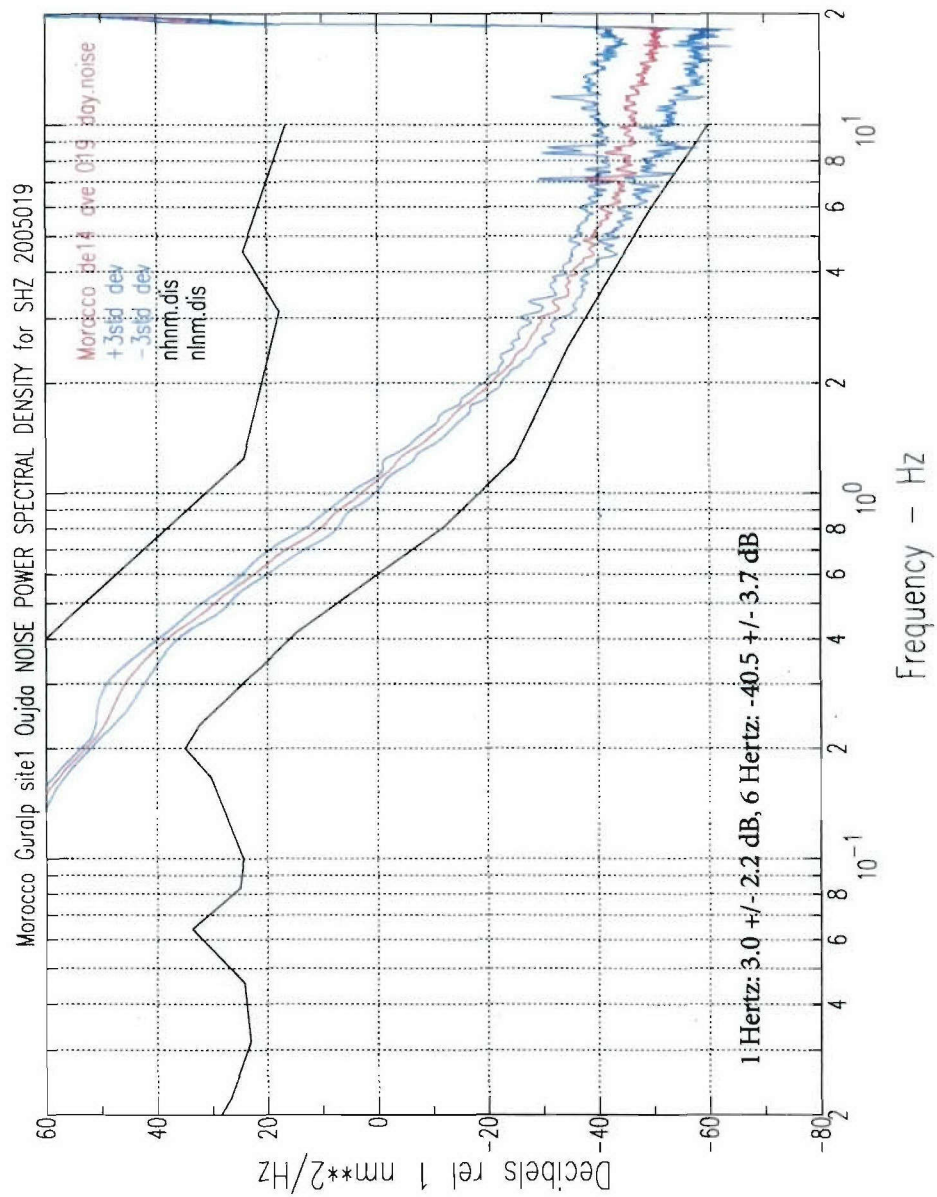


Figure C-2. Morocco Guralp Site 1, sensor DE14, DOY 019, day noise.

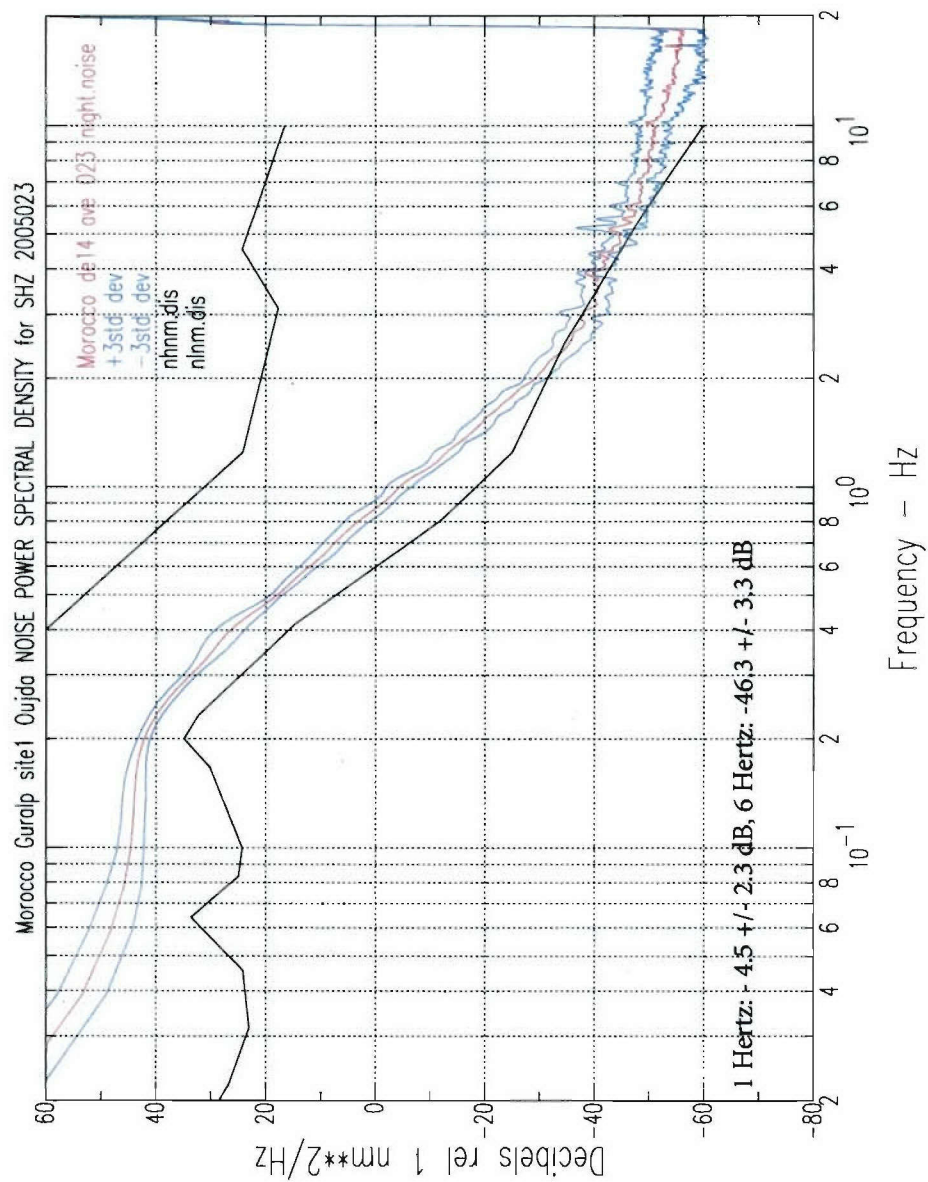


Figure C-3. Morocco Guralp Site 1, sensor DE14, DOY 023, night noise.

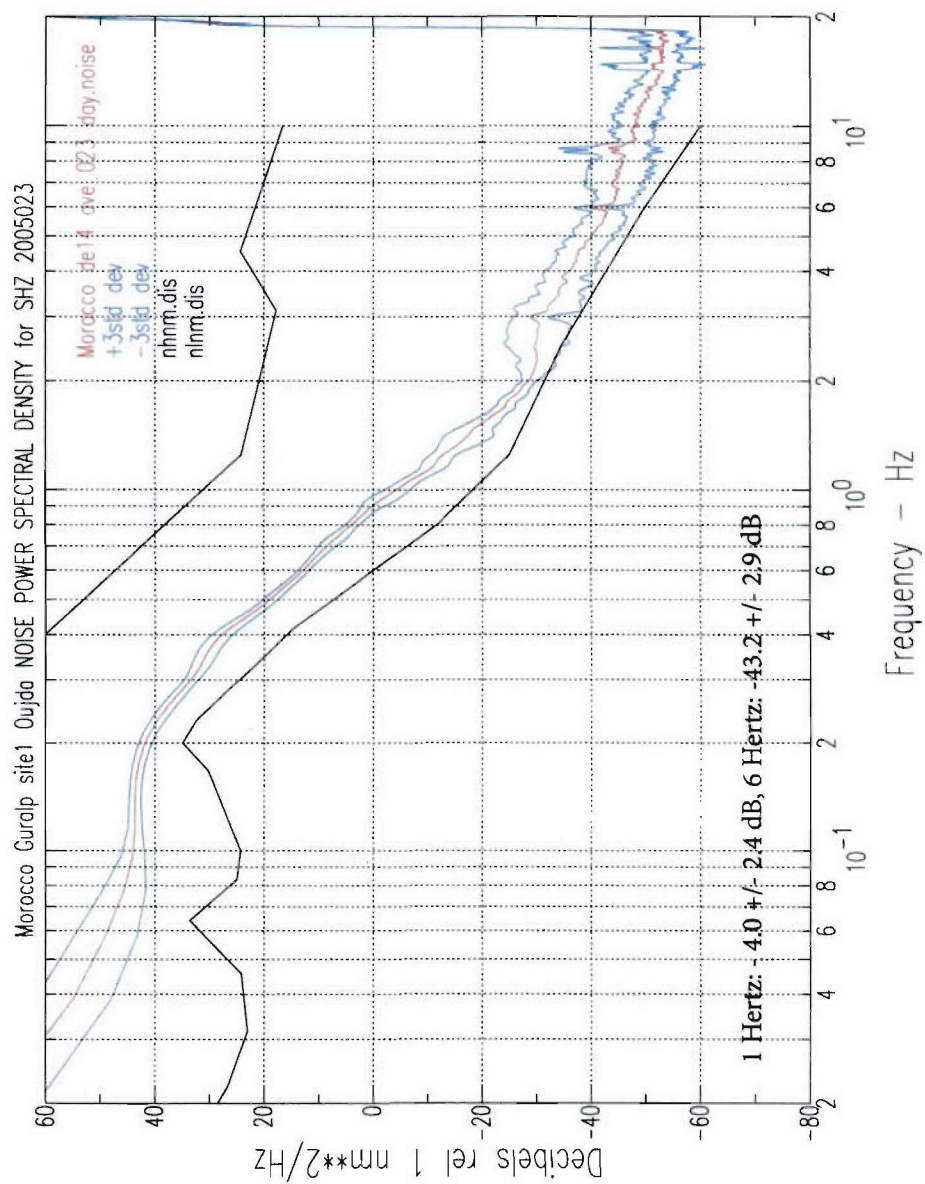


Figure C-4. Morocco Guralp Site 1, sensor DE14, DOY 023, day noise.

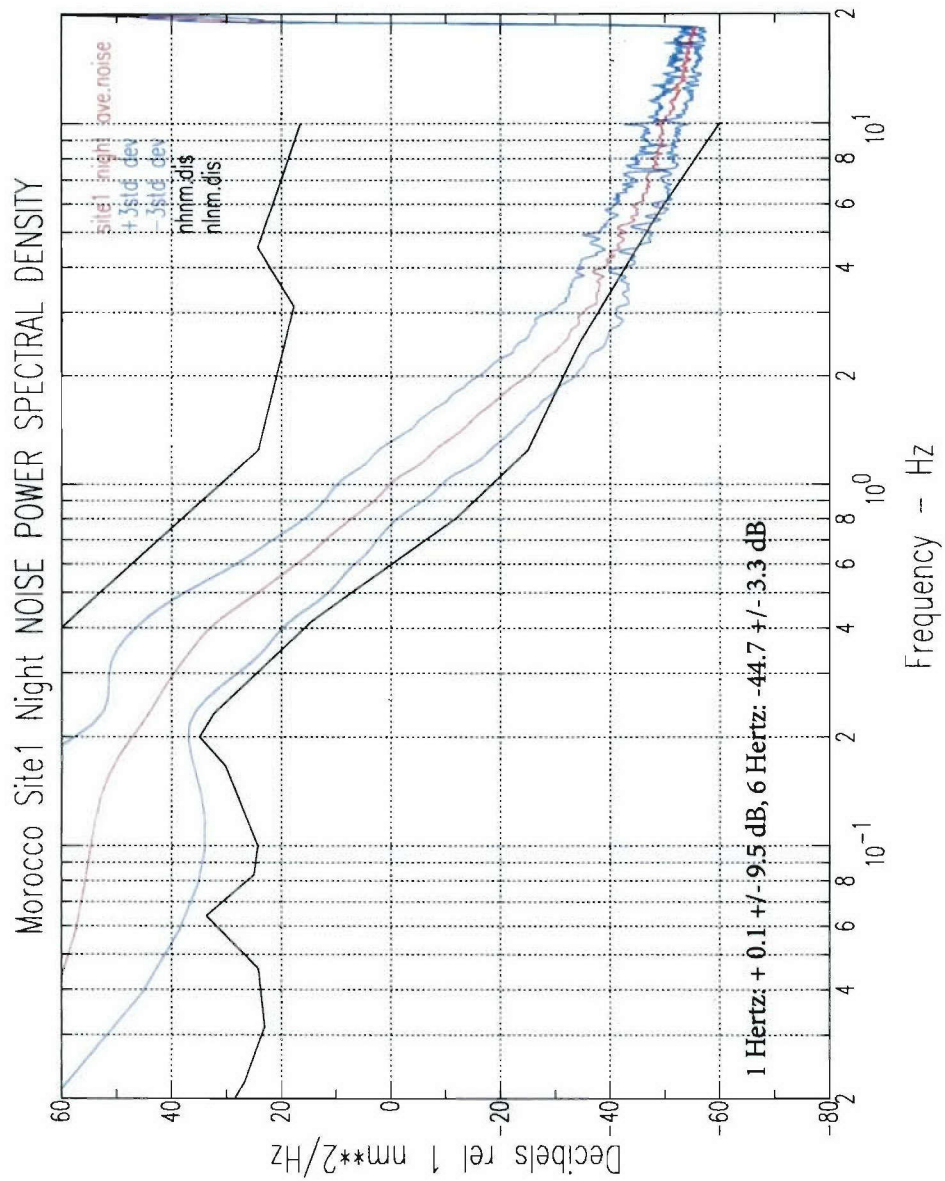


Figure C-5. Morocco Guralp Site 1, night average noise.

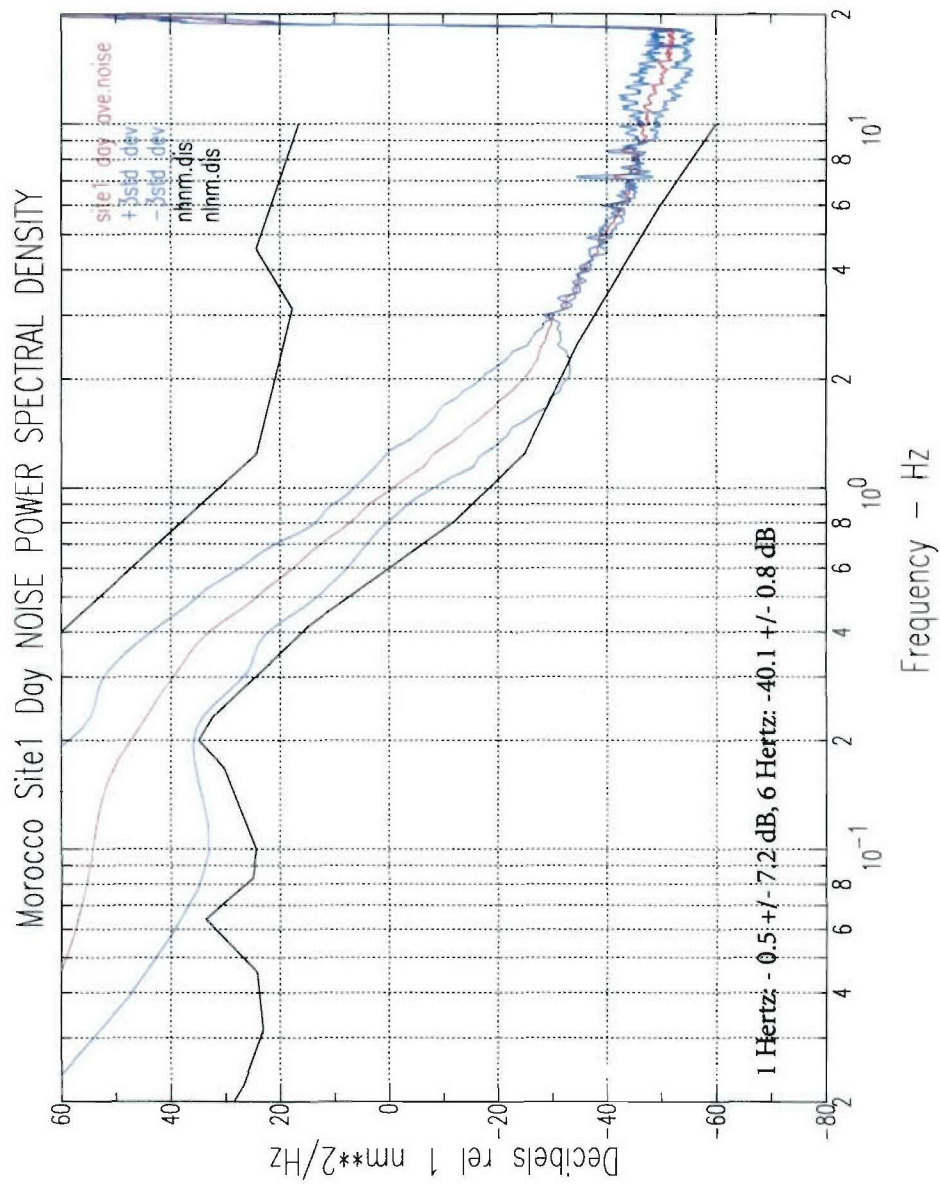


Figure C-6. Morocco Guralp Site 1, day average noise.

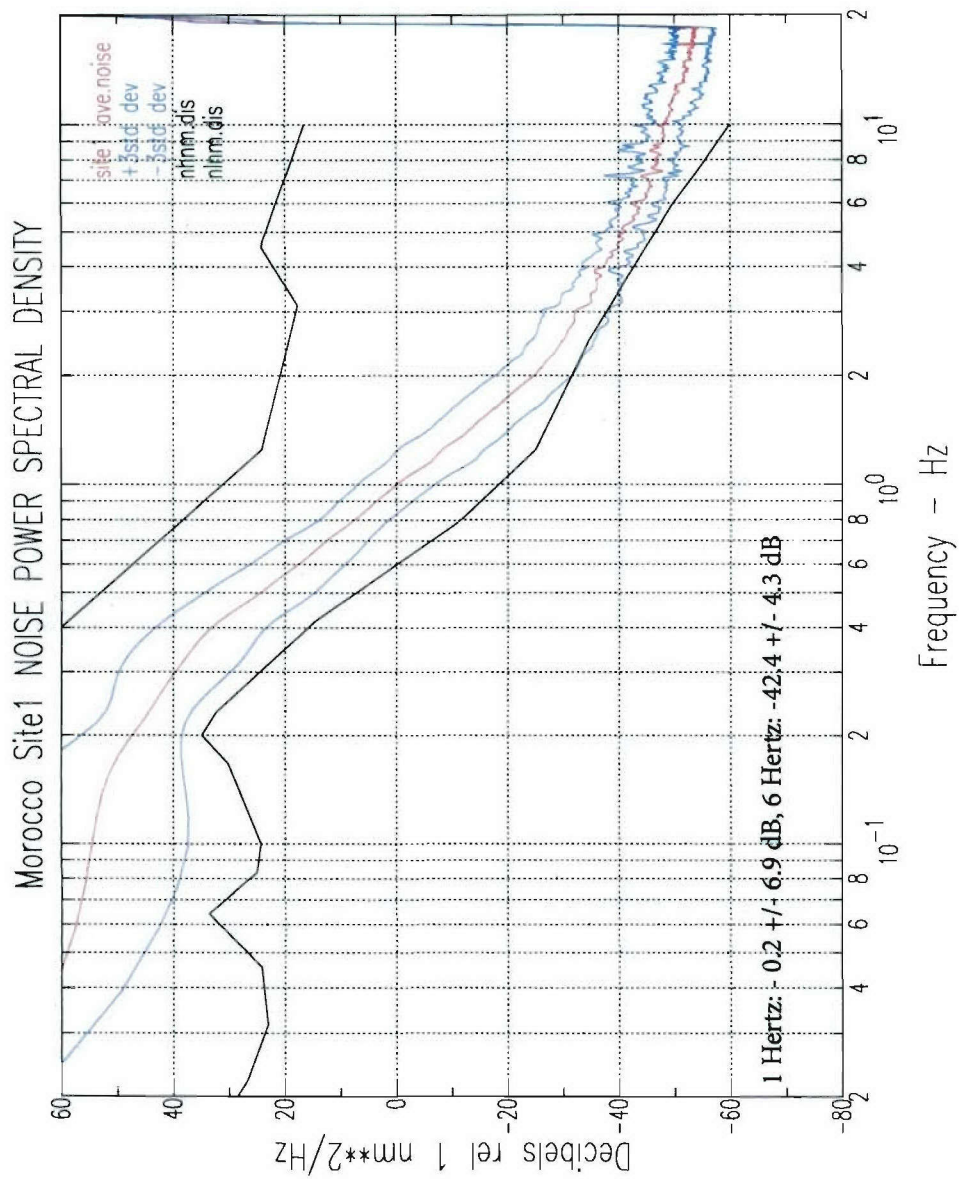


Figure C-7. Morocco Guralp Site 1, average noise.

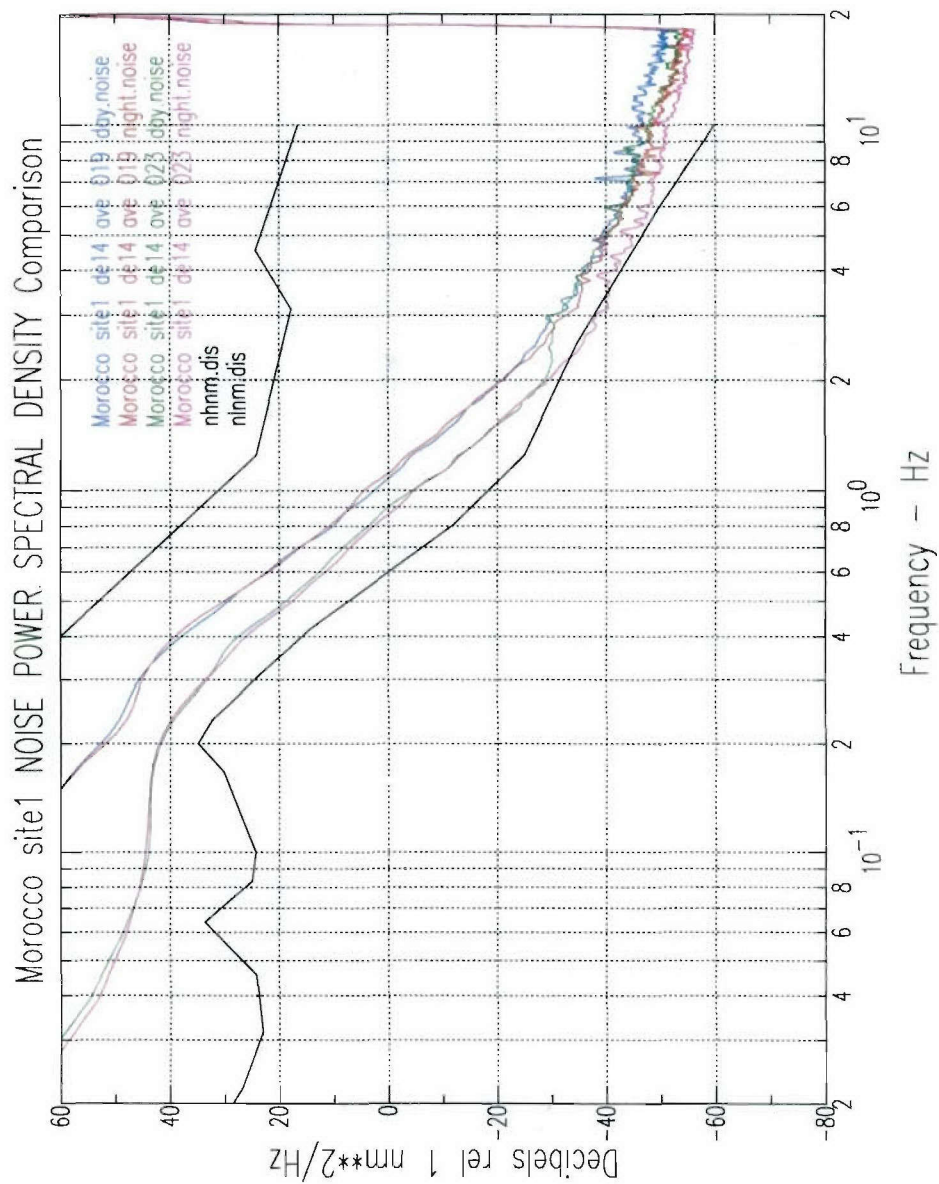


Figure C-8. Morocco Site 1, comparison day and night noise.

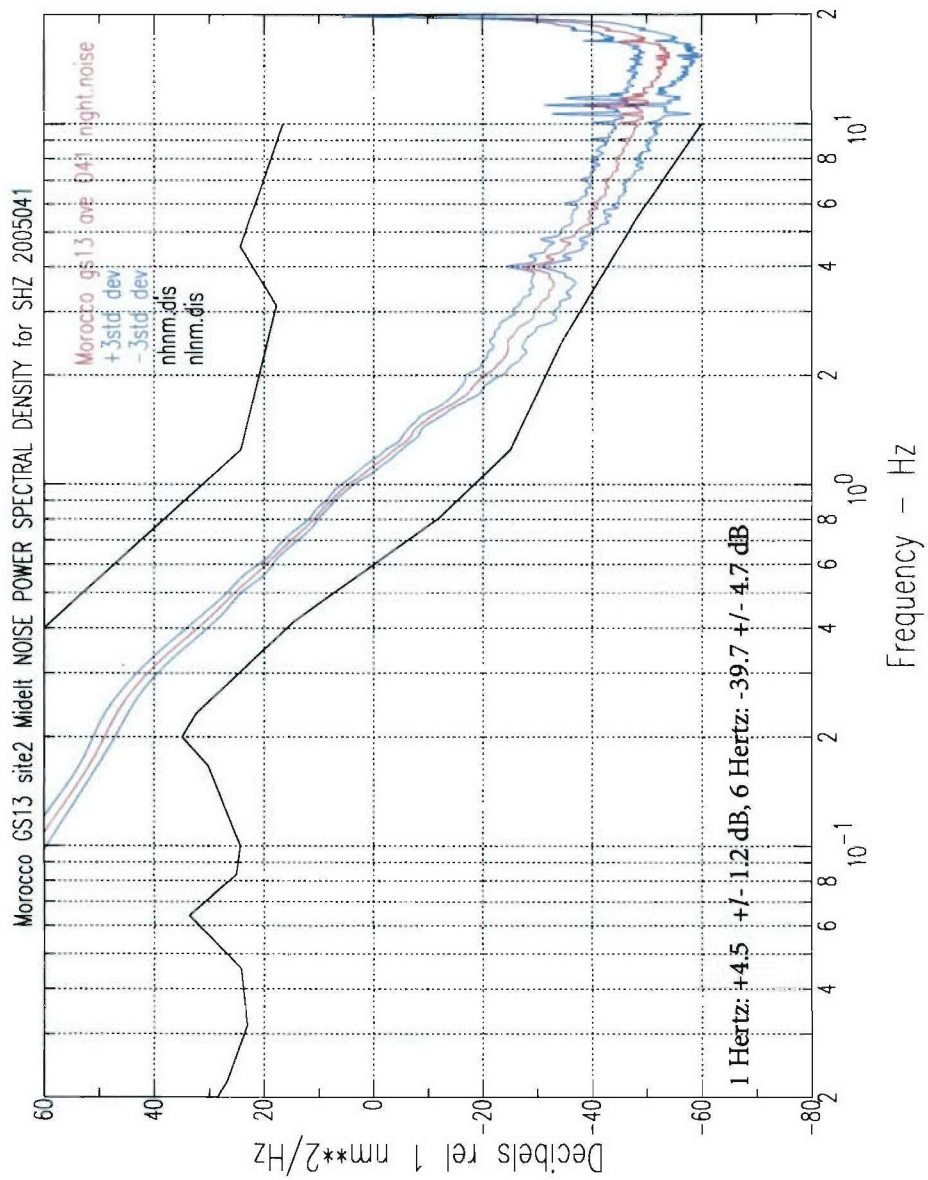


Figure C-9. Morocco GS13 Site 2, DOY 041, night noise

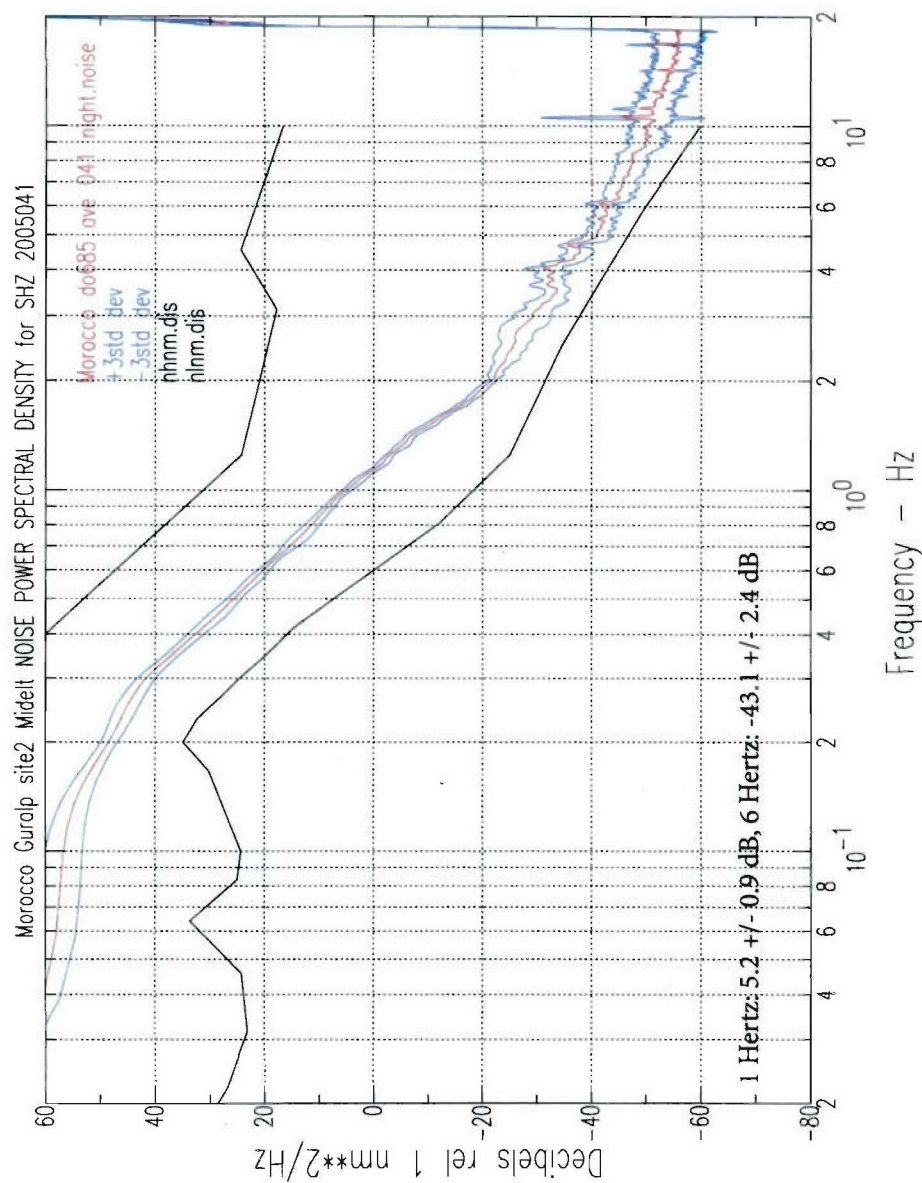


Figure C-10. Morocco Guralp Site 2, sensor DO685, DOY 041, night noise.

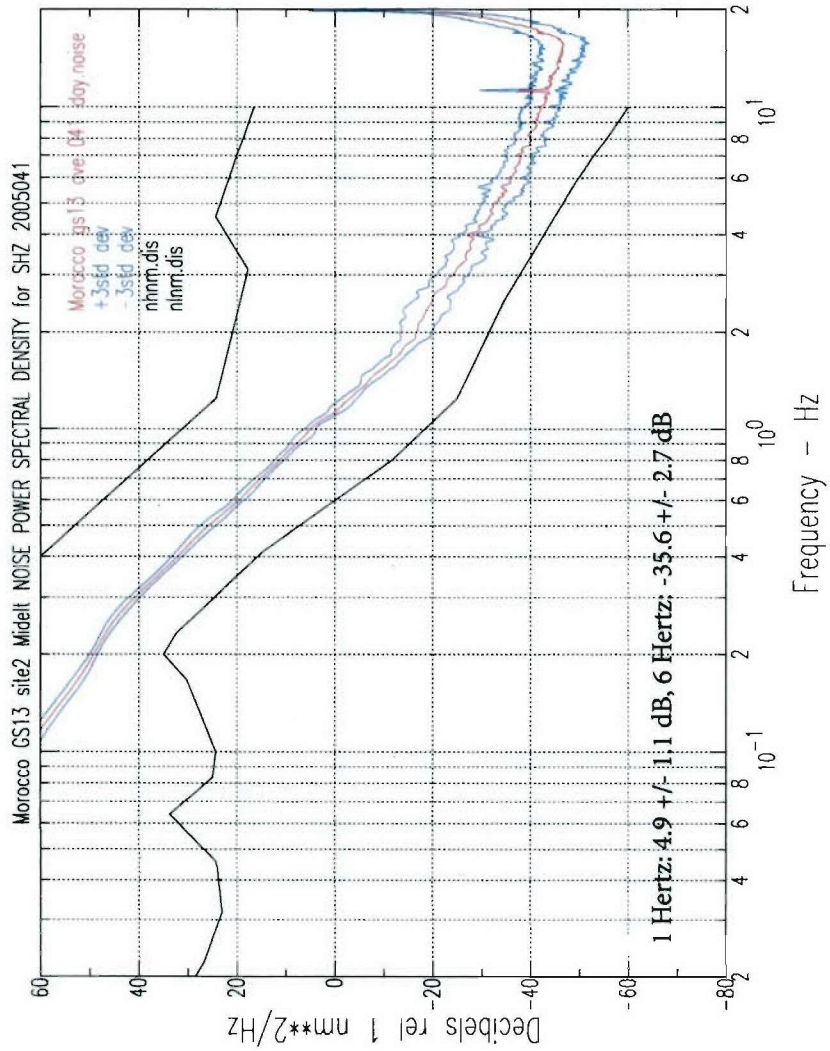


Figure C-11. GS13 Site 2, day noise for DOY 041.

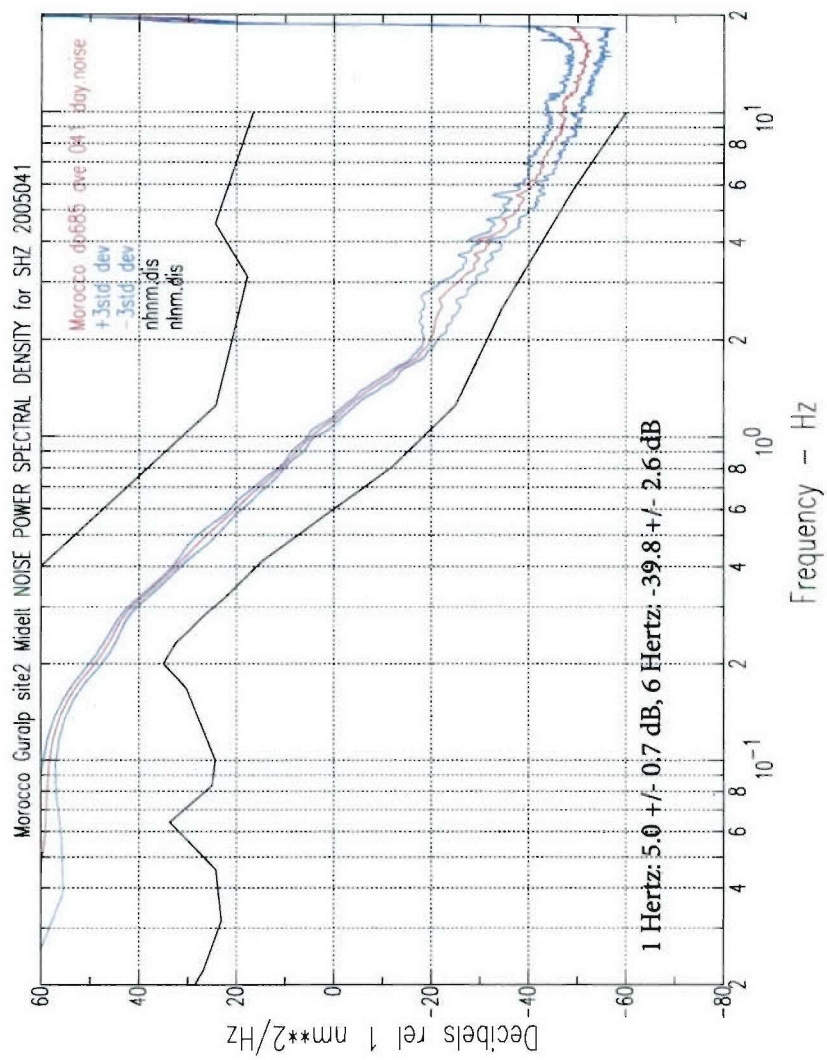


Figure C-12. Guralp DO685, DOY 041, day noise.

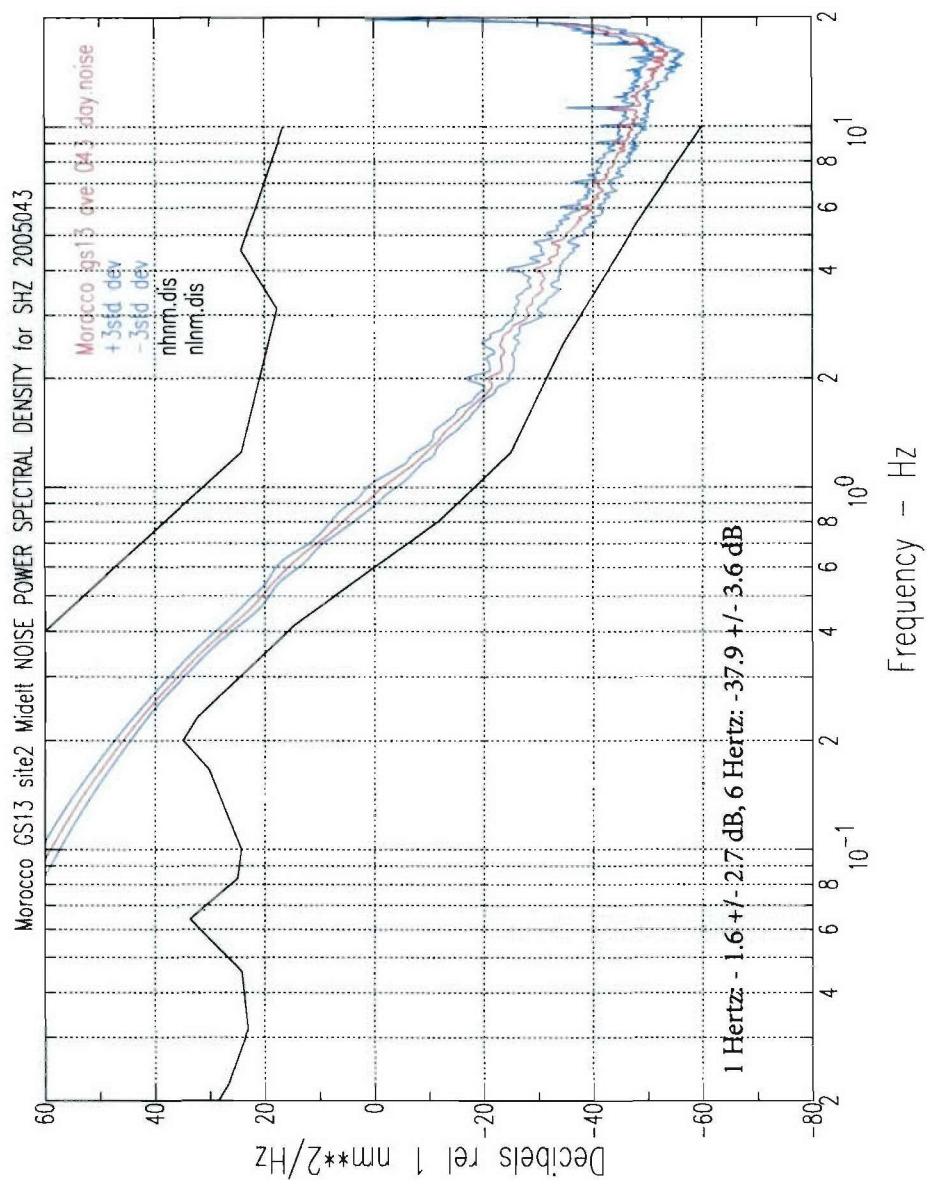


Figure C-13. Morocco GS13 Site 2, DOY 043, day noise.

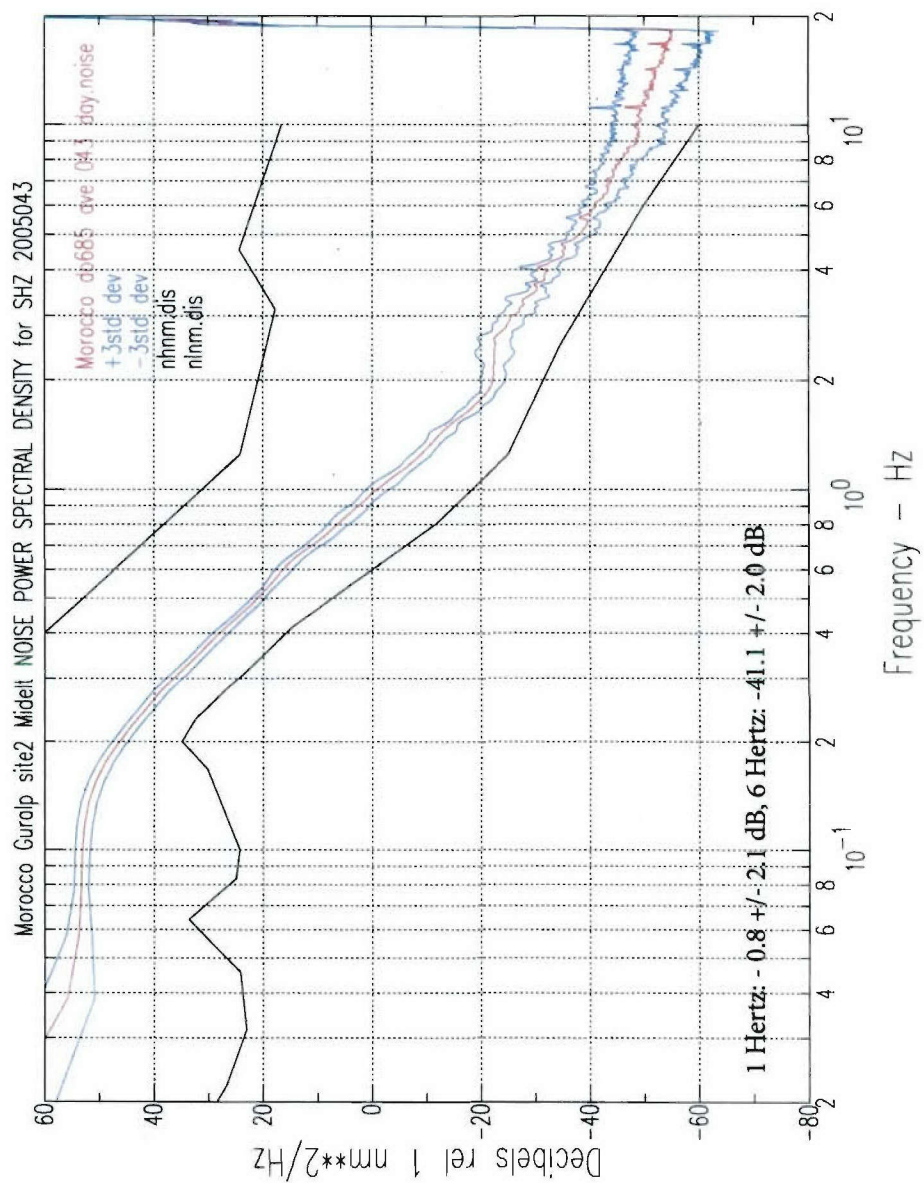


Figure C-14. Morocco Guralp Site 2, sensor DO685, DOY 043, day noise.

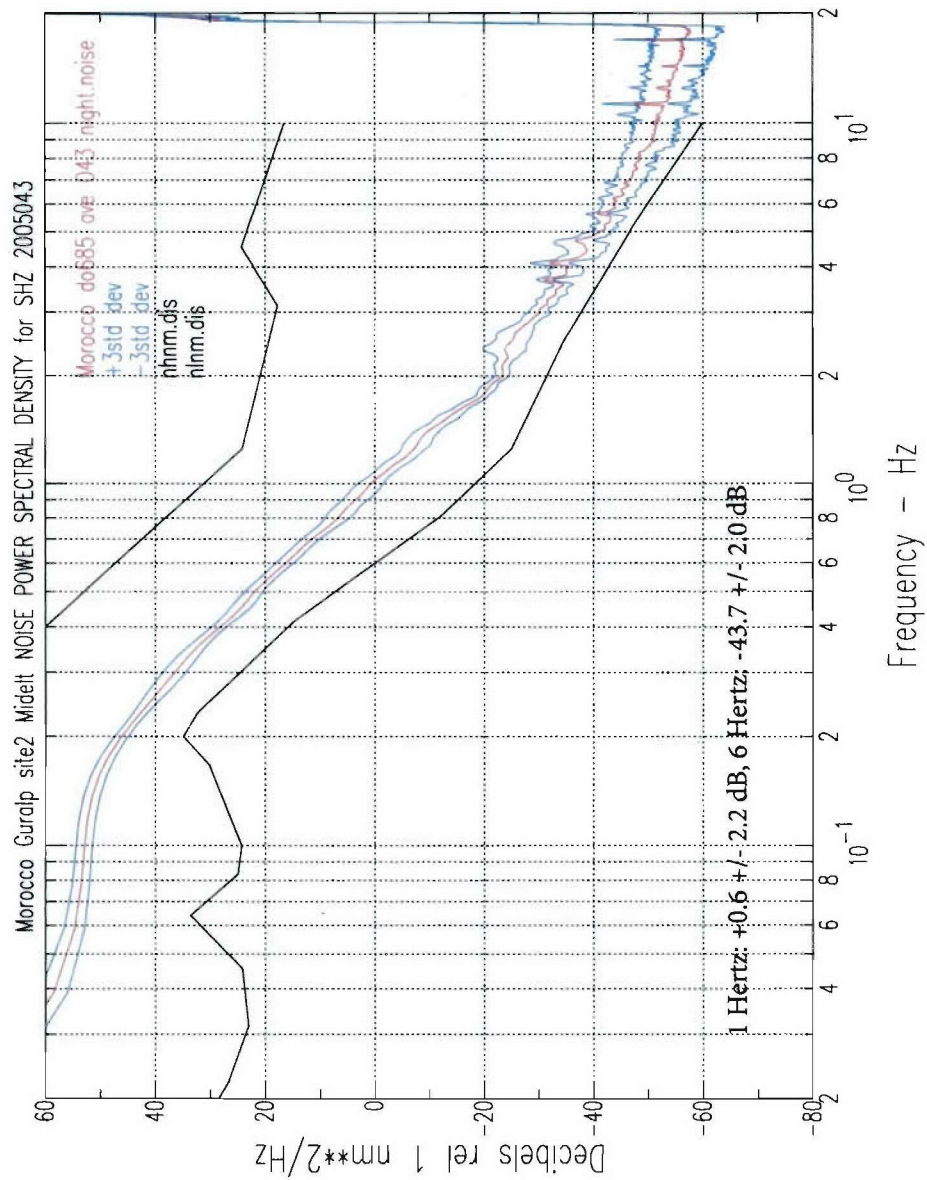


Figure C-15. Morocco Guralp Site 2, sensor DO685, DOY 043, night noise.

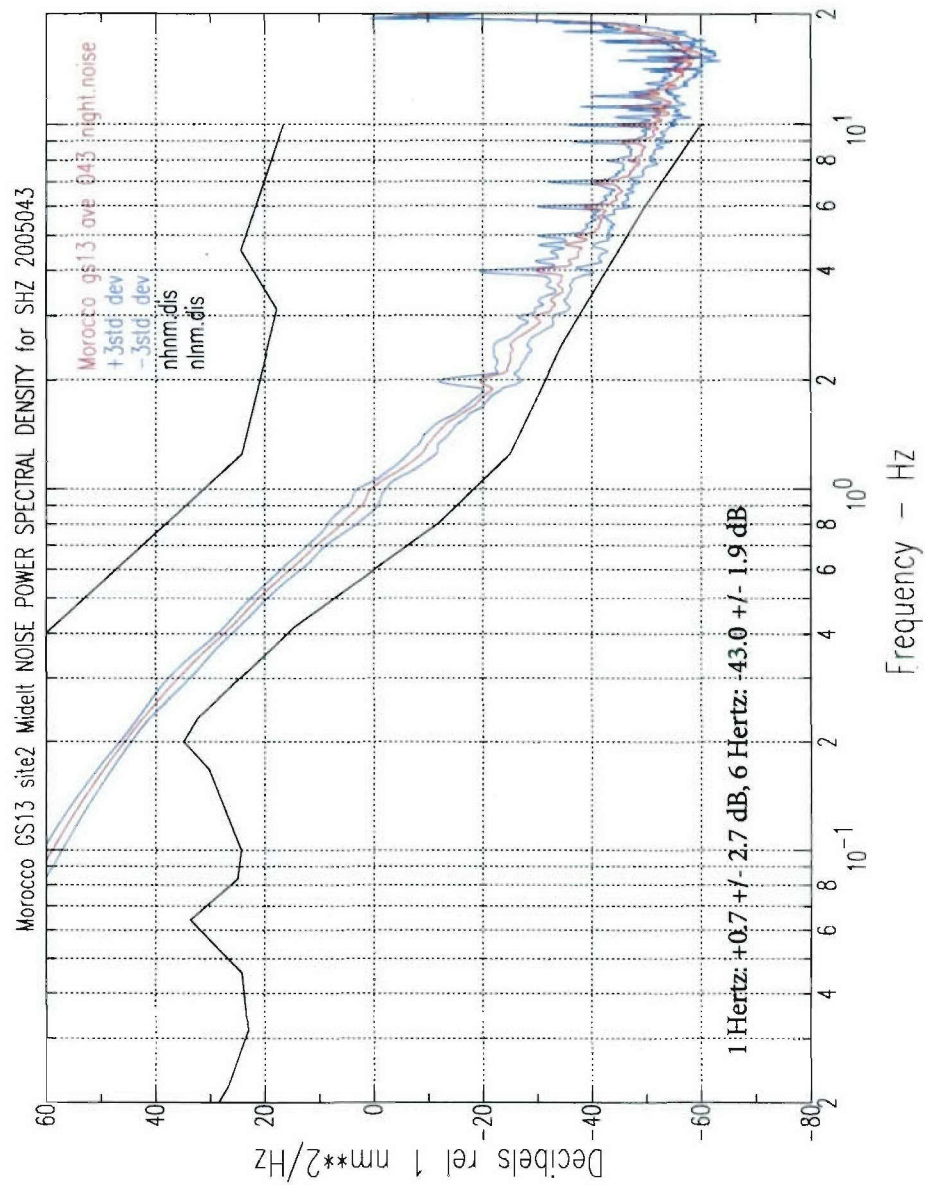


Figure C-16. Morocco GS13 Site 2, DOY 043, night noise.

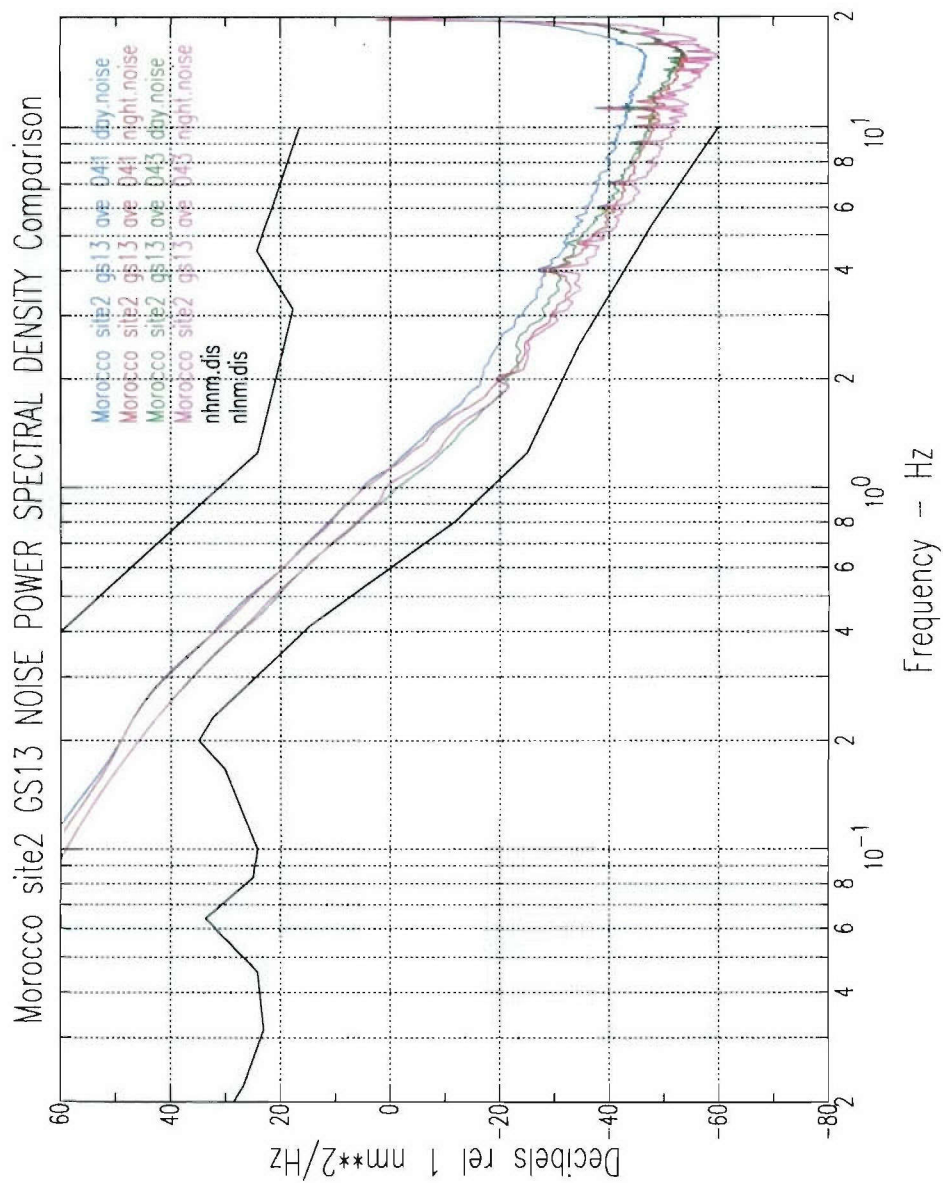


Figure C-17. Morocco Site 2 GS13, comparison day and night noise.

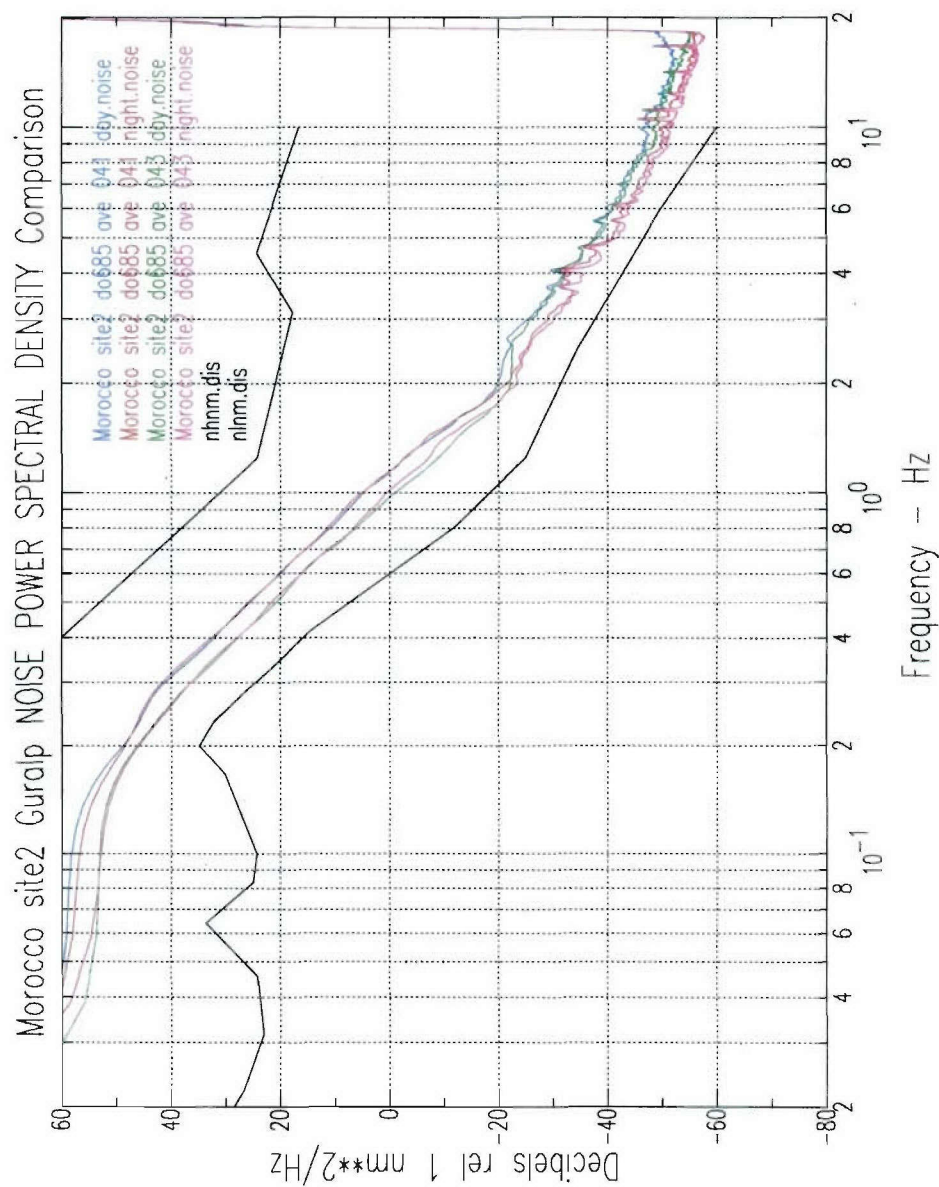


Figure C-18. Morocco Site 2 Guralp comparison day and night noise.

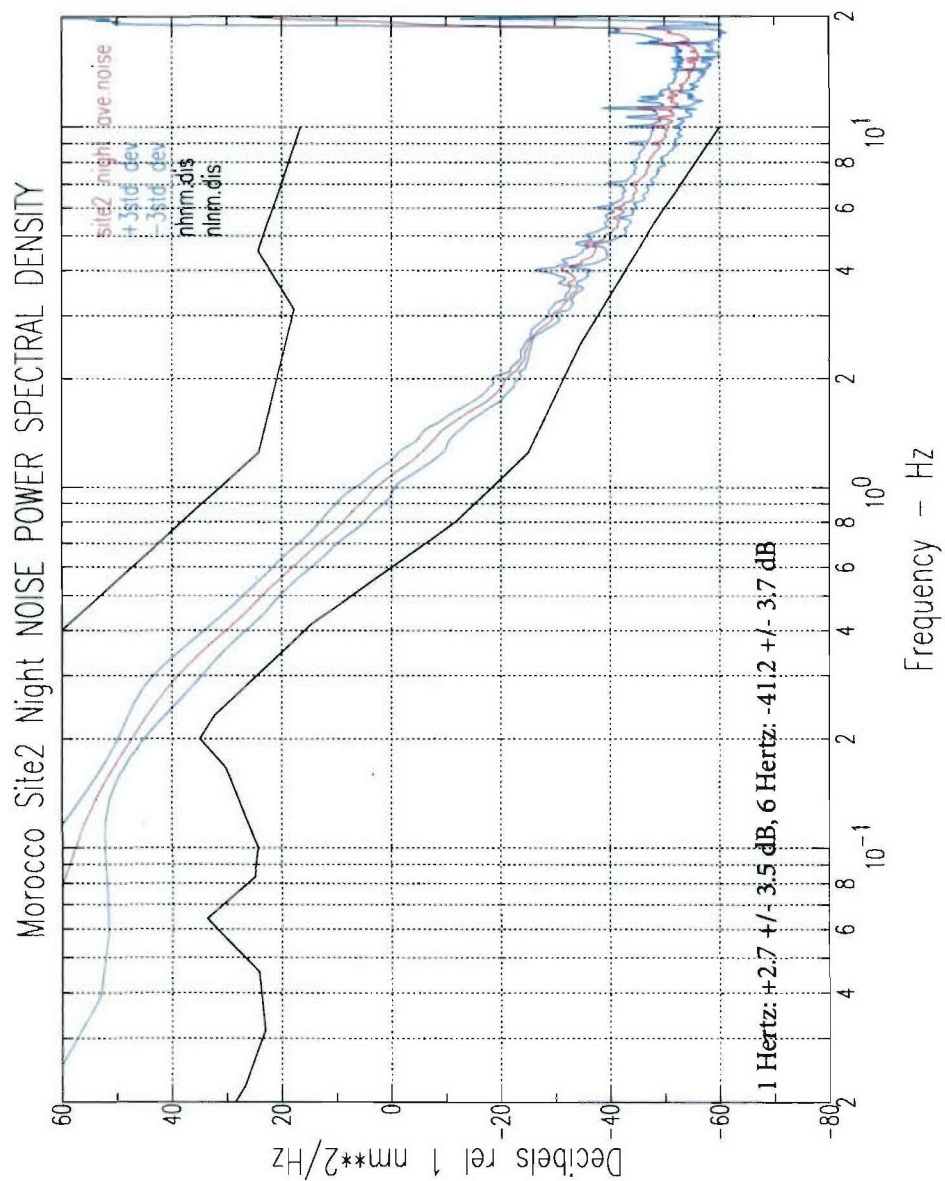


Figure C-19. Morocco Site 2, night average noise.

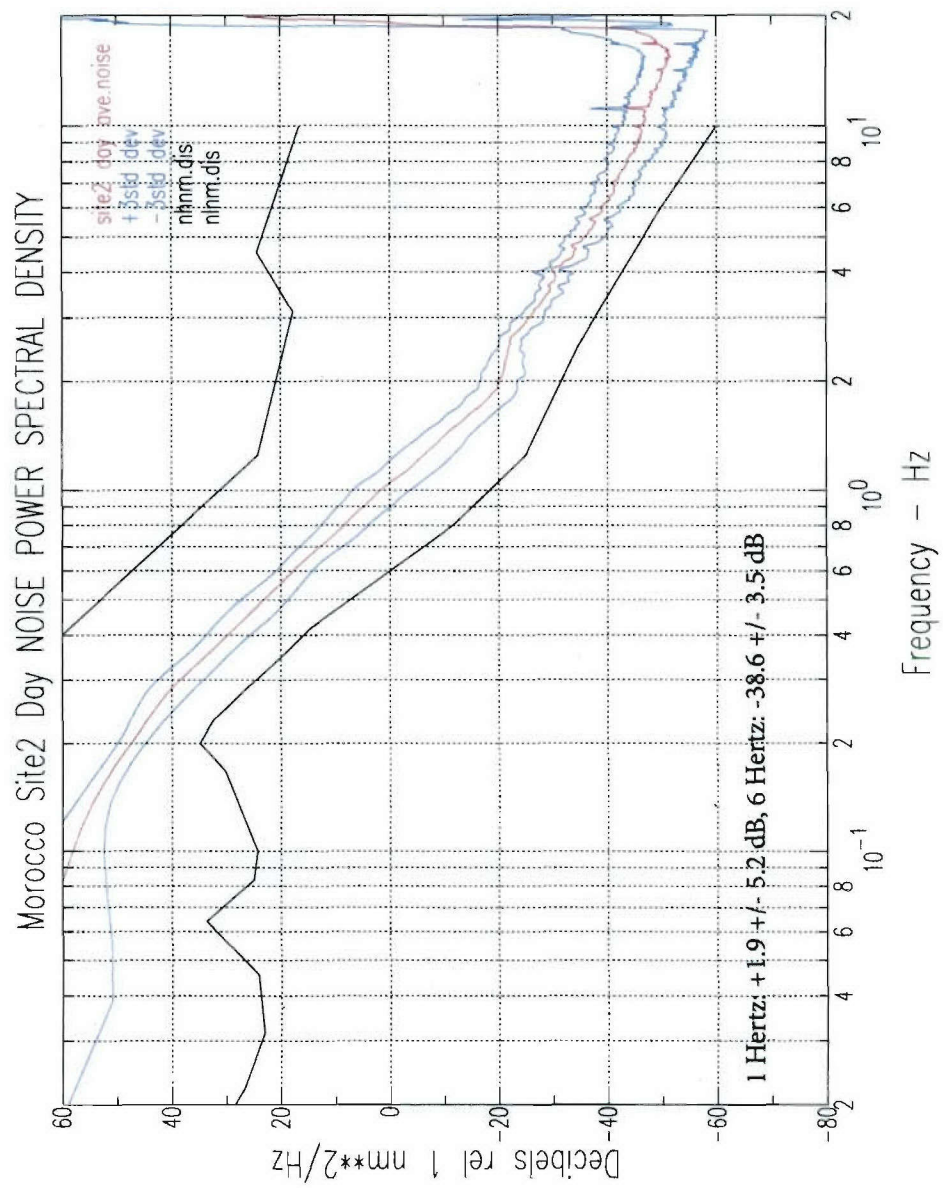


Figure C-20. Morocco Site 2, day average noise.

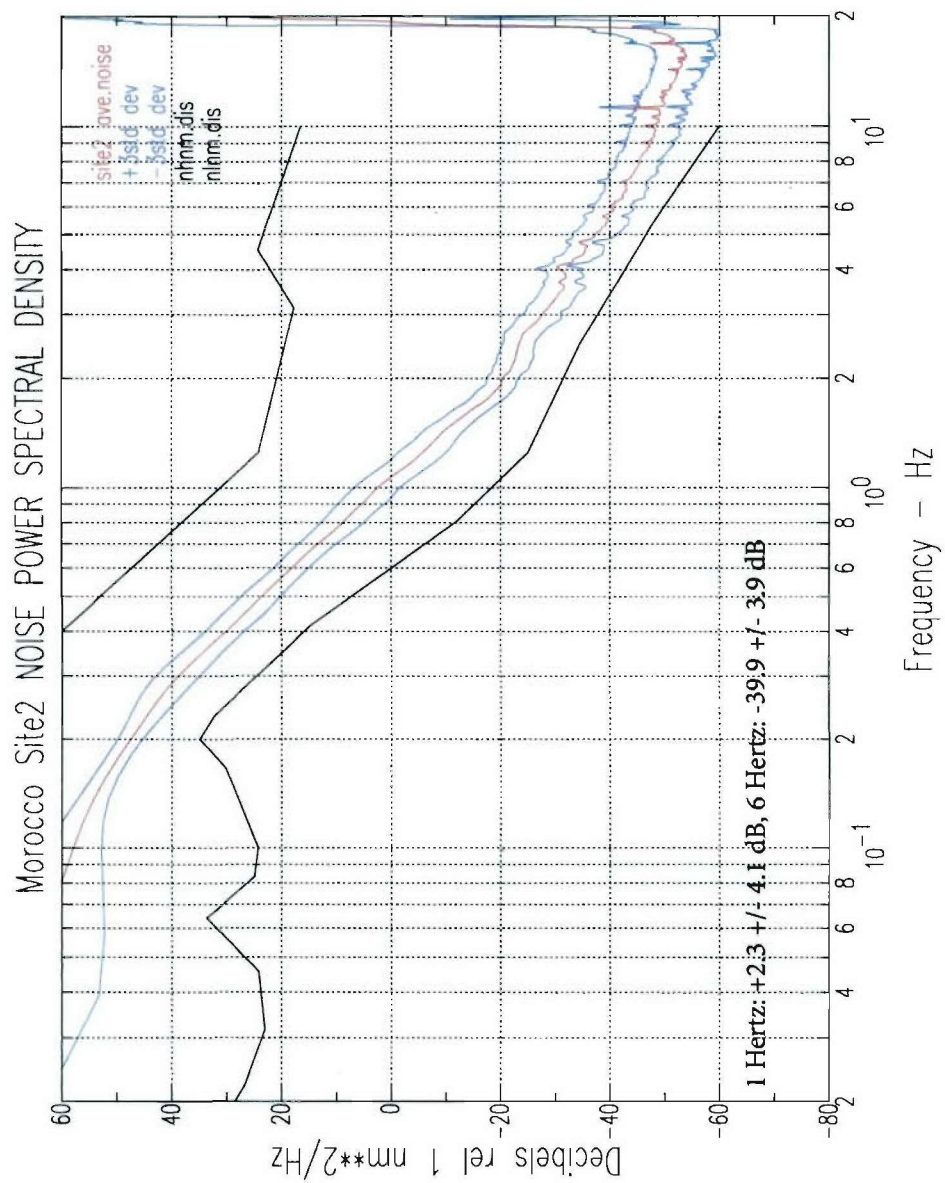


Figure C-21. Morocco Site 2, average noise

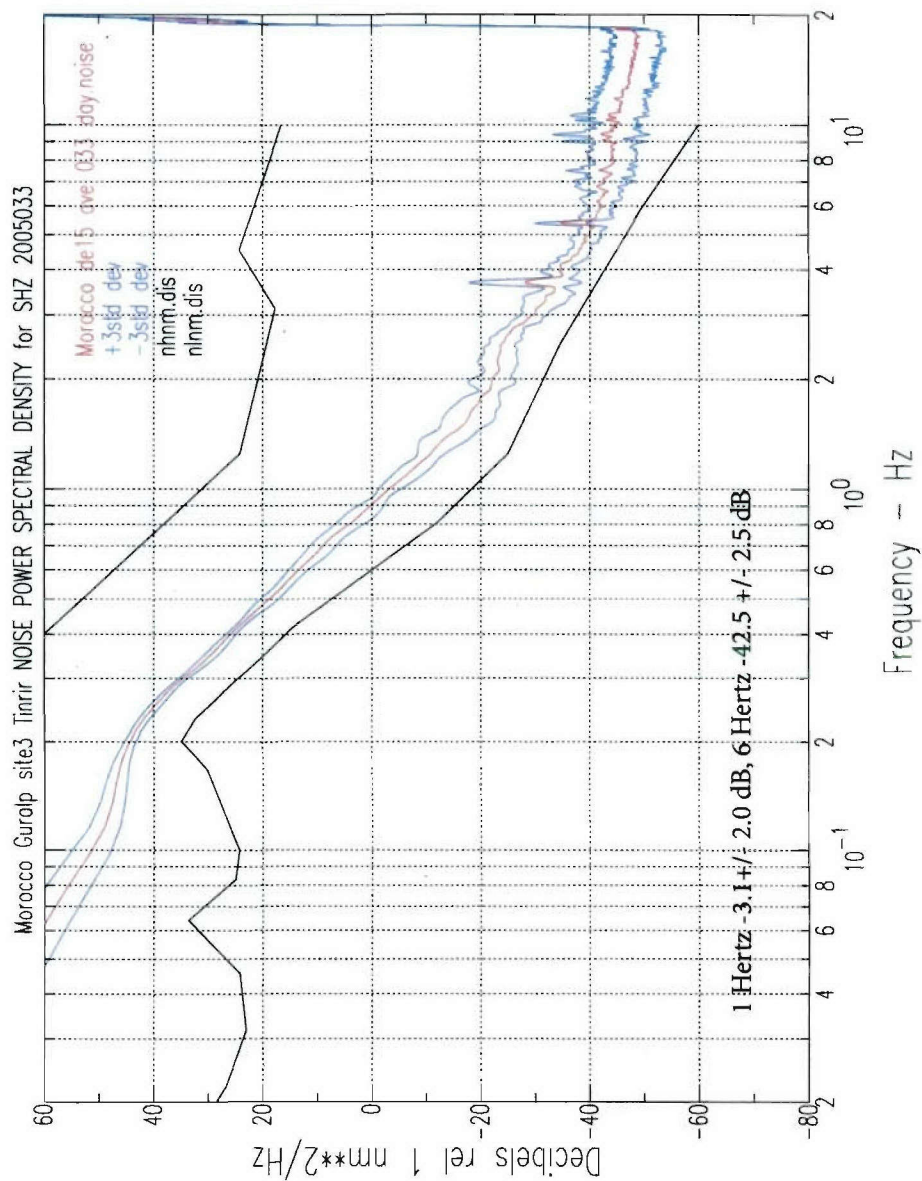


Figure C-22. Morocco Guralp Site 3, sensor DE15, DOY 033, day noise.

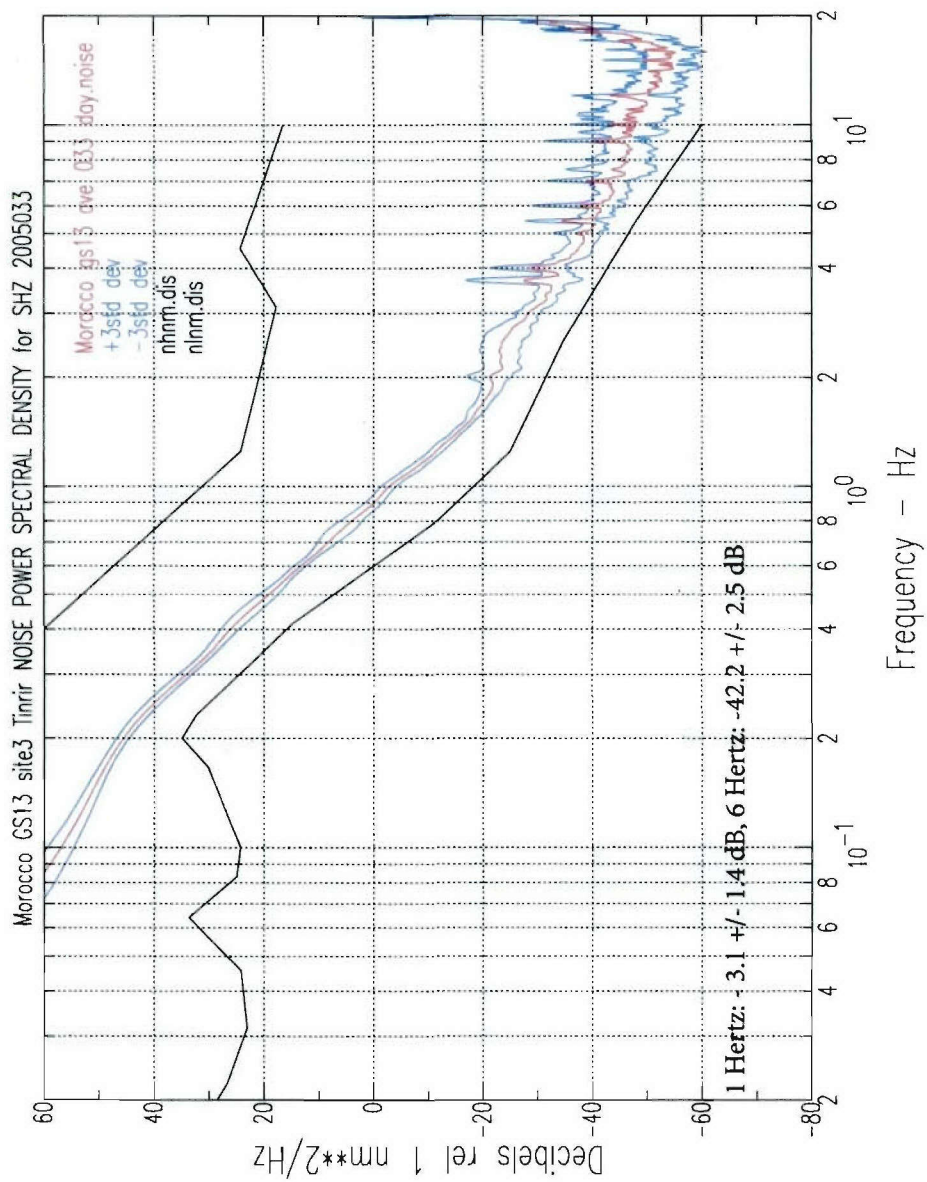


Figure C-23. Morocco GS13 Site 3, DOY 033, day noise.

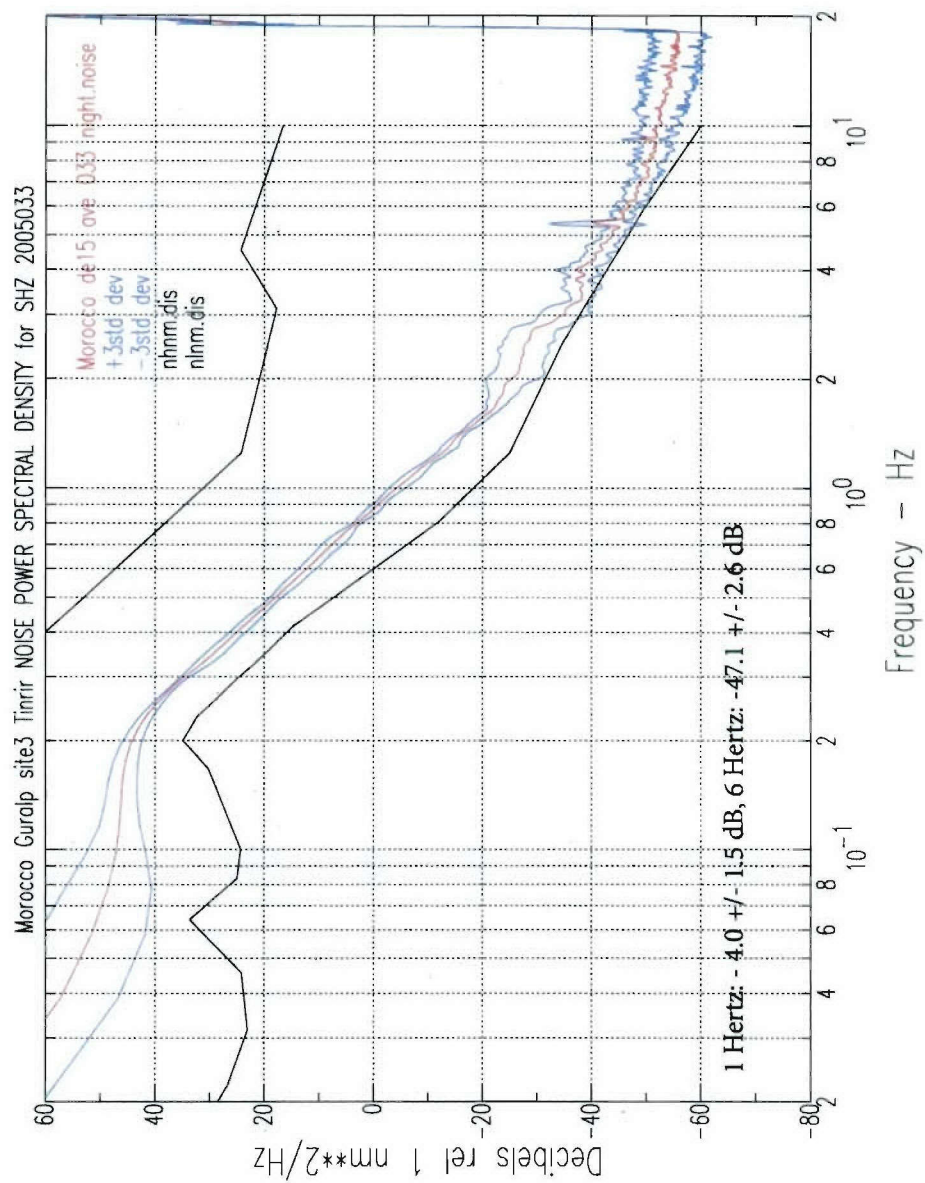


Figure C-24. Morocco Guralp Site 3, sensor DE15, DOY 033, night noise.

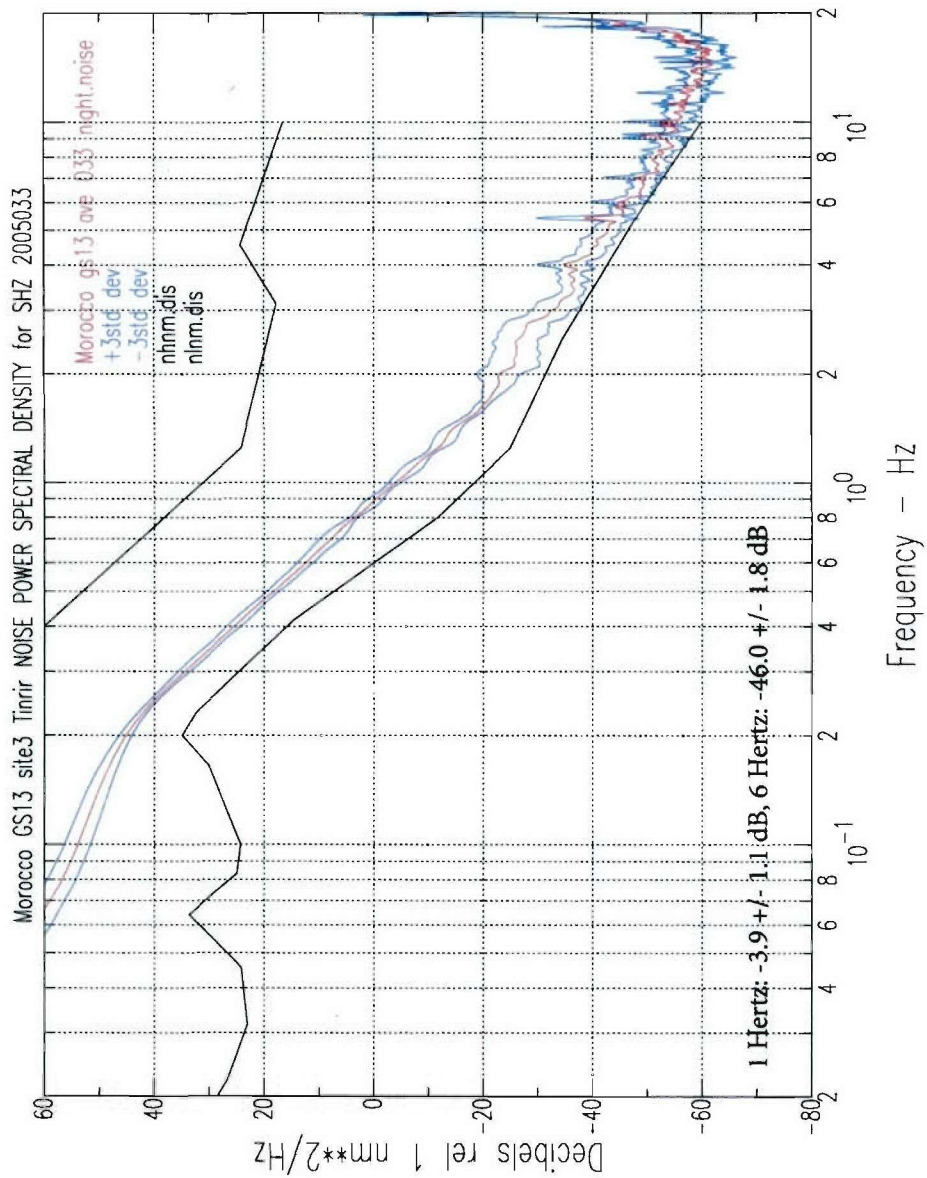


Figure C-25. Morocco GS13 Site 3, DOY 033, night noise.

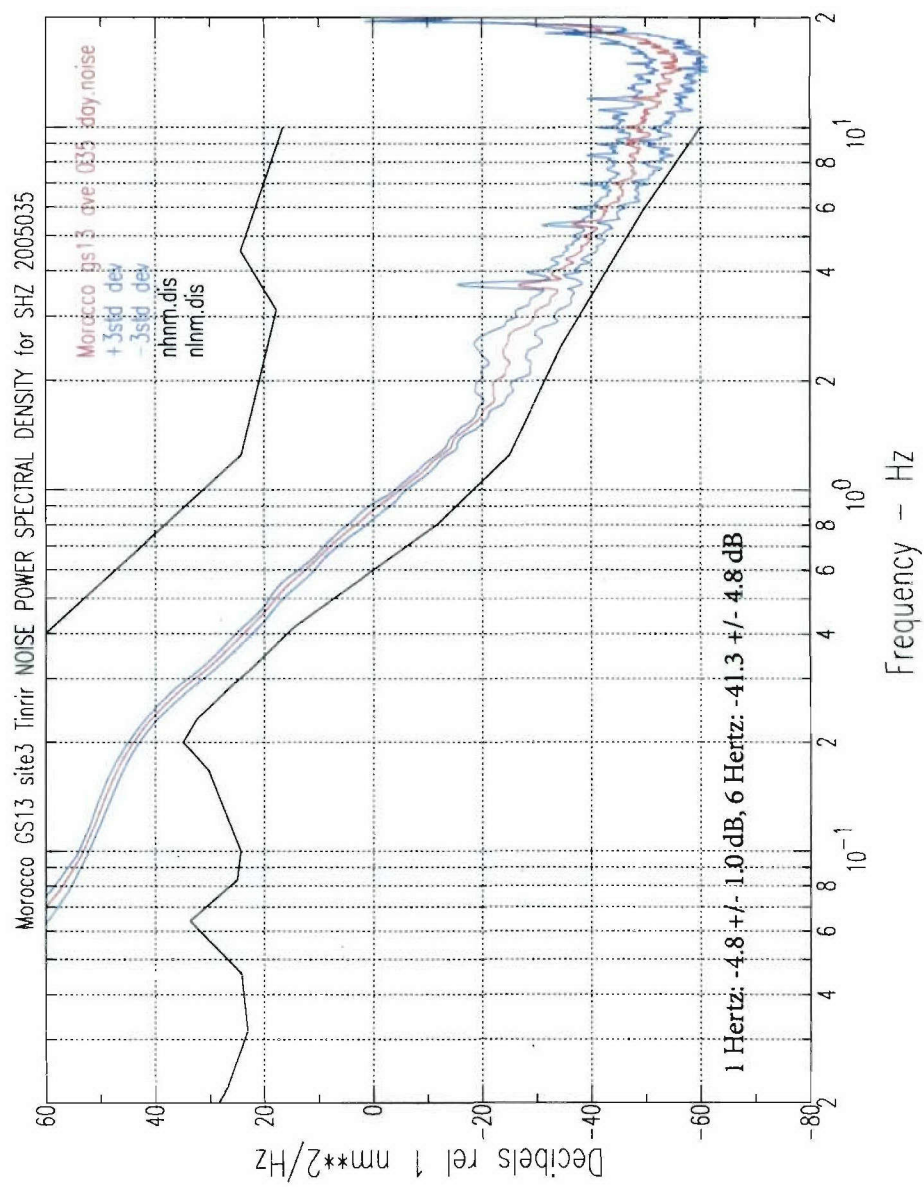


Figure C-26. Morocco GS13 Site 3, DOY 035, day noise.

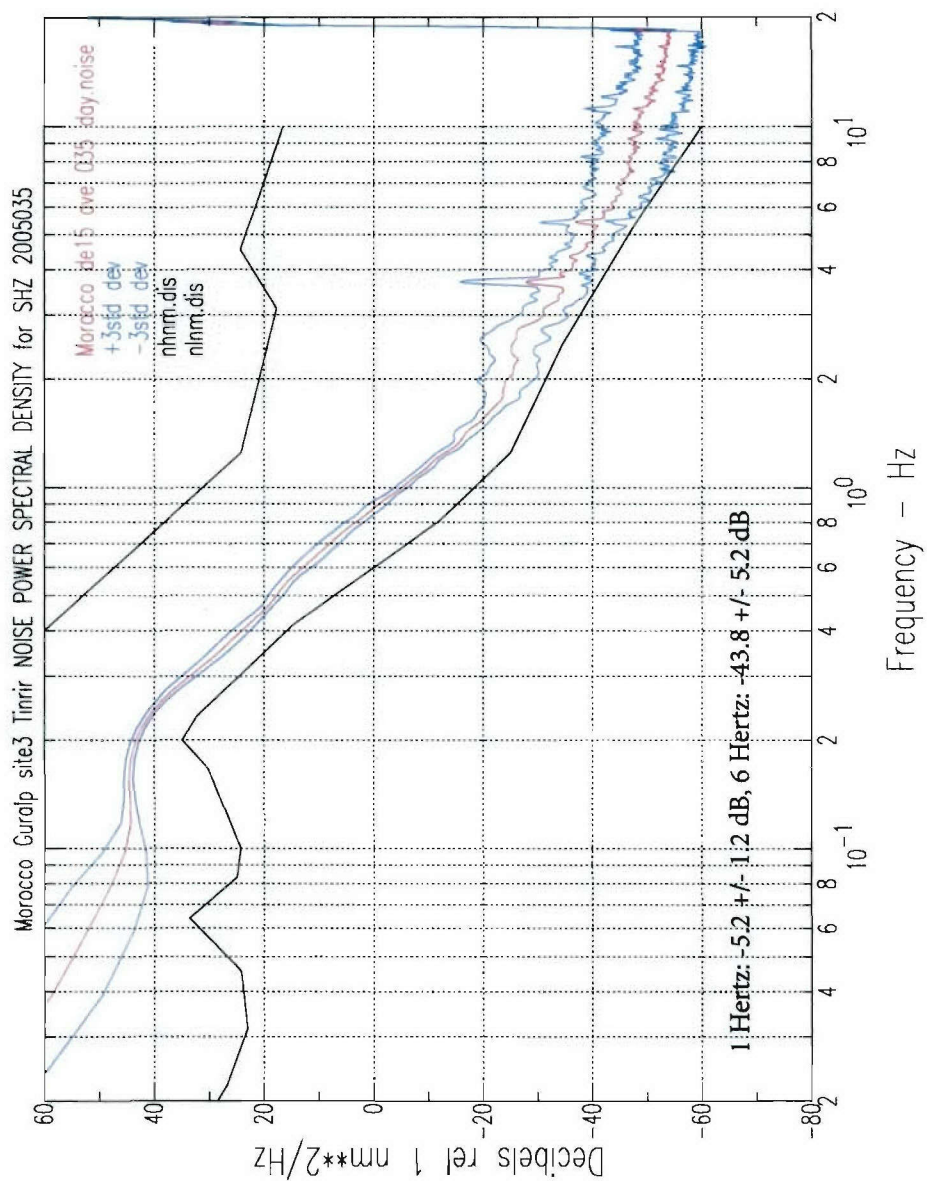


Figure C-27. Morocco Guralp Site 3, sensor DE15, DOY 035, day noise.

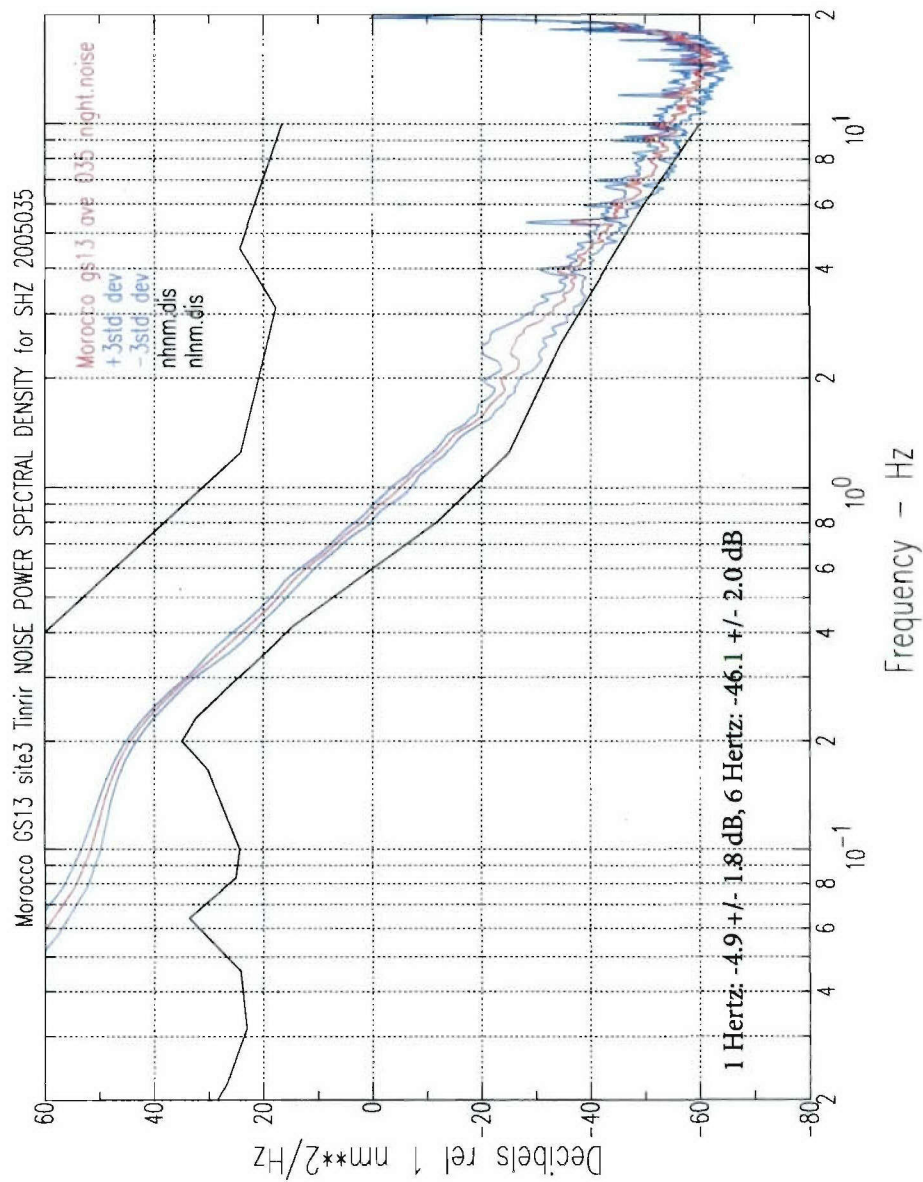


Figure C-28. Morocco GS13 Site 3, DOY 035, night noise.

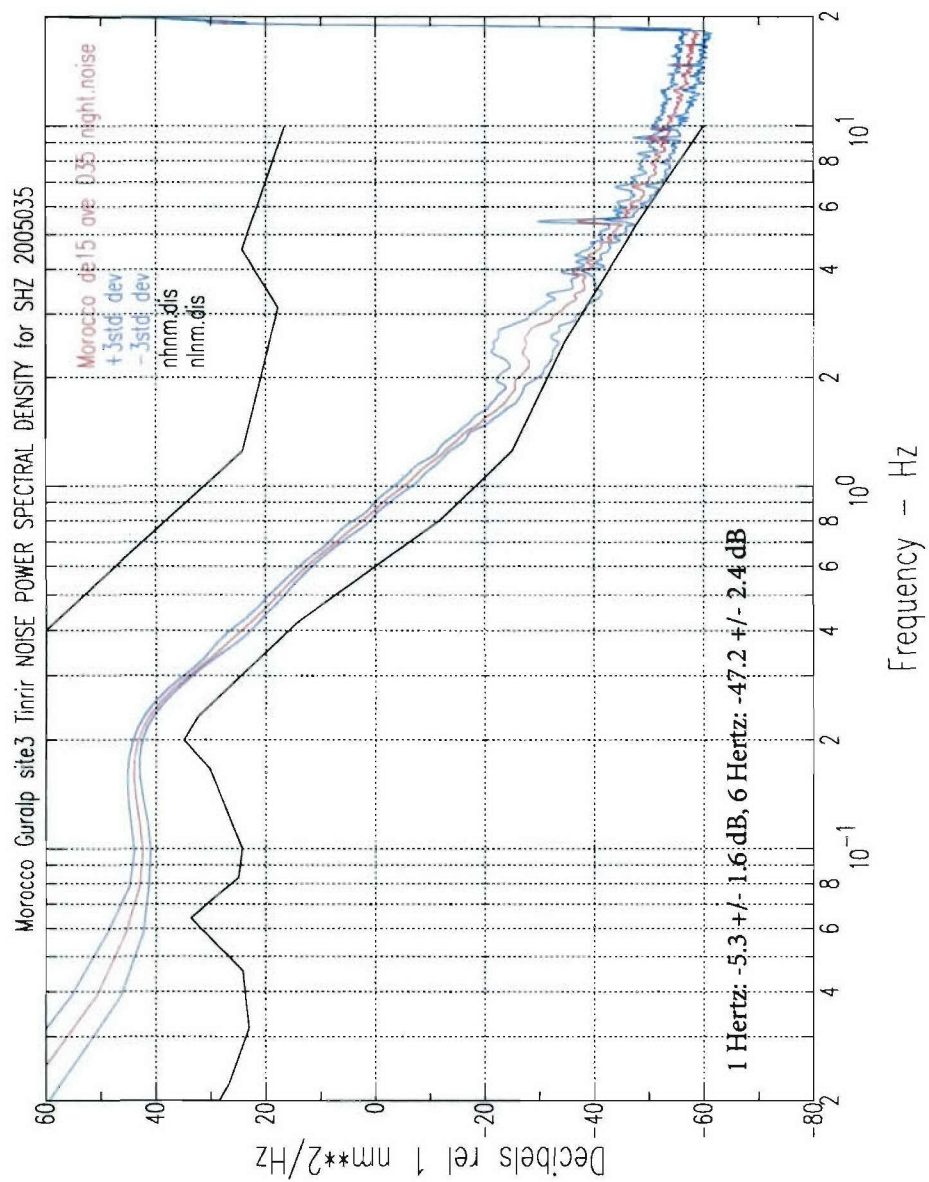


Figure C-29. Morocco Guralp Site 3, sensor DE15, DOY 035, night noise.

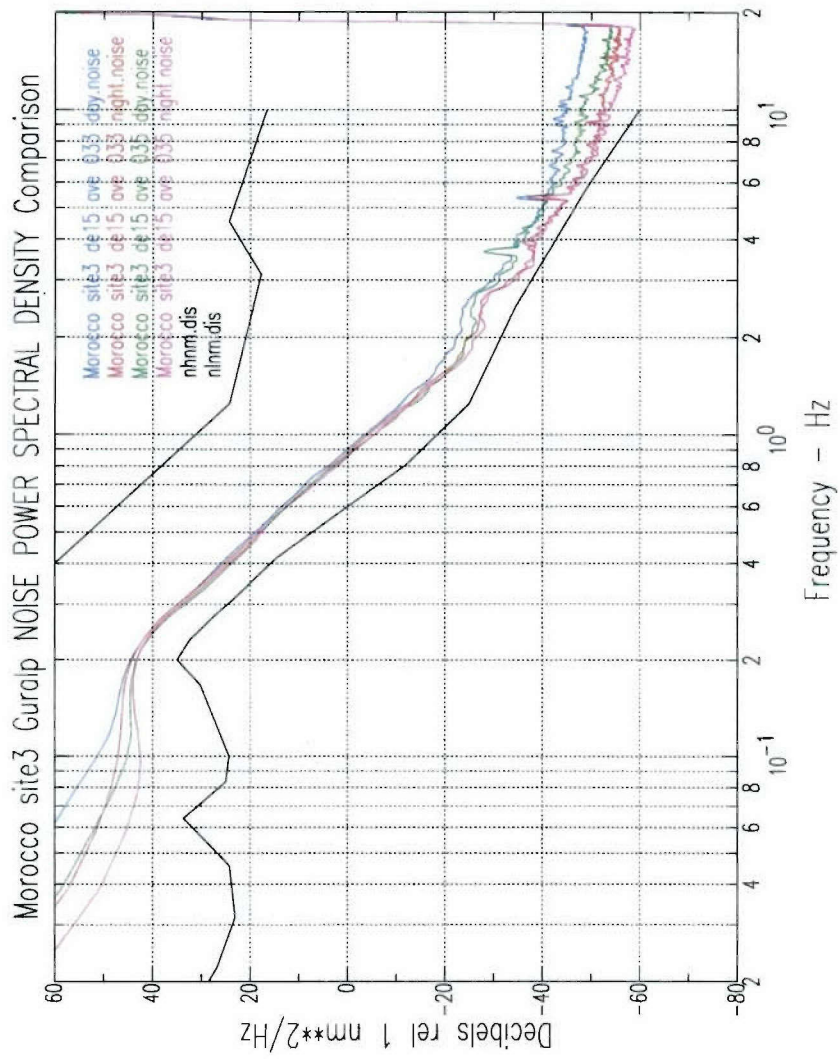


Figure C-30. Guralp Site 3 noise comparison.

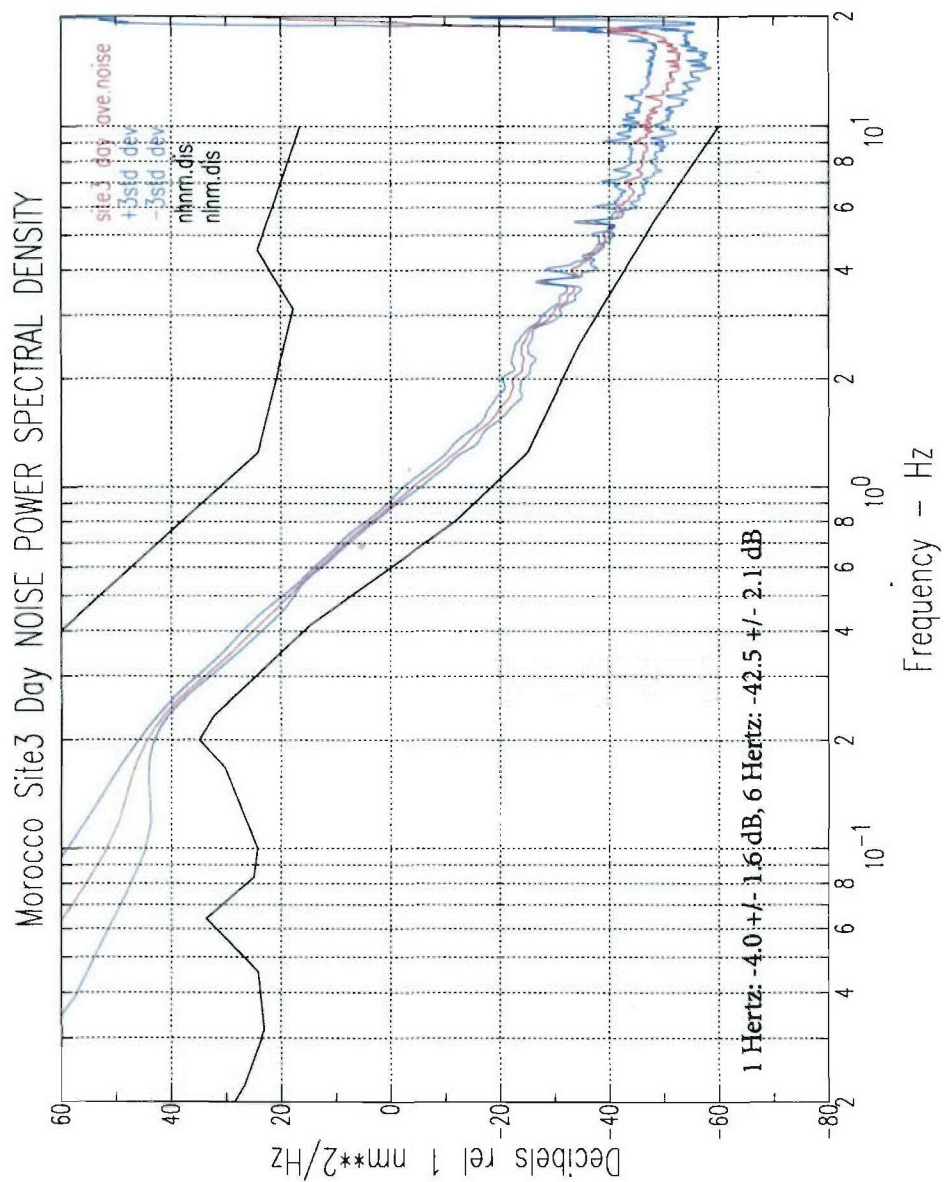


Figure C-31. Morocco Site 3, day average noise.

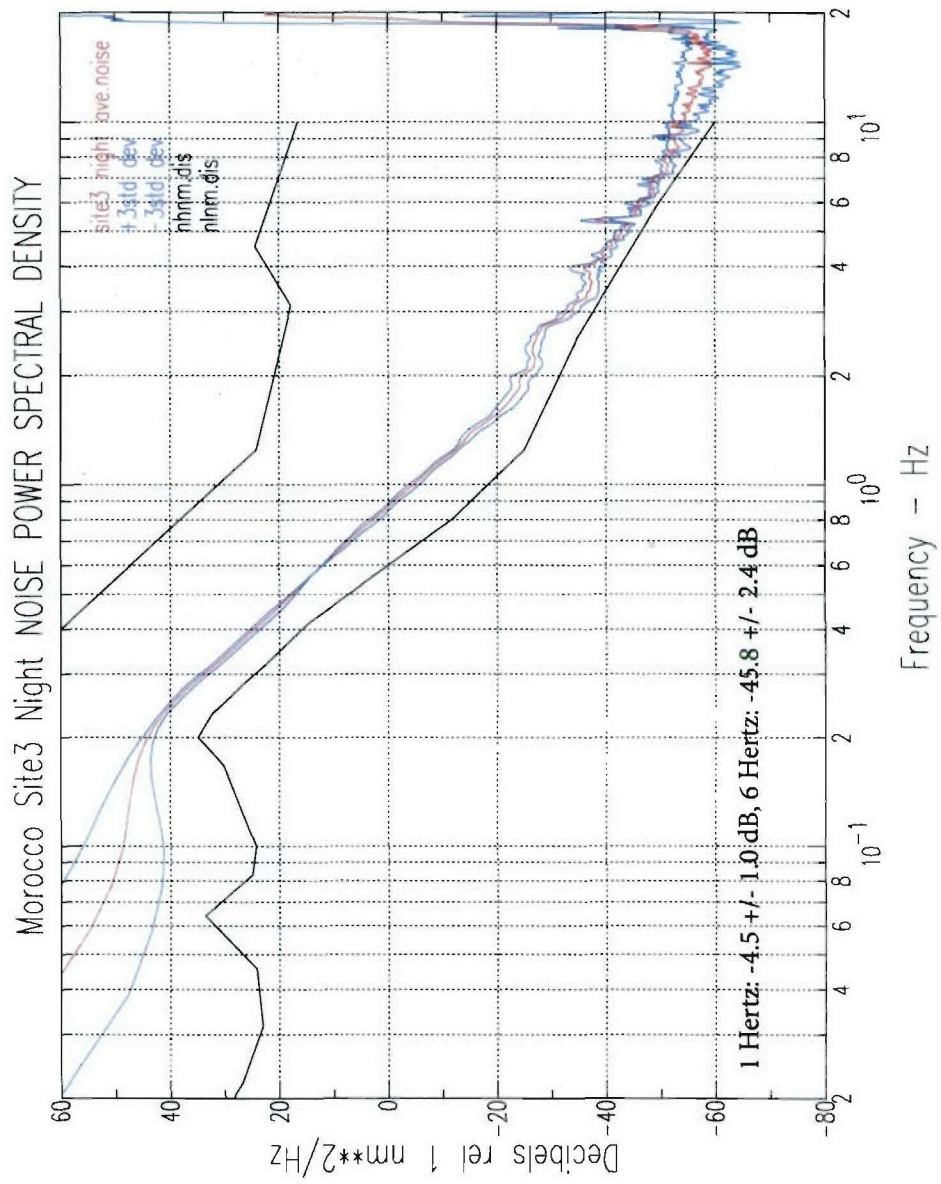


Figure C-32. Morocco Site 3, night average noise.

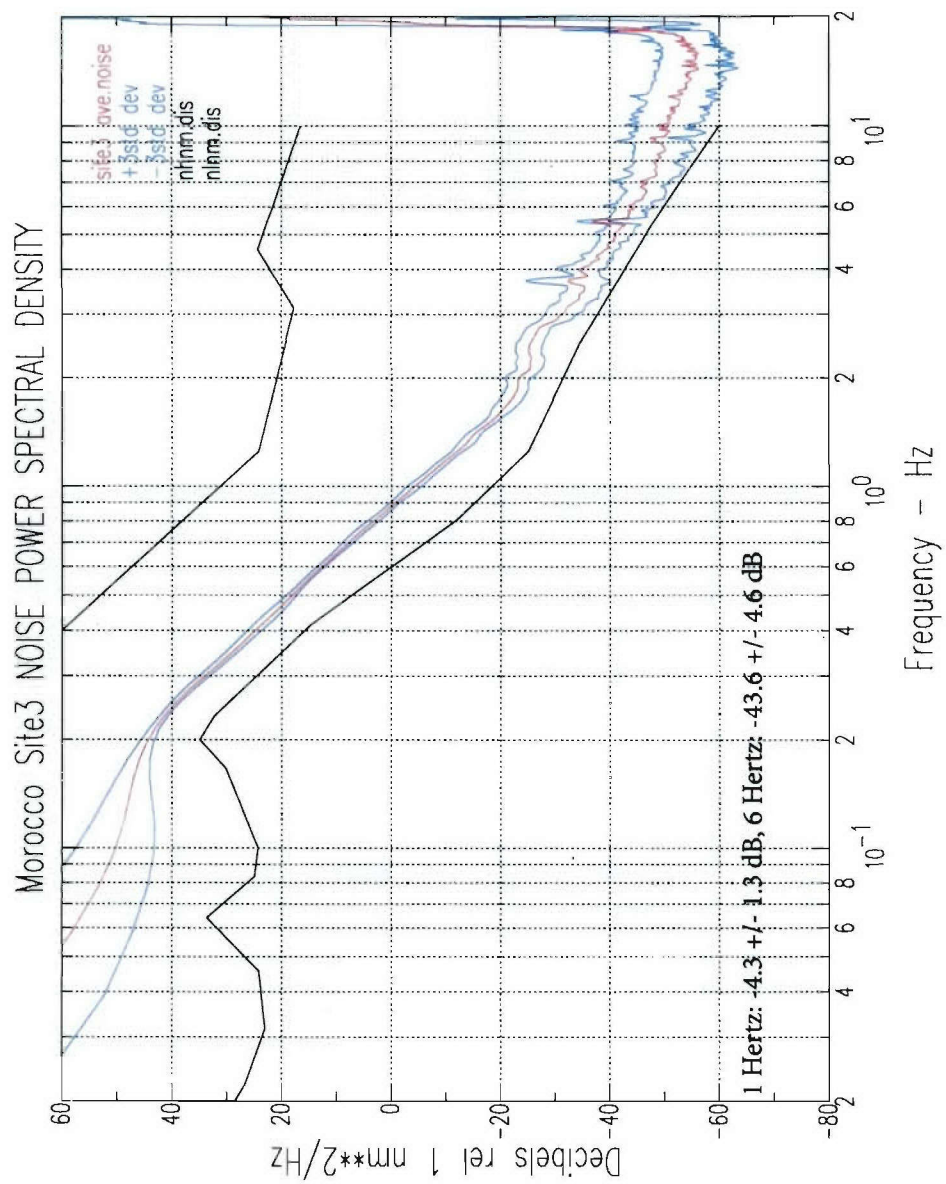


Figure C-33. Morocco Site 3, average noise.

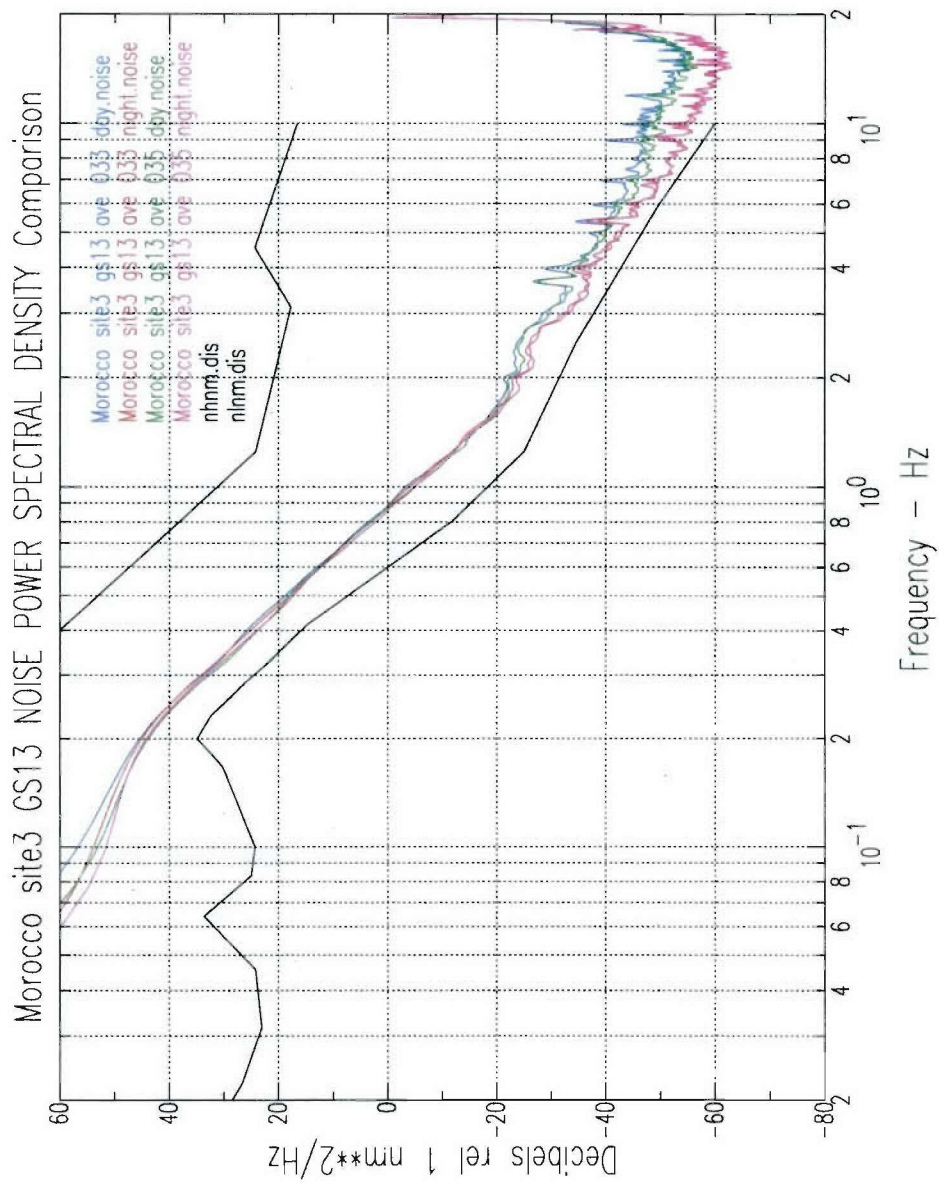


Figure C-34. Morocco Site 3 GS13 comparison day and night noise.

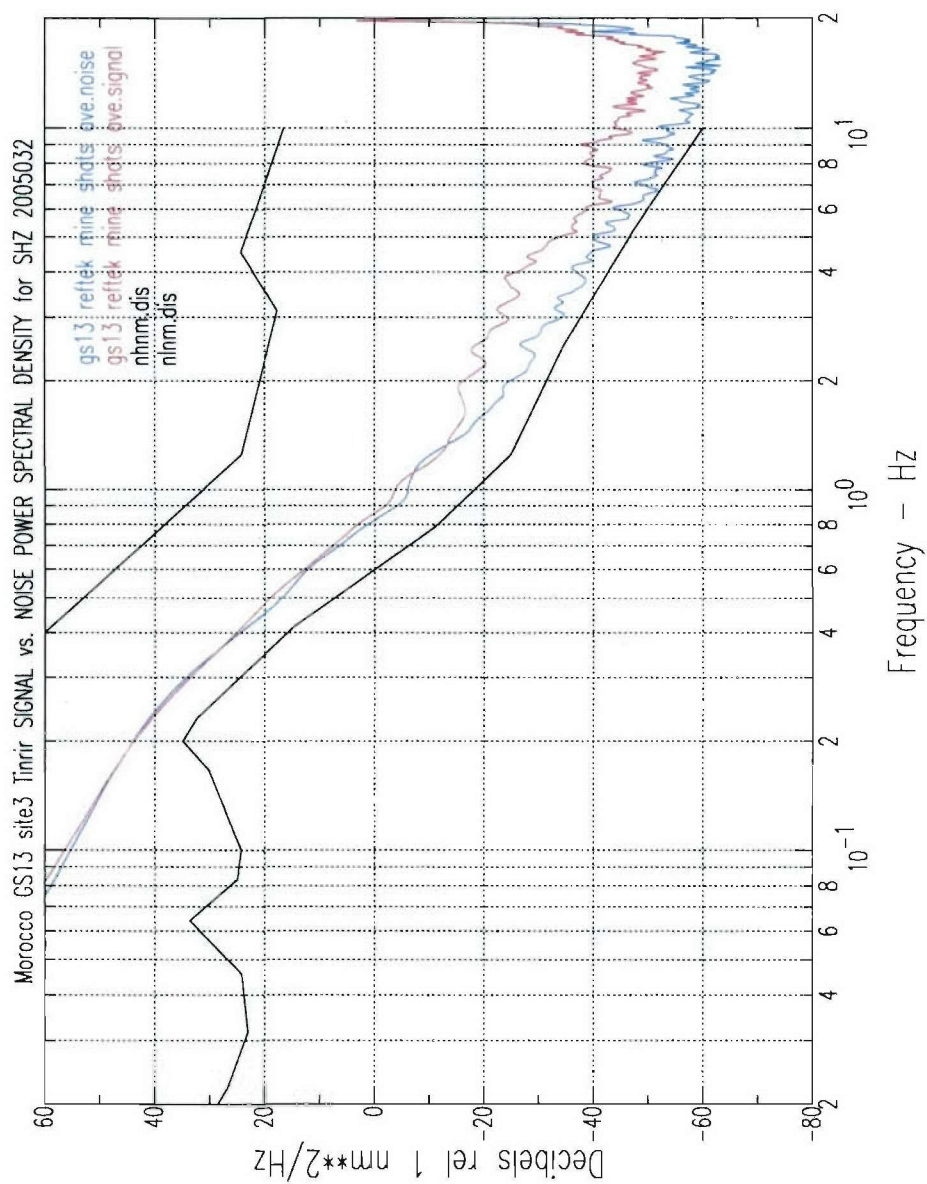


Figure C-35. Morocco Site 3 GS13 signal vs. noise spectra of local mine shots, DOY 032.

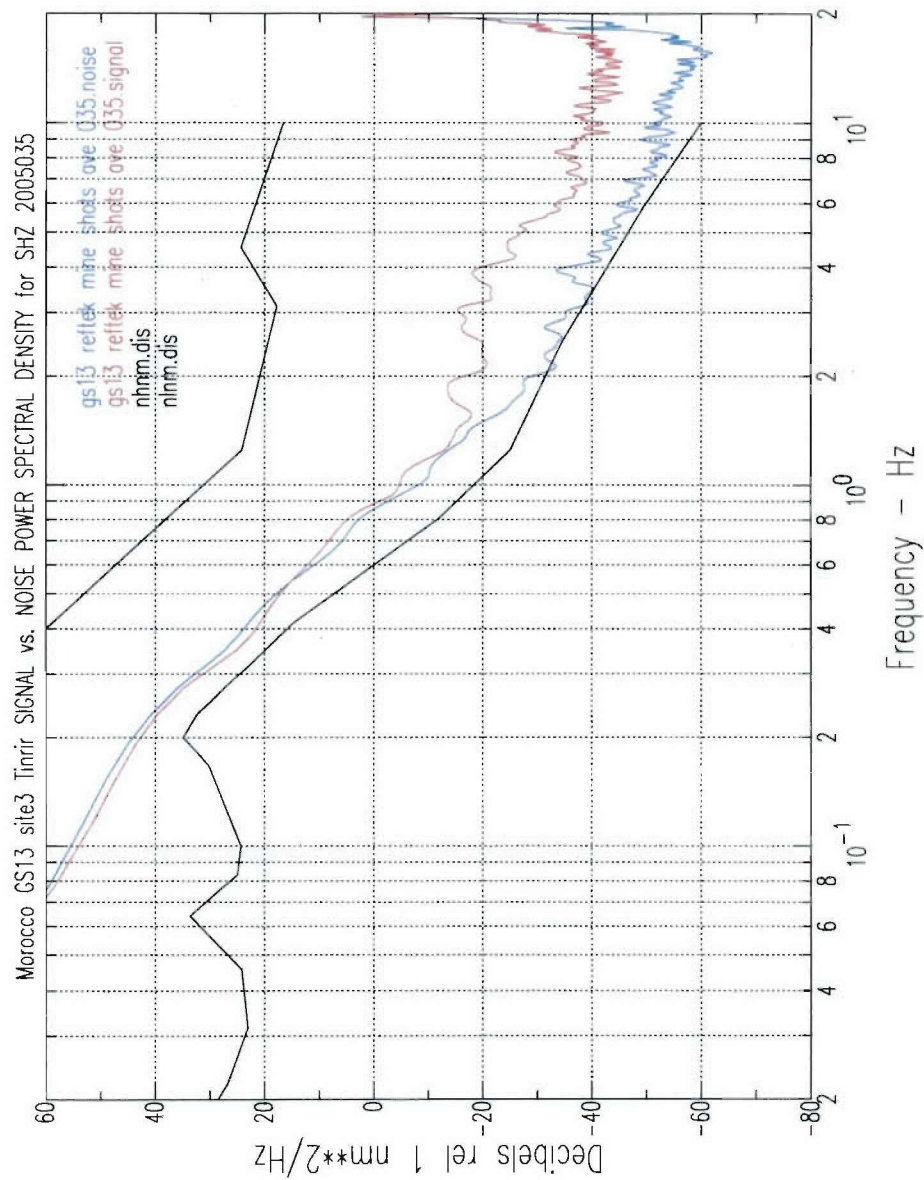


Figure C-36. Morocco Site 3 GS13 signal vs. noise spectra of local mine shots, DOY 035.

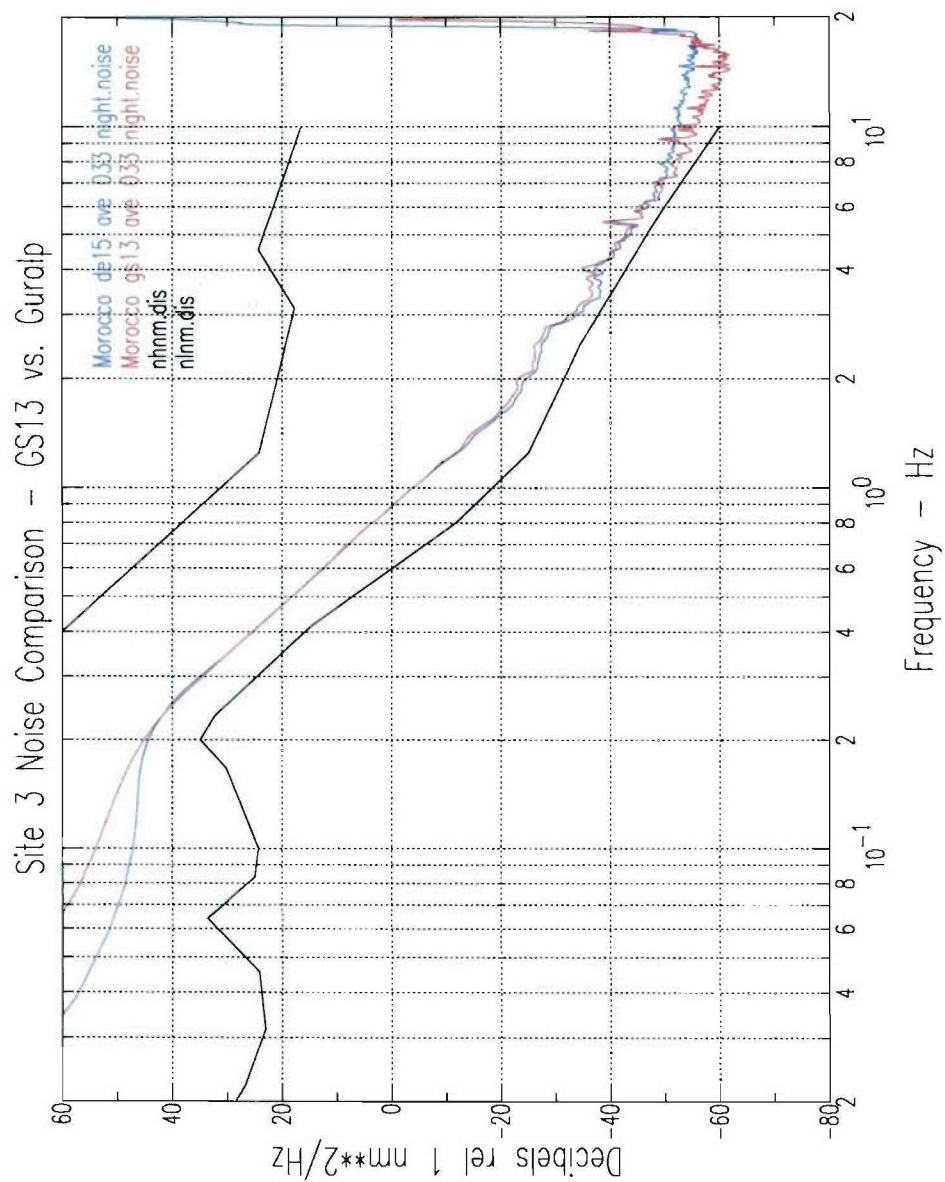


Figure C-37. Noise comparison between the GS13 Reftek and co-located Guralp system.

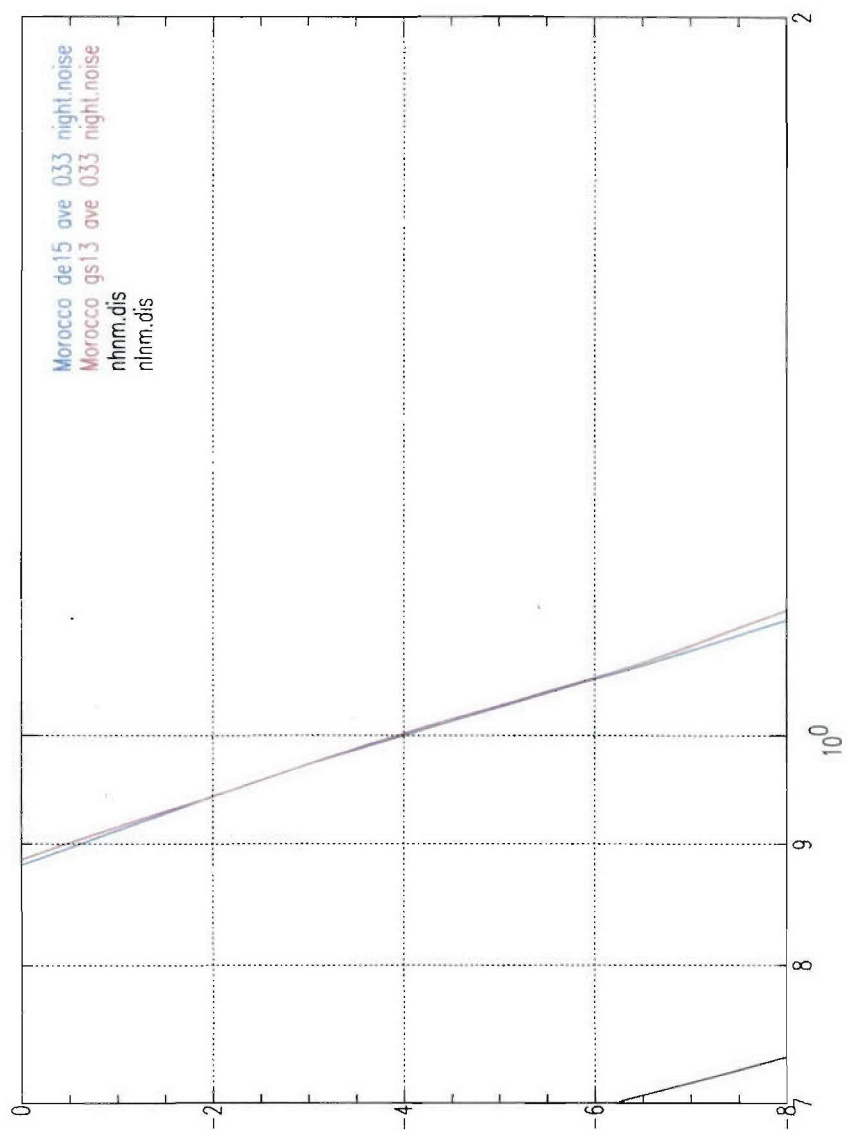


Figure C-38. Noise comparison between the GS13 Reftek and co-located Guralp system (zoom in at 1 Hz).

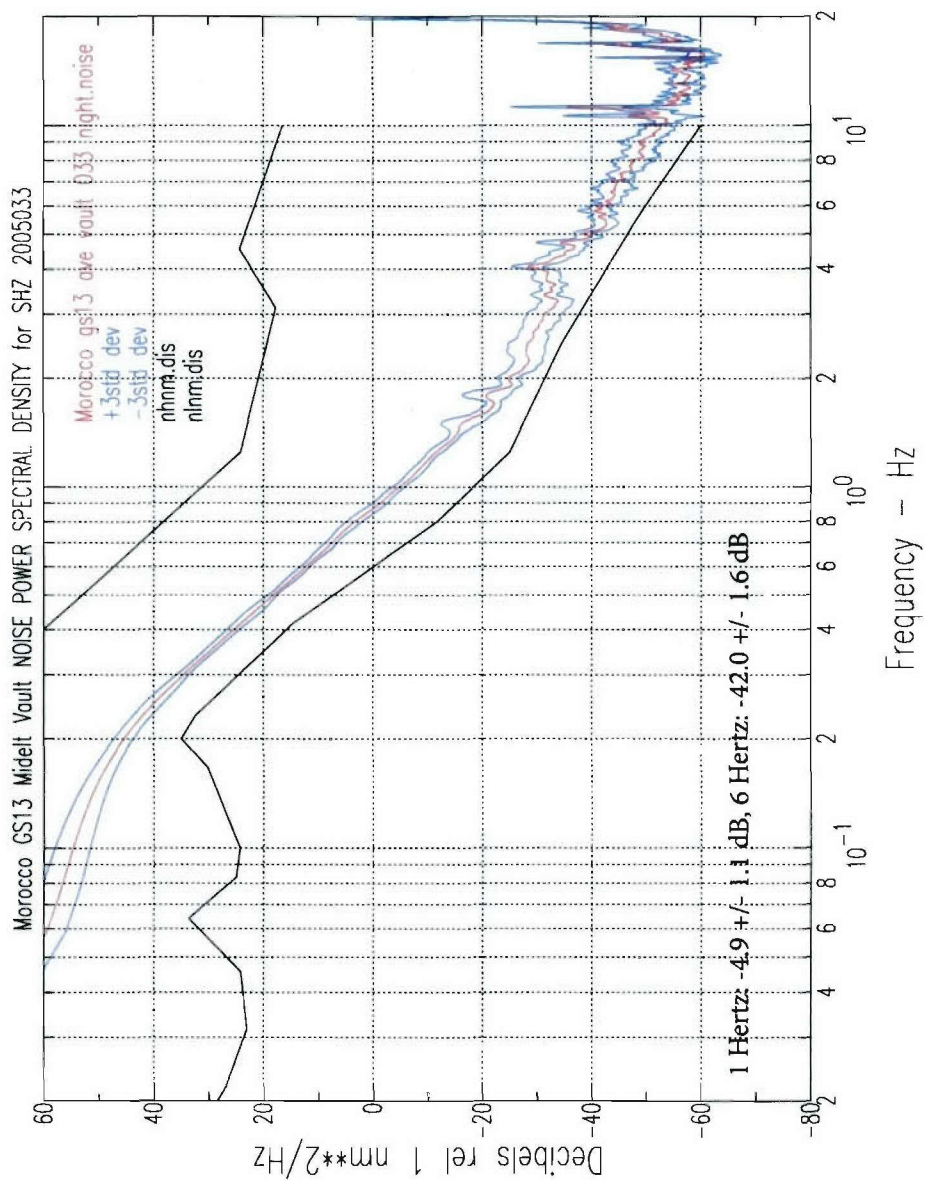


Figure C-39. Morocco GS13 Vault, DOY 033, night noise.

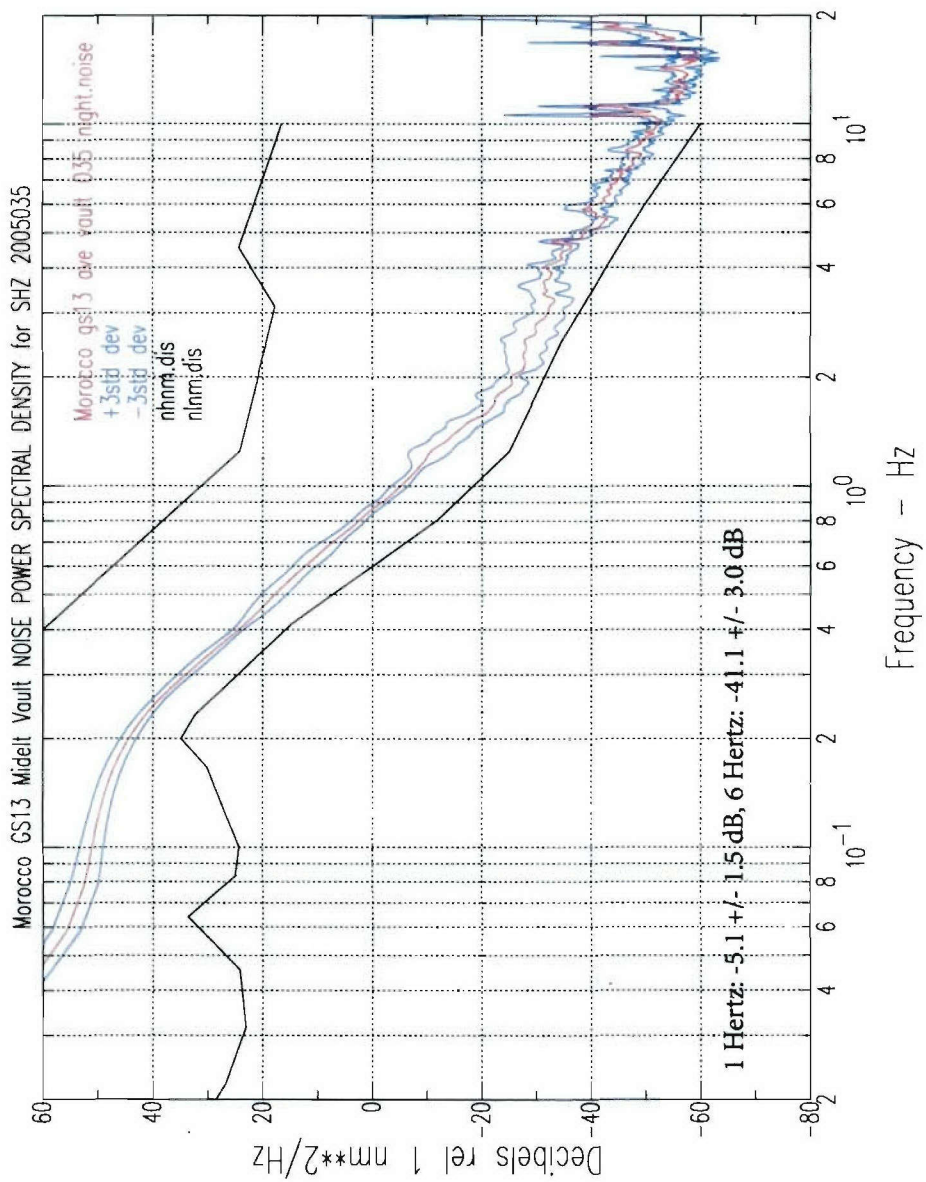


Figure C-41. Morocco GS13 Vault, DOY 035, night noise.

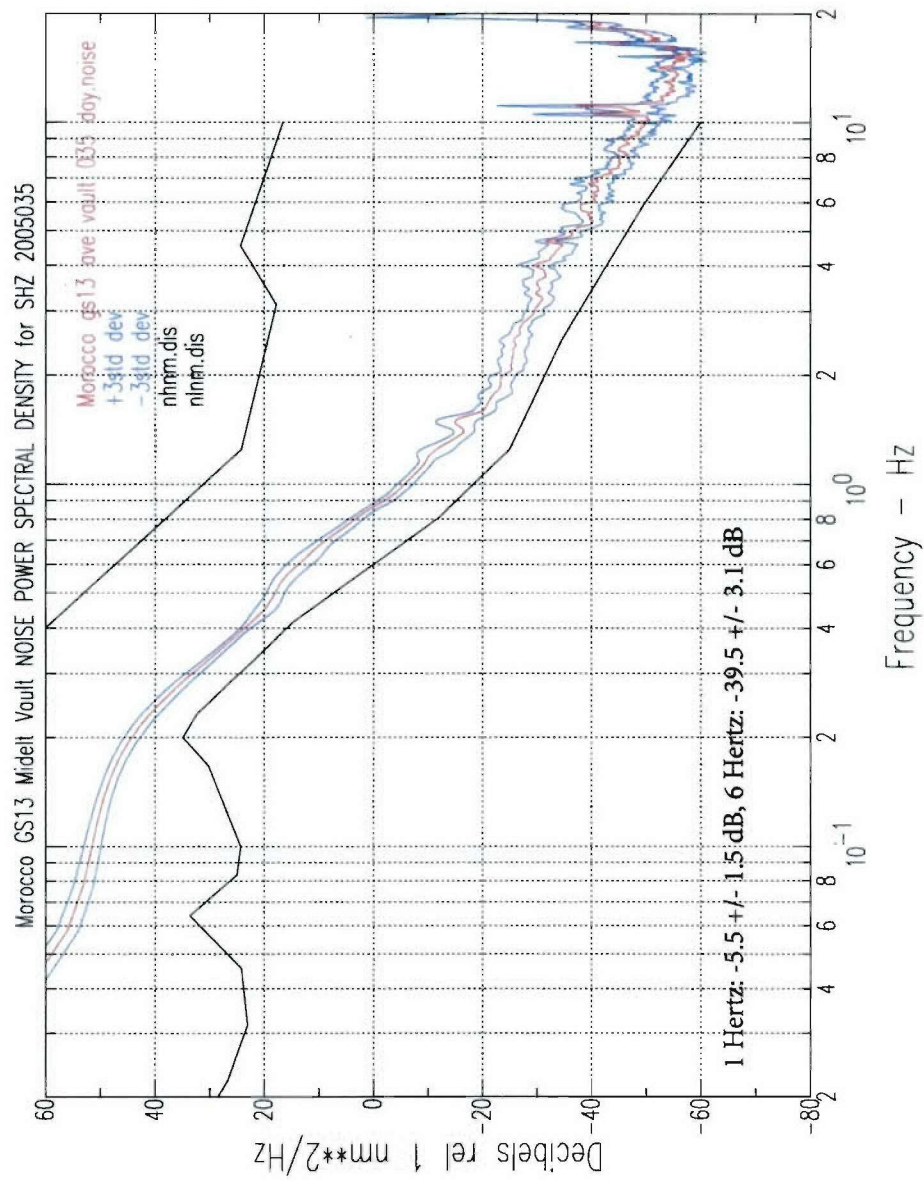


Figure C-42. Morocco GS13 Vault, DOY 035, day noise.

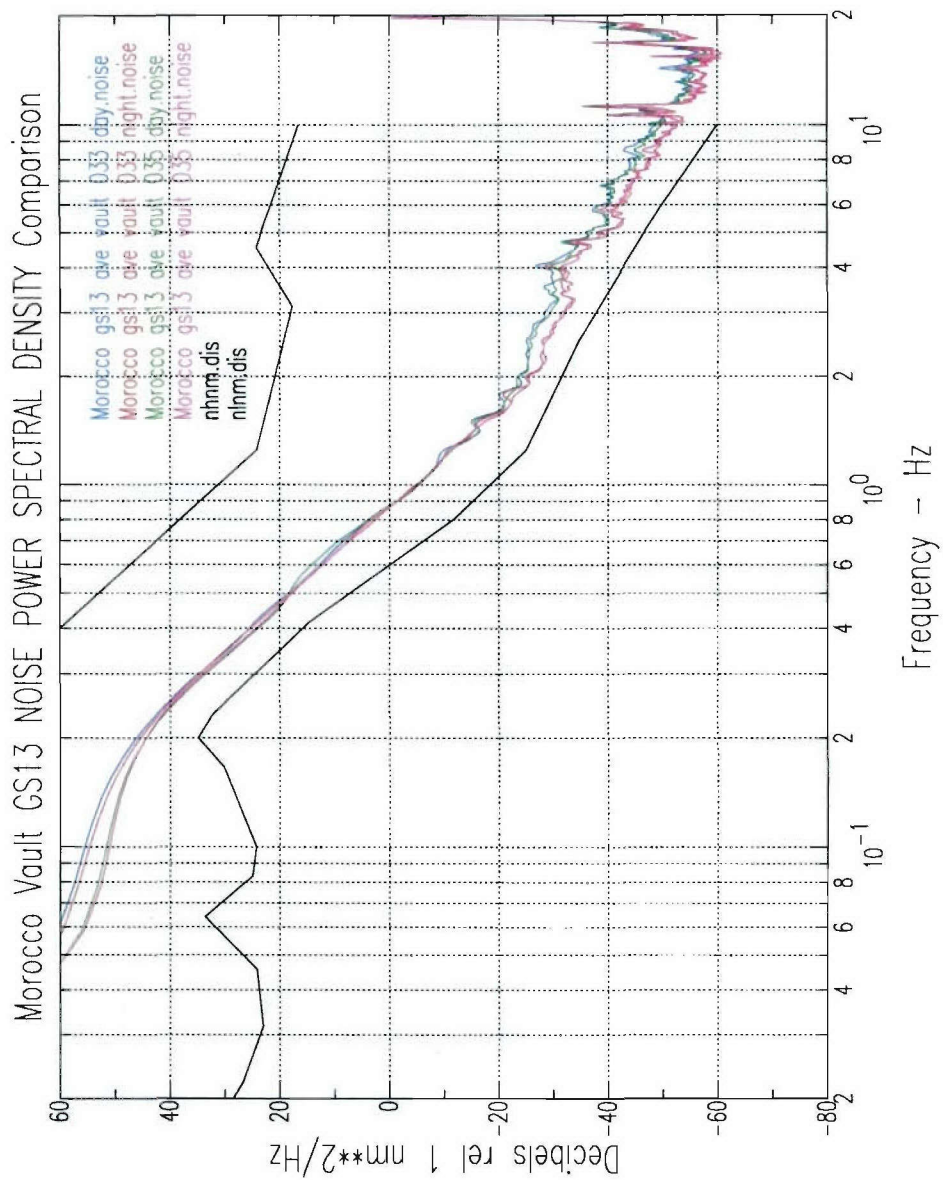


Figure C-43. Morocco Vault GS13 comparison day and night noise.

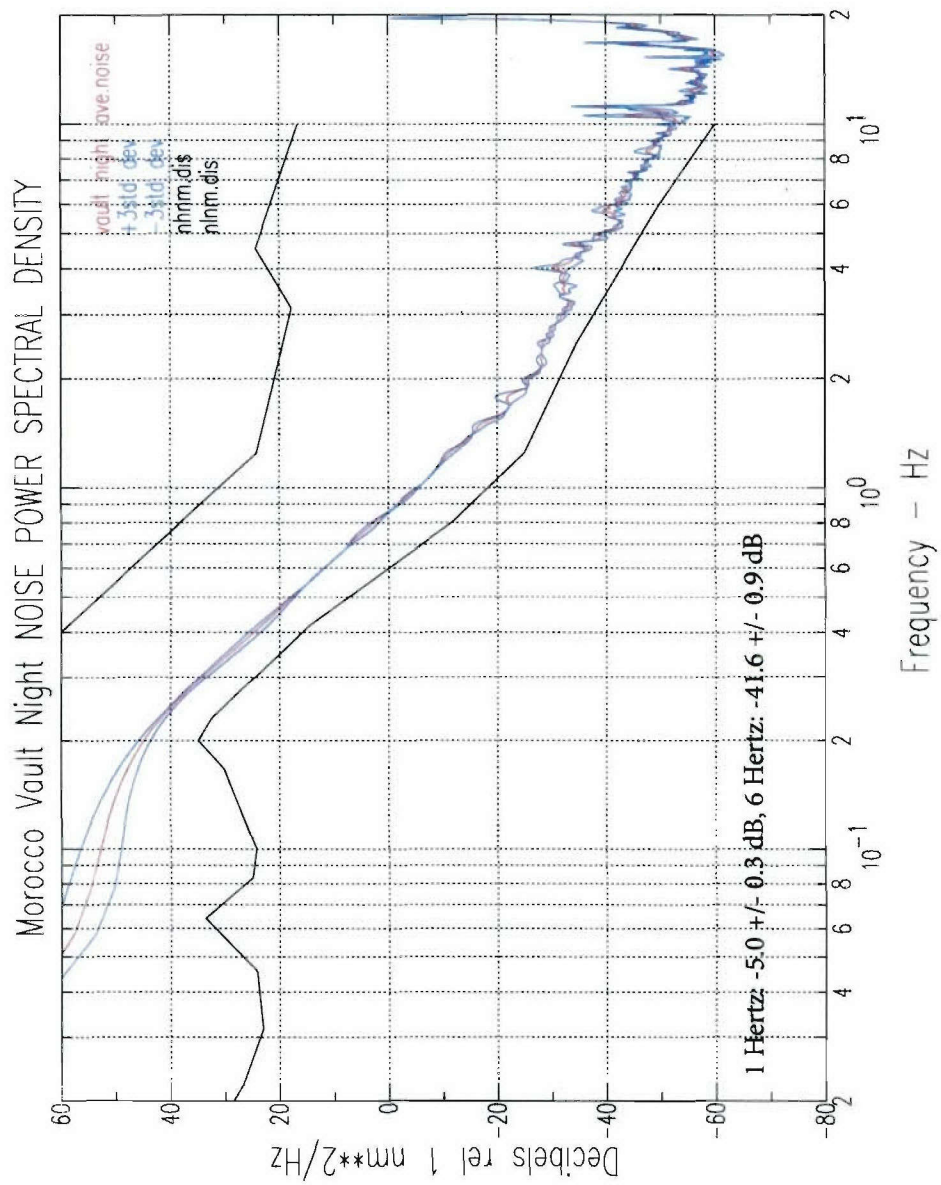


Figure C-44. Morocco Vault, night average noise.

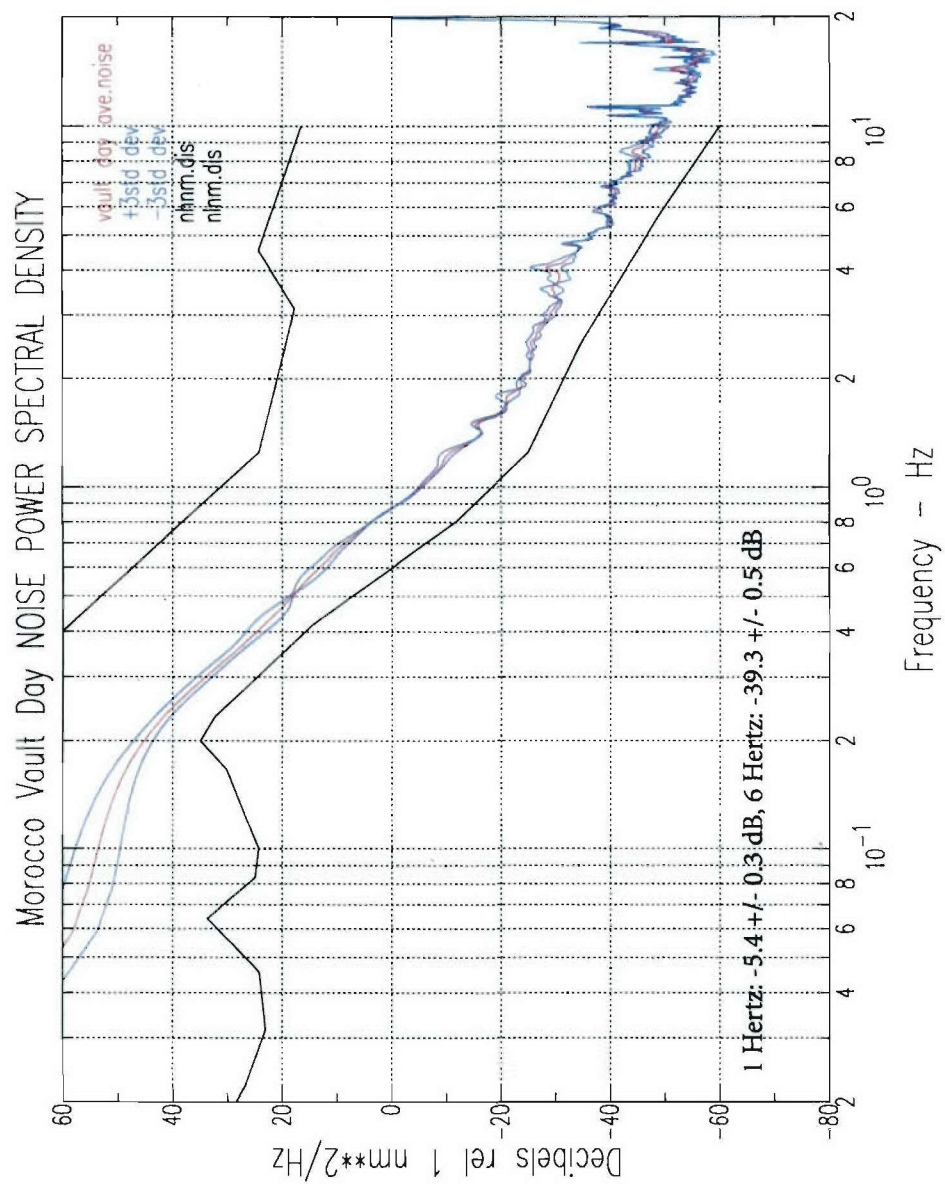


Figure C-45. Morocco Vault, day average noise.

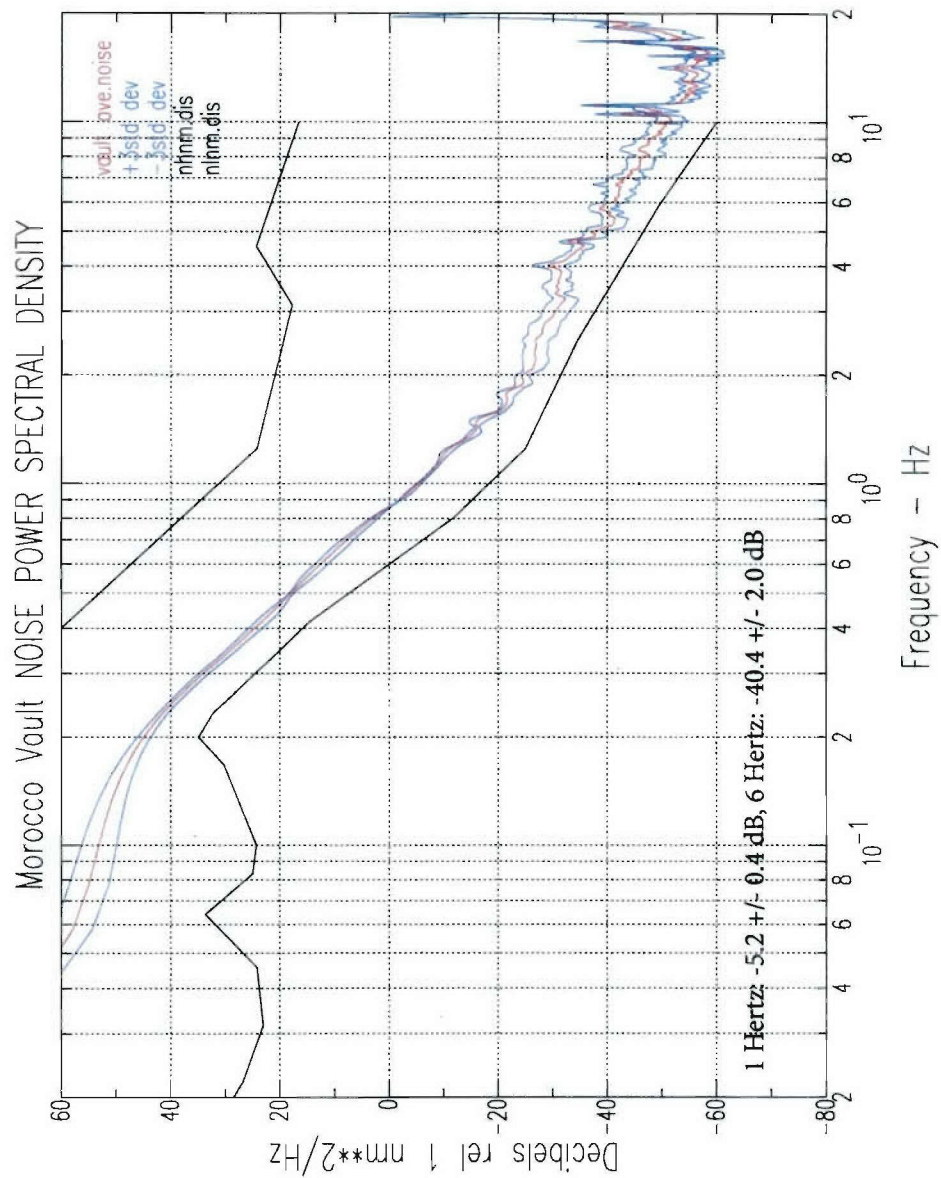


Figure C-46. Morocco Vault, average noise.

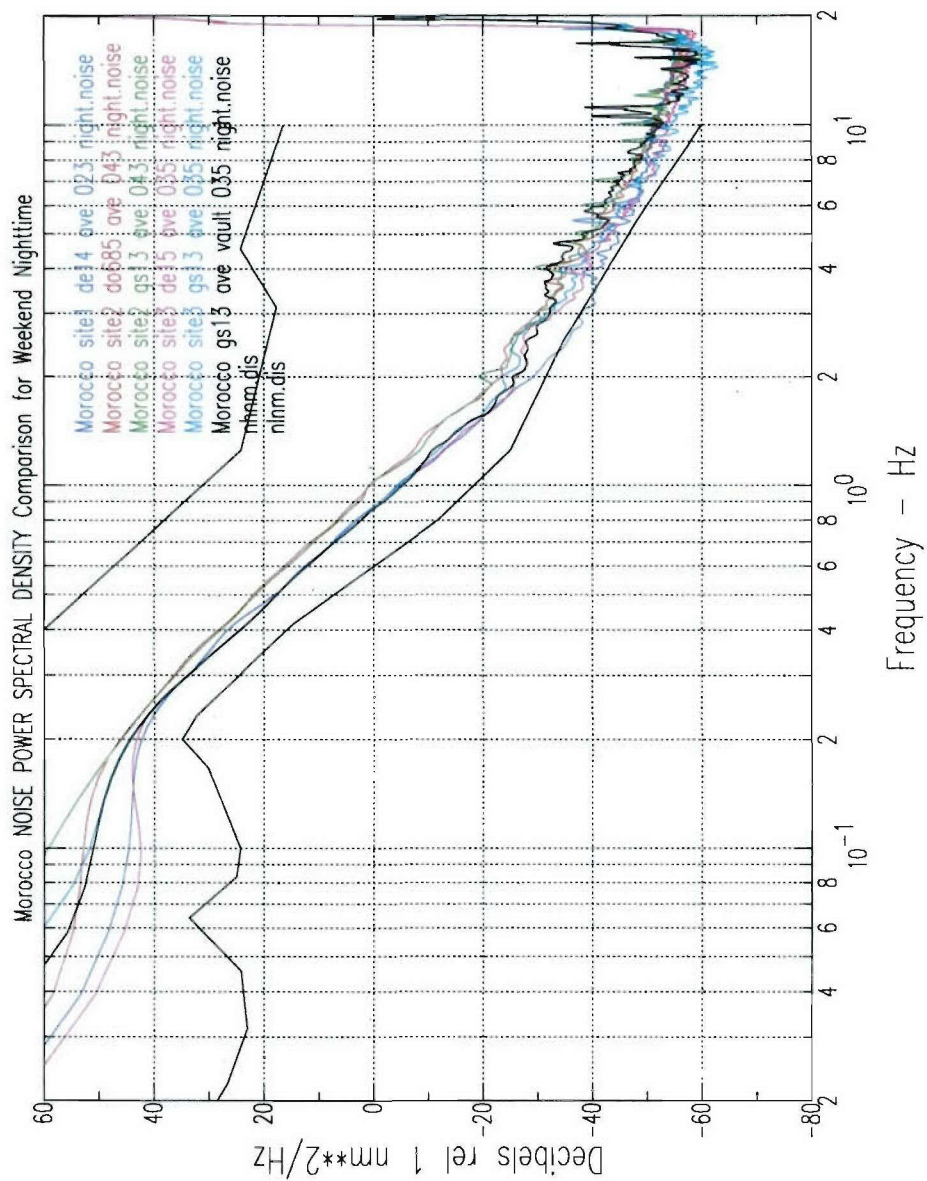


Figure C-47. Morocco site comparison of weekend nighttime noise.

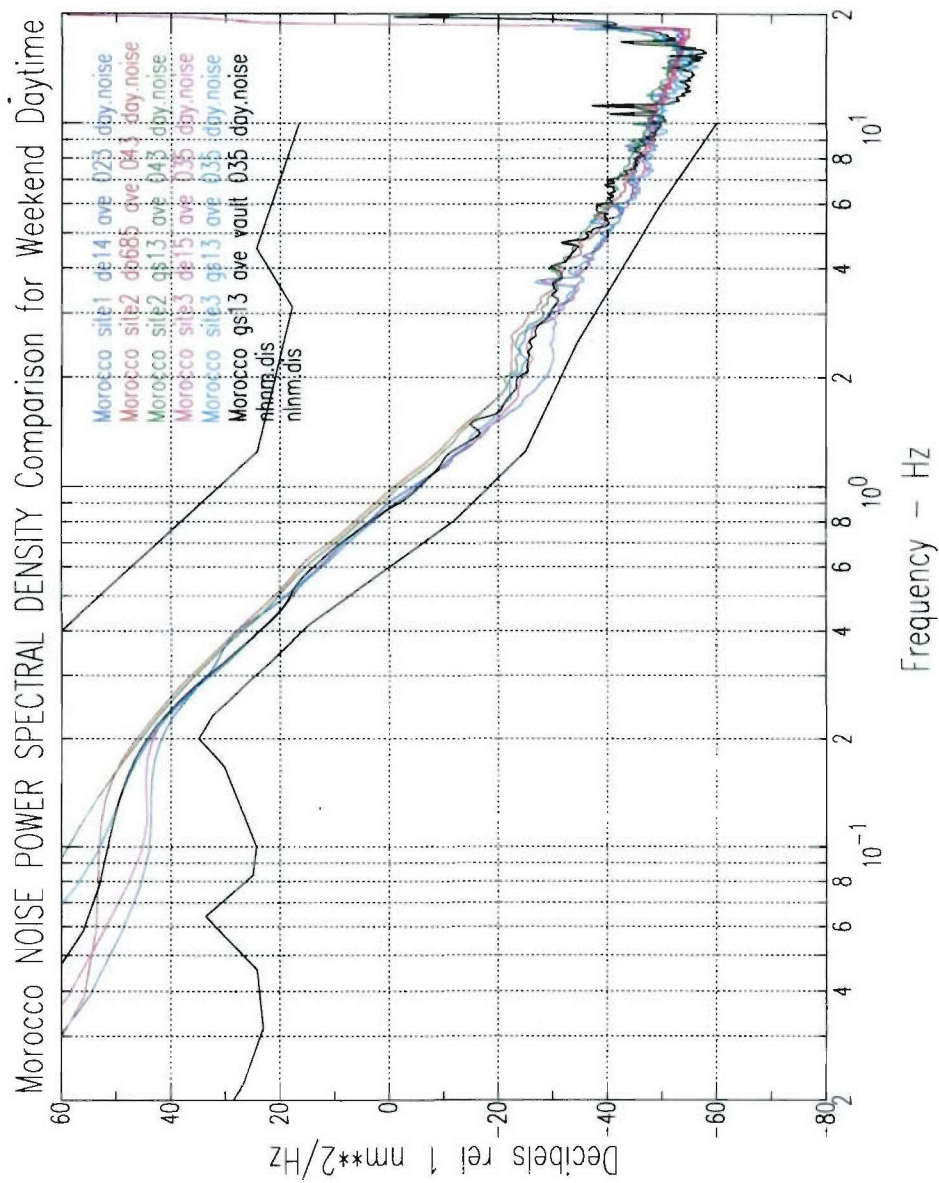


Figure C-48. Morocco site comparison of weekend daytime noise.

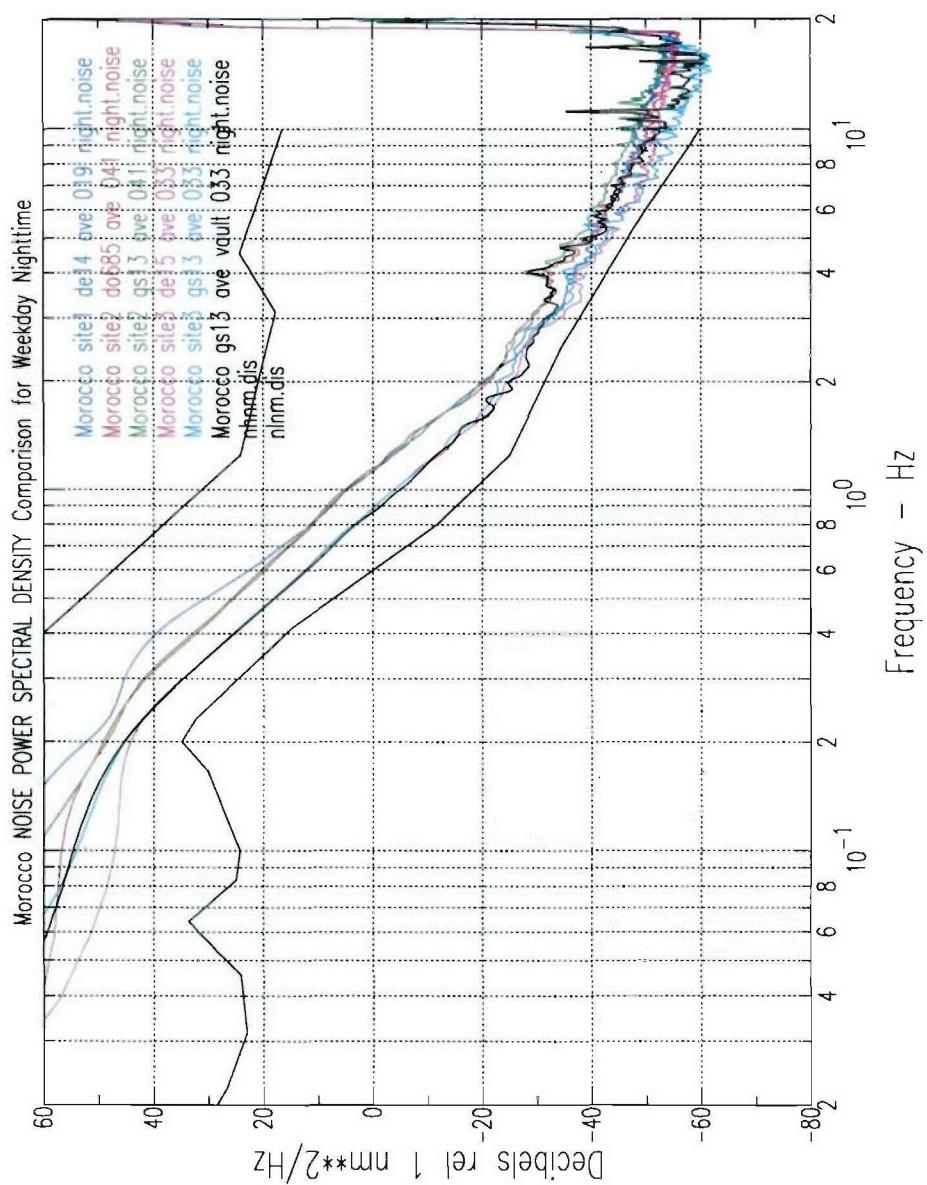


Figure C-49. Morocco site comparison of weekday nighttime noise.

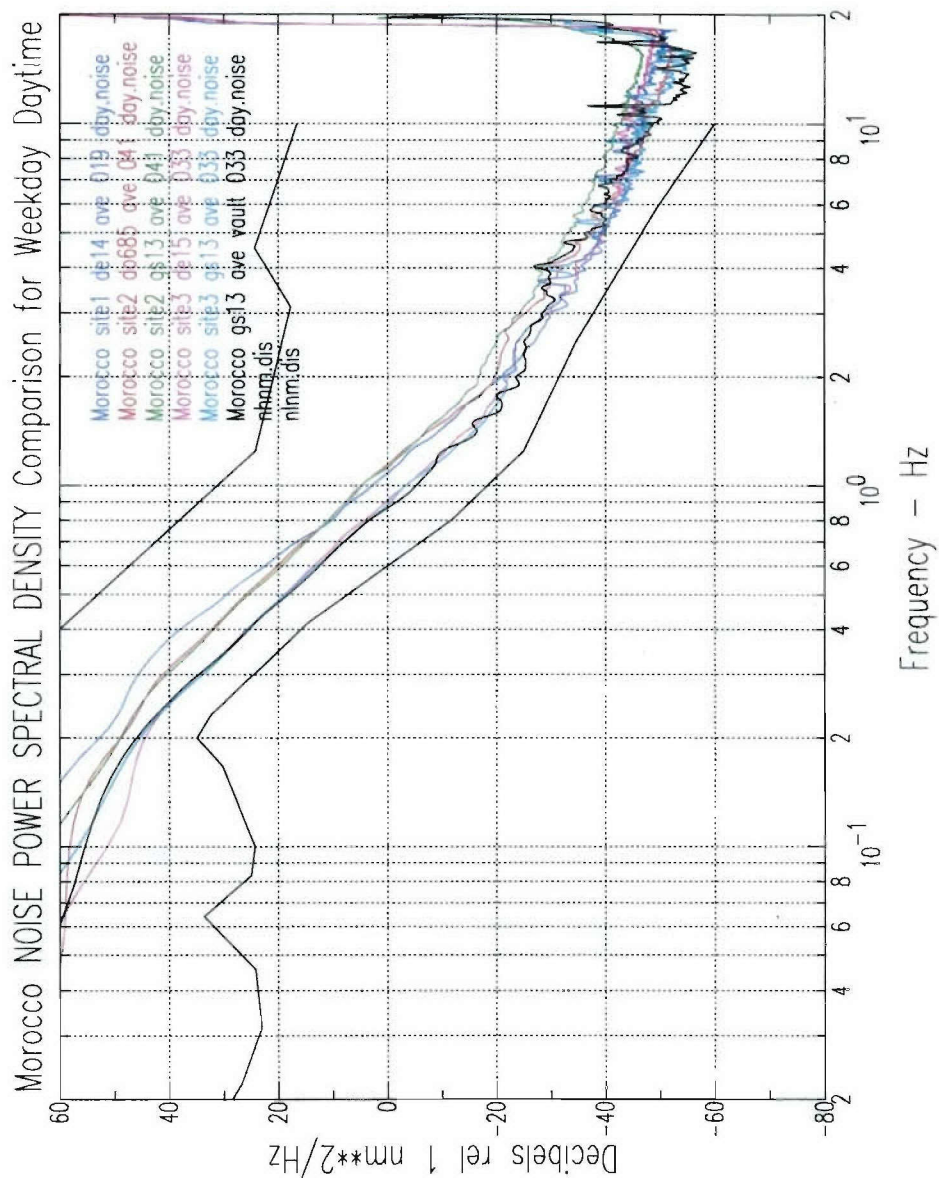


Figure C-50. Morocco site comparison of weekday daytime noise.

Appendix D

Event Tables

Table D-1: Site 1 Event Position and Origin Time

Latitude	Longitude	Day	DOY	Time
34.988000	-3.897000	1/17/2005	(017)	18:38:12.390
34.950000	-2.873000	1/17/2005	(017)	22:30:40.020
34.971411	-2.906061	1/19/2005	(019)	0:31:28.228
34.967290	-2.955439	1/19/2005	(019)	1:06:29.252
34.985895	-2.958919	1/19/2005	(019)	1:18:22.404
34.934913	-2.898553	1/19/2005	(019)	1:43:48.673
35.001594	-2.972717	1/19/2005	(019)	2:04:31.226
34.995796	-2.933108	1/19/2005	(019)	2:35:29.552
34.928795	-2.934995	1/19/2005	(019)	3:16:29.898
34.944259	-2.928110	1/19/2005	(019)	3:43:09.840
34.988557	-2.938889	1/19/2005	(019)	3:43:40.400
34.947853	-2.963360	1/19/2005	(019)	6:05:44.071
34.933638	-2.948807	1/19/2005	(019)	6:14:49.001
34.960400	-2.968760	1/19/2005	(019)	6:41:51.490
34.988935	-2.971320	1/19/2005	(019)	7:11:09.958
34.915397	-2.944190	1/19/2005	(019)	8:12:06.047
34.661679	-2.809619	1/19/2005	(019)	10:11:34.830
35.261332	-3.048699	1/19/2005	(019)	10:16:59.367
34.975013	-2.930184	1/19/2005	(019)	19:47:55.942
34.953015	-2.977555	1/19/2005	(019)	19:56:41.906
35.036000	-3.719000	1/19/2005	(019)	21:28:14.100
35.032287	-2.956368	1/19/2005	(019)	23:56:15.071
35.056000	3.692000	1/20/2005	(020)	0:07:17.100
35.085465	-3.692857	1/20/2005	(020)	0:07:17.956
35.090416	-3.345715	1/20/2005	(020)	0:12:58.895
34.653010	-2.004549	1/20/2005	(020)	0:14:40.739
33.880903	-4.195534	1/20/2005	(020)	0:46:25.370
34.691222	-2.231619	1/20/2005	(020)	0:47:21.791
34.569944	-2.310638	1/20/2005	(020)	0:54:40.672
34.992663	-3.848189	1/20/2005	(020)	2:01:15.415
34.946227	-3.849268	1/20/2005	(020)	2:02:51.889
34.958450	-2.922124	1/20/2005	(020)	2:06:08.234

Table D-1: Site 1 Event Position and Origin Time (Continued)

Latitude	Longitude	Day	DOY	Time
34.938879	-2.972363	1/20/2005	(020)	2:31:49.765
34.952762	-2.871081	1/20/2005	(020)	2:42:39.071
34.979128	-3.033539	1/20/2005	(020)	2:51:02.430
34.596527	-2.248206	1/20/2005	(020)	2:52:32.834
34.933326	-2.890187	1/20/2005	(020)	4:37:17.187
34.959954	-2.963655	1/20/2005	(020)	4:38:40.527
34.919172	-2.914681	1/20/2005	(020)	4:45:36.306
34.544642	-2.311595	1/20/2005	(020)	4:54:22.947
35.072820	-3.914181	1/20/2005	(020)	4:59:54.032
34.616862	-2.263461	1/20/2005	(020)	5:06:34.035
34.596284	-2.230349	1/20/2005	(020)	5:28:35.333
34.531620	-2.209080	1/20/2005	(020)	6:04:37.590
34.939452	-2.935548	1/20/2005	(020)	6:08:52.470
34.908550	-2.958444	1/20/2005	(020)	7:39:29.340
35.205354	-3.329341	1/20/2005	(020)	17:23:42.547
34.964438	-2.992996	1/20/2005	(020)	18:21:17.945
34.940407	-2.910454	1/20/2005	(020)	18:30:51.532
34.909314	-2.978242	1/20/2005	(020)	18:41:51.761
34.977973	-2.953738	1/20/2005	(020)	19:18:37.852
34.929520	-2.942944	1/20/2005	(020)	19:51:17.934
34.532834	-2.967901	1/20/2005	(020)	21:07:08.662
34.999818	-2.940910	1/20/2005	(020)	23:01:48.099
34.976157	-2.891847	1/20/2005	(020)	23:53:57.867
39.255717	2.811676	1/21/2005	(021)	1:54:29.788
34.917170	-2.979033	1/21/2005	(021)	5:56:20.839
34.916212	-3.842892	1/21/2005	(021)	6:43:41.567
34.904692	-2.956757	1/21/2005	(021)	7:04:44.297
35.044192	-3.987050	1/21/2005	(021)	9:50:07.863
34.963197	-2.985611	1/21/2005	(021)	10:10:51.221
34.971066	-3.000058	1/21/2005	(021)	10:17:25.346
34.863831	-2.949411	1/21/2005	(021)	10:20:53.558
34.967243	-3.027054	1/21/2005	(021)	10:21:37.524
35.222785	-1.057744	1/21/2005	(021)	12:45:37.268
34.925351	-2.942242	1/21/2005	(021)	14:51:22.774
34.975379	-2.961173	1/21/2005	(021)	16:31:47.748

Table D-1: Site 1 Event Position and Origin Time (Continued)

Latitude	Longitude	Day	DOY	Time
34.907047	-2.985830	1/21/2005	(021)	17:20:11.653
34.887015	-2.979738	1/21/2005	(021)	17:33:50.934
34.954114	-2.944855	1/21/2005	(021)	17:34:14.440
34.950585	-2.965731	1/21/2005	(021)	17:36:46.641
34.917907	-2.947178	1/21/2005	(021)	17:47:24.037
35.039717	-3.439943	1/21/2005	(021)	17:56:05.641
33.502229	-2.989833	1/21/2005	(021)	18:20:10.746
35.081000	2.801000	1/21/2005	(021)	18:39:07.800
34.943774	-2.973469	1/21/2005	(021)	18:39:09.094
34.902656	-2.994055	1/21/2005	(021)	18:50:50.780
34.915629	-2.945243	1/21/2005	(021)	19:07:20.308
34.915661	-2.924315	1/21/2005	(021)	19:12:10.992
34.927419	-2.938210	1/21/2005	(021)	19:53:10.197
34.957302	-2.961955	1/21/2005	(021)	20:42:52.318
34.831285	-2.874362	1/21/2005	(021)	20:55:09.399
33.517950	-3.045353	1/21/2005	(021)	21:27:40.577
34.937008	-3.002233	1/21/2005	(021)	23:47:17.036
34.925886	-3.010706	1/21/2005	(021)	23:48:01.831
34.916413	-2.917875	1/22/2005	(022)	2:05:43.219
34.944802	-2.973500	1/22/2005	(022)	2:48:14.115
35.460444	-4.271442	1/22/2005	(022)	2:53:03.651
34.879070	-2.973662	1/22/2005	(022)	3:05:18.004
34.745054	-4.136021	1/22/2005	(022)	3:43:22.141
34.852168	-3.921000	1/22/2005	(022)	3:54:34.172
34.962270	-3.037107	1/22/2005	(022)	4:05:02.834
34.887027	-2.996490	1/22/2005	(022)	4:13:52.141
34.855907	-3.963100	1/22/2005	(022)	4:15:28.181
34.758003	-3.866191	1/22/2005	(022)	4:16:45.232
34.874450	-3.878393	1/22/2005	(022)	4:24:37.573
35.069046	-3.545891	1/22/2005	(022)	5:39:54.532
34.769980	-2.811089	1/22/2005	(022)	5:46:38.274
34.939618	-3.036493	1/22/2005	(022)	6:21:34.805
34.929171	-2.943556	1/22/2005	(022)	7:06:10.842
34.934541	-2.946658	1/22/2005	(022)	8:39:39.392
34.972378	-2.967046	1/22/2005	(022)	9:59:06.590

Table D-1: Site 1 Event Position and Origin Time (Continued)

Latitude	Longitude	Day	DOY	Time
34.912338	-3.025605	1/22/2005	(022)	10:02:49.845
34.941293	-0.793678	1/22/2005	(022)	10:36:31.138
34.902264	-2.933869	1/22/2005	(022)	10:52:34.102
33.502905	-3.037716	1/22/2005	(022)	11:06:56.043
34.930632	-0.682615	1/22/2005	(022)	11:16:44.459
34.841485	-4.180378	1/22/2005	(022)	11:25:36.007
34.902451	-0.711014	1/22/2005	(022)	11:30:06.542
34.793550	-0.675461	1/22/2005	(022)	11:39:04.353
35.045482	-4.006267	1/22/2005	(022)	12:29:52.514
34.857429	-2.989385	1/22/2005	(022)	13:34:58.913
34.950643	-2.938420	1/22/2005	(022)	13:47:09.165
34.963113	-2.963436	1/22/2005	(022)	14:02:54.191
34.933678	-2.961959	1/22/2005	(022)	14:55:53.031
34.964459	-2.893927	1/22/2005	(022)	18:12:55.802
34.872190	-2.981821	1/22/2005	(022)	18:23:43.512
35.013794	-3.852666	1/22/2005	(022)	18:55:22.430
37.731752	-0.823241	1/22/2005	(022)	19:06:21.023
35.034224	-2.926450	1/22/2005	(022)	19:45:43.868
34.879041	-2.997254	1/22/2005	(022)	20:21:35.610
34.937613	-3.001611	1/22/2005	(022)	20:42:31.394
34.960746	-2.943086	1/22/2005	(022)	20:44:37.790
34.957332	-2.965457	1/22/2005	(022)	21:13:54.002
34.840708	-2.887076	1/22/2005	(022)	21:38:04.881
36.283857	-4.990392	1/22/2005	(022)	21:40:07.600
34.945200	-2.991113	1/22/2005	(022)	22:07:20.426
35.087116	-3.844920	1/22/2005	(022)	22:17:24.325
34.924137	-2.971547	1/22/2005	(022)	23:36:15.285
34.936976	-1.981712	1/23/2005	(023)	0:04:53.295
34.902414	-2.970820	1/23/2005	(023)	0:18:18.300
34.984944	-2.929801	1/23/2005	(023)	0:31:20.433
34.998288	-3.808611	1/23/2005	(023)	1:19:11.668
35.080384	-3.823107	1/23/2005	(023)	2:28:04.783
34.788821	-4.189773	1/23/2005	(023)	2:53:49.167
35.027356	-3.833667	1/23/2005	(023)	3:21:26.068
34.835810	-2.899265	1/23/2005	(023)	3:25:55.957

Table D-1: Site 1 Event Position and Origin Time (Continued)

Latitude	Longitude	Day	DOY	Time
34.944286	-2.989911	1/23/2005	(023)	5:00:29.855
35.000623	-3.809293	1/23/2005	(023)	5:30:29.342
36.709041	3.678693	1/23/2005	(023)	6:00:48.681
37.369106	-9.822544	1/23/2005	(023)	6:15:39.219
35.114717	-3.978258	1/23/2005	(023)	6:33:47.996
34.845206	-2.868530	1/23/2005	(023)	6:39:17.600
34.801214	-2.848055	1/23/2005	(023)	11:29:42.807
34.900803	-3.022373	1/23/2005	(023)	11:38:55.481
34.973764	-2.943882	1/23/2005	(023)	17:08:18.405
34.992002	-3.798328	1/23/2005	(023)	17:34:11.175
34.936392	-3.039383	1/23/2005	(023)	18:49:31.969
33.671000	-5.962000	1/23/2005	(023)	19:07:25.160
34.708055	-2.803736	1/23/2005	(023)	19:21:38.672
32.676942	-1.158144	1/23/2005	(023)	20:10:23.933
34.911495	-2.932935	1/23/2005	(023)	23:34:50.038
34.929556	-3.730432	1/23/2005	(023)	23:47:51.477
34.900707	-3.027832	1/24/2005	(024)	0:05:40.221
34.900707	-3.027832	1/24/2005	(024)	0:05:40.221
34.945669	-2.969801	1/24/2005	(024)	0:10:30.901
36.096732	-3.777392	1/24/2005	(024)	0:22:10.202
34.942551	-2.993619	1/24/2005	(024)	0:37:48.533
34.875626	-2.923802	1/24/2005	(024)	1:00:20.338
34.851514	-2.886998	1/24/2005	(024)	1:23:28.009
35.157734	-1.639266	1/24/2005	(024)	1:34:00.965
35.231082	-2.159604	1/24/2005	(024)	1:34:04.076
34.746194	-2.269535	1/24/2005	(024)	1:37:05.362
34.944543	-2.981147	1/24/2005	(024)	1:43:32.709
34.866614	-2.949084	1/24/2005	(024)	1:43:34.265
34.600888	-2.284541	1/24/2005	(024)	1:49:15.950
34.628749	-2.209680	1/24/2005	(024)	1:58:47.674
34.627130	-2.226048	1/24/2005	(024)	2:05:08.520
34.663400	-2.236454	1/24/2005	(024)	2:07:58.531
34.677654	-2.193239	1/24/2005	(024)	2:10:52.363
34.629586	-2.178835	1/24/2005	(024)	2:19:52.289
34.794297	-3.357796	1/24/2005	(024)	2:23:28.001

Table D-1: Site 1 Event Position and Origin Time (Continued)

Latitude	Longitude	Day	DOY	Time
34.630490	-2.201693	1/24/2005	(024)	2:25:01.781
34.628619	-2.160474	1/24/2005	(024)	2:28:57.054
34.605609	-2.194837	1/24/2005	(024)	2:31:54.963
34.572180	-2.171230	1/24/2005	(024)	2:41:46.458
34.600869	-2.182382	1/24/2005	(024)	2:46:33.188
34.643818	-2.197735	1/24/2005	(024)	3:03:47.521
34.946599	-3.004068	1/24/2005	(024)	3:09:23.339
34.617755	-2.213244	1/24/2005	(024)	3:28:34.267
34.964717	-3.876883	1/24/2005	(024)	4:51:42.047
35.489103	-1.540823	1/24/2005	(024)	5:41:25.166
34.930427	-2.972791	1/24/2005	(024)	5:56:47.591
34.933521	-3.022654	1/24/2005	(024)	8:22:57.298

Table D-2: Site 2 Event Position and Origin Time

Latitude	Longitude	Day	DOY	Time
34.488754	-6.437109	2/01/2005	(032)	22:28:53.967
33.126929	-3.614231	2/09/2005	(040)	14:59:49.932
31.064251	-7.247926	2/09/2005	(040)	15:09:57.899
31.808855	-6.334802	2/09/2005	(040)	15:47:11.311
34.413594	-7.727536	2/10/2005	(041)	16:44:07.455
31.881238	-8.013179	2/10/2005	(041)	16:44:09.775
33.818359	-4.174014	2/10/2005	(041)	19:25:50.225
32.956811	-5.058166	2/11/2005	(042)	1:22:00.894
30.282522	2.801233	2/11/2005	(042)	1:52:42.138
33.379062	-5.302364	2/11/2005	(042)	4:58:46.797
34.807215	-4.137963	2/11/2005	(042)	5:24:46.461
34.781592	-4.333142	2/11/2005	(042)	5:24:48.063
32.814020	-5.106167	2/11/2005	(042)	7:04:52.861
34.136580	-4.965693	2/11/2005	(042)	8:52:21.180
33.474152	-5.586085	2/11/2005	(042)	12:33:55.653
34.485902	-7.020010	2/11/2005	(042)	12:58:21.484
34.608894	-4.773588	2/11/2005	(042)	14:44:13.705
34.608894	-4.773588	2/11/2005	(042)	14:44:13.705
33.126354	-6.811830	2/11/2005	(042)	16:24:07.489
33.126354	-6.811830	2/11/2005	(042)	16:24:07.489

Table D-2: Site 2 Event Position and Origin Time (Continued)

Latitude	Longitude	Day	DOY	Time
32.532504	-6.785168	2/11/2005	(042)	17:01:19.220
32.177959	-4.224363	2/12/2005	(043)	1:38:02.946
32.503951	-2.979886	2/12/2005	(043)	3:41:27.902
32.801658	-4.790549	2/12/2005	(043)	5:39:32.086
33.307781	-5.270079	2/12/2005	(043)	7:15:22.807
36.099483	-8.927822	2/12/2005	(043)	8:00:45.296
33.885664	-5.025936	2/12/2005	(043)	10:46:04.948
33.646481	-4.800319	2/12/2005	(043)	12:13:00.782
33.876845	-2.180027	2/12/2005	(043)	13:04:07.068
33.607567	-2.752791	2/12/2005	(043)	13:16:42.059
33.911209	-4.961653	2/12/2005	(043)	13:32:20.329
33.931726	-3.982994	2/12/2005	(043)	15:31:27.081
34.509268	-7.478536	2/12/2005	(043)	15:38:20.830
34.623770	-3.597107	2/12/2005	(043)	16:03:12.056
32.482078	-3.447753	2/12/2005	(043)	16:16:24.467
33.614496	-4.843181	2/12/2005	(043)	17:59:32.155
34.575926	-6.057895	2/12/2005	(043)	19:11:12.807
33.438870	-4.638174	2/13/2005	(044)	0:14:27.972
37.381936	-9.035518	2/13/2005	(044)	0:23:36.800
32.645907	-4.773123	2/13/2005	(044)	5:01:01.219
33.123833	-6.025350	2/13/2005	(044)	7:29:29.835

Table D-3: Site 3 Event Position and Origin Time

Latitude	Longitude	Origin Time
35.037000	-3.802000	1/30/2005 (030) 17:09:55.540
35.311481	-9.956352	1/30/2005 (030) 19:35:16.179
31.369002	-5.763530	1/30/2005 (030) 22:07:15.817
35.045000	-3.798000	1/30/2005 (030) 22:19:16.600
31.187843	-5.218374	1/31/2005 (031) 2:41:29.333
32.683745	-5.133385	1/31/2005 (031) 3:40:49.535
32.708136	-5.144037	1/31/2005 (031) 4:04:45.155
30.555351	-7.003837	1/31/2005 (031) 5:17:31.043
31.511662	-5.759745	1/31/2005 (031) 5:42:01.192
33.423220	-6.142889	1/31/2005 (031) 13:22:41.907
34.453258	-4.114174	1/31/2005 (031) 15:28:00.973

Table D-3: Site 3 Event Position and Origin Time (Continued)

Latitude	Longitude	Origin Time
31.651888	-5.583669	1/31/2005 (031) 15:29:24.733
32.463331	-7.013117	1/31/2005 (031) 16:08:23.808
31.507055	-6.141322	1/31/2005 (031) 16:10:31.479
33.420702	-2.034745	1/31/2005 (031) 16:57:53.602
32.396803	-6.044701	1/31/2005 (031) 20:35:32.119
35.871232	-9.645744	2/01/2005 (032) 1:49:41.865
35.344196	-9.907622	2/01/2005 (032) 1:49:45.581
35.344137	-9.907643	2/01/2005 (032) 1:49:45.582
32.610045	-5.654530	2/01/2005 (032) 5:31:09.902
35.630670	-11.10201	2/01/2005 (032) 11:46:17.545
35.630209	-11.10229	2/01/2005 (032) 11:46:17.546
32.609790	-6.820489	2/01/2005 (032) 13:26:44.160
32.498807	-6.958069	2/01/2005 (032) 13:26:44.272
32.498807	-6.958069	2/01/2005 (032) 13:26:44.272
31.342449	-5.711852	2/01/2005 (032) 13:54:51.432
32.512527	-7.063299	2/01/2005 (032) 14:40:55.854
33.543517	-6.382771	2/01/2005 (032) 14:42:24.719
31.752502	-8.192057	2/01/2005 (032) 14:42:26.760
32.508243	-7.254356	2/01/2005 (032) 14:55:01.709
32.789083	-7.061566	2/01/2005 (032) 15:49:31.852
32.521758	-7.016625	2/01/2005 (032) 15:49:35.409
31.837189	-6.624709	2/01/2005 (032) 18:44:18.486
31.345402	-5.709557	2/01/2005 (032) 21:37:39.371
31.328031	-5.669420	2/01/2005 (032) 21:40:07.354
31.345384	-5.688810	2/01/2005 (032) 21:46:27.085
31.342352	-5.699913	2/01/2005 (032) 21:55:52.137
31.318488	-5.694599	2/01/2005 (032) 21:57:09.285
31.150939	-7.087147	2/02/2005 (033) 8:24:41.863
32.510154	-6.771067	2/02/2005 (033) 14:55:12.120
32.510033	-6.770907	2/02/2005 (033) 14:55:12.122
32.559967	-6.842499	2/02/2005 (033) 14:58:41.120
32.441973	-6.855465	2/02/2005 (033) 15:19:56.673
32.461092	-6.916794	2/02/2005 (033) 16:14:35.512
31.750961	-8.203209	2/02/2005 (033) 17:16:01.992
31.564895	-8.871284	2/02/2005 (033) 17:49:10.937

Table D-3: Site 3 Event Position and Origin Time (Continued)

Latitude	Longitude	Origin Time
33.744734	-6.467133	2/02/2005 (033) 19:57:32.594
32.303767	-5.373532	2/02/2005 (033) 21:01:05.012
32.292431	-5.355046	2/02/2005 (033) 21:01:05.113
31.339932	-5.731601	2/02/2005 (033) 22:00:38.751
35.063000	-3.791000	2/03/2005 (034) 0:47:05.000
35.264508	-11.01000	2/03/2005 (034) 3:20:06.338
34.015209	-6.131742	2/03/2005 (034) 11:34:51.093
33.481334	-5.966348	2/03/2005 (034) 11:34:58.205
37.938000	1.740000	2/03/2005 (034) 11:40:33.970
32.500977	-6.809942	2/03/2005 (034) 14:30:46.080
32.572105	-6.999828	2/03/2005 (034) 15:06:50.342
32.530677	-6.856385	2/03/2005 (034) 15:14:33.491
32.532942	-6.921215	2/03/2005 (034) 15:29:22.143
31.665732	-7.925041	2/03/2005 (034) 15:42:09.708
32.438753	-6.869946	2/03/2005 (034) 15:45:04.451
35.624150	-10.52803	2/03/2005 (034) 16:08:46.831
32.691464	-3.419102	2/03/2005 (034) 18:34:20.678
31.280406	-5.877584	2/03/2005 (034) 23:41:32.599
37.884000	-1.636000	2/04/2005 (035) 1:09:41.800
38.077628	-5.562016	2/04/2005 (035) 1:09:43.697
32.371447	-6.298191	2/04/2005 (035) 3:23:03.751
35.825153	-10.76870	2/04/2005 (035) 3:34:01.638
31.336022	-5.724263	2/04/2005 (035) 5:56:04.408
31.744482	-8.451558	2/04/2005 (035) 12:16:00.972
33.685384	-5.578584	2/04/2005 (035) 13:09:49.991
31.845868	-7.962522	2/04/2005 (035) 13:34:16.049
31.939281	-6.447602	2/04/2005 (035) 14:52:10.307
31.285418	-7.012685	2/04/2005 (035) 15:19:47.538
32.471791	-6.859651	2/04/2005 (035) 16:25:58.313
32.451615	-6.747319	2/04/2005 (035) 16:43:13.201
31.483419	-8.704057	2/04/2005 (035) 16:55:02.104
32.503832	-6.959961	2/04/2005 (035) 17:46:42.483
31.376105	-5.168121	2/04/2005 (035) 19:30:47.002
33.128000	5.318000	2/05/2005 (036) 3:56:04.700
32.063791	-5.552067	2/05/2005 (036) 4:11:14.639

(This page intentionally left blank.)